1987

Superconductivity, magnetism, and charge density wave formation in ternary compounds with the Sc5Co4Si10-type structure

Hung-Duen Yang
Iowa State University

INFORMATION TO USERS

While the most advanced technology has been used to photograph and reproduce this manuscript, the quality of the reproduction is heavily dependent upon the quality of the material submitted. For example:

- Manuscript pages may have indistinct print. In such cases, the best available copy has been filmed.

- Manuscripts may not always be complete. In such cases, a note will indicate that it is not possible to obtain missing pages.

- Copyrighted material may have been removed from the manuscript. In such cases, a note will indicate the deletion.

Oversize materials (e.g., maps, drawings, and charts) are photographed by sectioning the original, beginning at the upper left-hand corner and continuing from left to right in equal sections with small overlaps. Each oversize page is also filmed as one exposure and is available, for an additional charge, as a standard 35mm slide or as a 17"x 23" black and white photographic print.

Most photographs reproduce acceptably on positive microfilm or microfiche but lack the clarity on xerographic copies made from the microfilm. For an additional charge, 35mm slides of 6"x 9" black and white photographic prints are available for any photographs or illustrations that cannot be reproduced satisfactorily by xerography.

Yang, Hung-Duen

SUPERCONDUCTIVITY, MAGNETISM, AND CHARGE DENSITY WAVE FORMATION IN TERNARY COMPOUNDS WITH THE SCANDIUM(5)COBALT(4)SILICON(10)-TYPE STRUCTURE

Iowa State University PH.D. 1987

PLEASE NOTE:

In all cases this material has been filmed in the best possible way from the available copy. Problems encountered with this document have been identified here with a check mark __√__.

1. Glossy photographs or pages _____
2. Colored illustrations, paper or print _____
3. Photographs with dark background _____
4. Illustrations are poor copy _____
5. Pages with black marks, not original copy _____
6. Print shows through as there is text on both sides of page _____
7. Indistinct, broken or small print on several pages __√__
8. Print exceeds margin requirements _____
9. Tightly bound copy with print lost in spine _____
10. Computer printout pages with indistinct print _____
11. Page(s) _____ lacking when material received, and not available from school or author.
12. Page(s) _____ seem to be missing in numbering only as text follows.
13. Two pages numbered _____. Text follows.
14. Curling and wrinkled pages _____
15. Dissertation contains pages with print at a slant, filmed as received _____
16. Other _____

_____

_____

University
Microfilms
International

Superconductivity, magnetism, and charge density wave formation in ternary compounds with the $Sc_5Co_4Si_{10}$-type structure

by

Hung-Duen Yang

A Dissertation Submitted to the
Graduate Faculty in Partial Fulfillment of the
Requirements for the Degree of
DOCTOR OF PHILOSOPHY

Department: Physics
Major: Solid State Physics

Approved:

Signature was redacted for privacy.
In Charge of Major Work

Signature was redacted for privacy.
For the Major Department

Signature was redacted for privacy.
For the Graduate College

Iowa State University
Ames, Iowa

1987

TABLE OF CONTENTS

I. INTRODUCTION

A. Superconductivity and Superconducting Materials

Superconductivity was discoverd in 1911 by Onnes,[1,2] who found the abrupt and complete disappearance of resistance in certain metals when they are cooled below a critical temperature T_c. In 1933, Meissner and Ochsenfeld[3] observed that the superconducting state was destroyed at a thermodynamic critical field H_c, where the energy cost per unit volume ($H_c^2/8\pi$) of excluding the field exceeded the decrease in free energy of superconducting state relative to the normal state. Two years later, the London brothers[4] proposed two phenomenological equations that neatly described the perfect conductivity and perfect diamagnetism at low field. In 1950, Ginzburg and Landau[5] proposed a profoundly suggestive phenomenological theory of superconductivity as a macroscopic quantum state described by a macroscopic wavefunction ψ. Three years later, Pippard's[6] insight in interpreting microwave surface-impedance measurements led him to introduce a coherence length ξ_0 measuring the nonlocality of superconducting electrons.

However, the major breakthrough in the understanding of microscopic superconductivity was presented by Bardeen, Cooper, and Schrieffer.[7] The BCS theory described the superconducting state in terms of "Cooper pairs" of electrons and showed how electron-phonon coupling could, at a critical temperature, produce a superconducting state with an energy gap of the observed magnitude and with appropriate values for the other measured parameters, such as H_c (thermodynamic critical field), λ

(penetration depth), and ξ (coherence length). Incorporation of the lattice via an electron-phonon interaction also accounted for the experimentally observed isotope effect.[8,9] Theoretical understanding of the many remarkable features of type II superconductors was soon achieved in terms of extreme parametric regimes of existing phenomenological theories of Ginzburg and Landau,[5] and Abrikosov,[10] which were linked to the BCS theory by Gor'kov[11] two years later.

So far, most superconductors can be understood on the basis of the standard predictions of the BCS theory and elementary solid state physics.[12] Superconductivity almost from its beginning has depended upon an interplay between materials research and condensed-matter physics. Two questions often come to mind: Why do some materials have much higher transition temperatures than others? Why do so many novel superconductors with unusual physical properties continue to be discovered? Several such classes of superconducting materials are discussed briefly below.

The high critical temperature found in the A15 system[13] has been the subject of both theoretical and experimental investigations, but with few definite answers. Many of the proposed models suggest the enhancement of T_c is exclusively due to peaks in the electronic density of states at the Fermi energy. Experimentally, the electron-phonon coupling increases in overall magnitude and strength at low frequencies (that is, soft mode phonons) and was analyzed from tunneling spectroscopy.

In 1958,[14] it was shown that as little as 1 percent of magnetic impurities can destroy superconductivity in metals. Beginning in the

mid-1970s,[15] the competition between superconductivity and magnetism has been re-explored in rare-earth ternary compounds. For example, $ErRh_4B_4$ [16,17] becomes a superconductor near 9 K. As it is cooled further, the rare-earth ions begin to order magnetically until the superconductivity is destroyed near the Curie temperature just below 1 K. Recent small-angle neutron scattering experiments suggest that some of these compounds exhibit a new phase of matter in which superconductivity coexists with magnetic order in periodic structures with a wavelength of about 200 Å with superconductivity surviving. In general, it is found that superconductivity can occur together with antiferromagnetism and spiral magnetic order. Purely ferromagnetic ordering will destroy superconductivity and is referred to as reentrant superconductivity.

Heavy-fermion superconductors[18] with enormous electronic specific heats have been found, such as $CeCu_2Si_2$, UBe_{13}, and UPt_3. There is some evidence that one or more of the heavy-fermion superconductors might have p-type pairing. If so, there is the additional question as to whether the attractive interaction giving rise to the pairing is phonon induced (BCS type) or due to another microscopic interaction, possibly localized spin fluctuations.

At the opposite extreme from heavy-fermion system, the $Ba(Bi_{1-x}Pb_x)O_3$[19] system becomes superconducting at 13 K with a very low electron density. This is quite interesting because superconductivity has been known to be a function of carrier number density. A complete understanding of the origins of the superconductivity of this material is not clear because (1) the heat capacity jump at the transition is so small, and in some cases nondetectable for this low electron density

state, and (2) it is difficult to prepare a single-phase sample to establish whether the superconductivity is a bulk or an interface effect.

Some quasi-one-dimensional systems, such as $TlMo_3Se_3$, TaS_3, and $NbSe_3$, quasi-two-dimensional conductors, such as the transition-metal dichalcogenides, artificially layered compounds, and organic system, such as $(TMTSF)_2PF_6$ are proven superconductors. The low dimensional superconductors[20] have provided a cornucopia of interesting competitive interaction effects (charge-density-wave, spin-density-wave and superconductivity) due to the well-known propensity toward instability of the Fermi surface in reduced-dimensional systems.

Most recently, the record high T_c superconductors based on the Ba-La-Cu-O (~ 40 K)[21], Ba-Y-Cu-O (~ 90 K)[22], and Ba-Lu-Cu-O (~ 90 K)[23] systems were found. This exciting discovery encourages scientists to challenge the T_c limit and push it toward even higher temperatures.

B. Charge Density Wave Formation

It was suggested more than 30 years ago[24] that a one-dimensional metal is unstable toward the formation of a periodic lattice distortion (PLD) associated with a spatially periodic modulation of the electronic charge density, the latter called a charge-density-wave (CDW). The wave vector Q of the CDW is related to the Fermi wavevector k_F by $Q = 2k_F$, and consequently the formation of a CDW opens a gap at the Fermi level, lowering the kinetic energy of the conduction electrons. The argument is due to Peierls, and phase transitions which lead to the development of a CDW ground state are called Peierls transitions.

The theoretical conjecture of CDW formation remained untested until the discovery of solids built of chains of atoms with highly anisotropic crystal and electronic structures. Early examples of so-called low-dimensional solids which have been widely studied from the stucture point of view, include the inorganic chain compound potassium cyanoplatinate (KCP)[25] and a large family of organic compounds of which the charge transfer salt tetrathiafulvalene-tetracyanoquinodimethane (TTF-TCNQ) has been the most prominent example.[26] In a family of inorganic chain compounds called the transition metal dichalcogenides[27] the electronic structure is two-dimensional (2D), leading to a 2D CDW stucture.

In linear chain compounds, the lattice distortion and periodically modulated charge density occur along the chain direction, and the position-dependent charge density modulation can be described as

$$\Delta\rho(x)=\rho_0 \cos(2k_F x + \phi) \qquad (1)$$

where ρ_0 and ϕ are the amplitude and phase of the CDW respectively, and x is the position along the chain. A 1D metallic system, together with the CDW ground state, is shown in Fig. 1. The static properties of the CDW and the periodic lattice distortion, both wavelength $\lambda = \pi/k_F$, are readily studied by X-ray, electron, or neutron diffraction methods.[24]

It was suggested by Fröhlich in 1954[28] that when the wavelength λ of the CDW is not a simple multiple of the original lattice constant (and hence the CDW is incommensurate), the energy associated with CDW is independent of the phase ϕ. In fact, in real systems, as shown by Lee et al.[29] and Rice[30], the translational invariance is broken because the

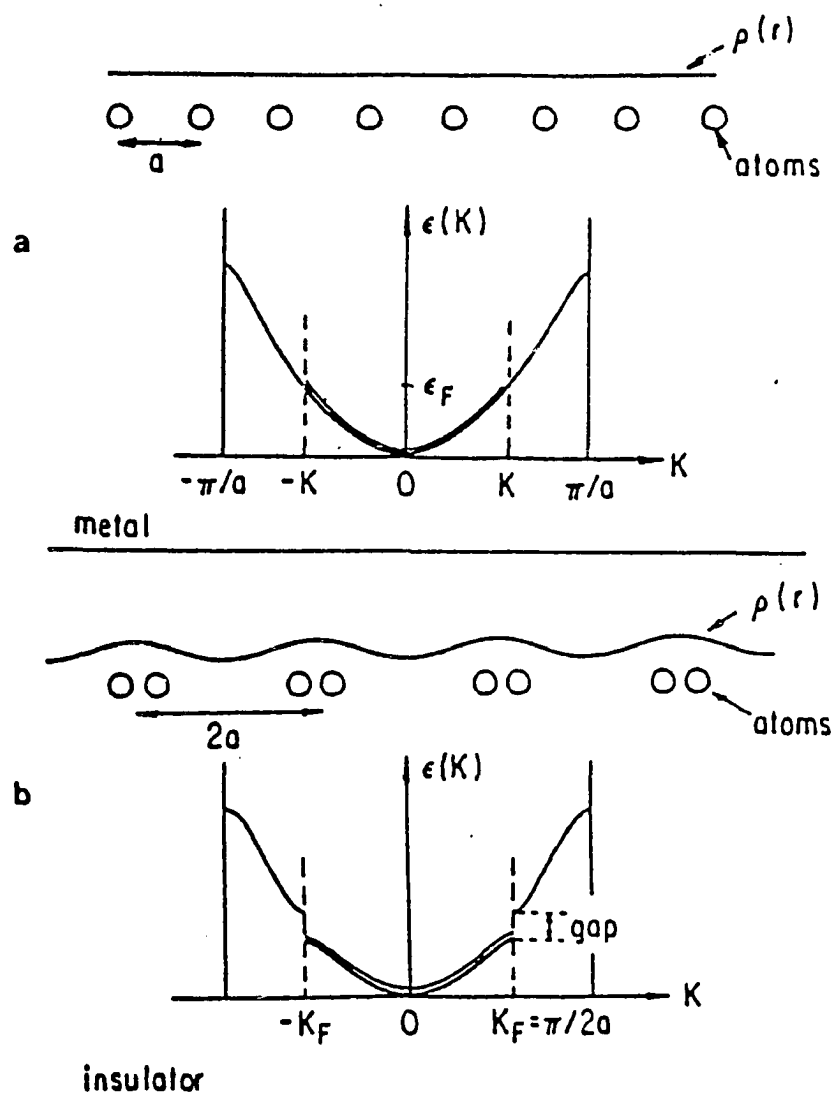

Fig. 1. Peierls distortion in a one-dimensional electron gas. (a) undistorted lattice (b) distorted lattice with gap in the single particle excitation

phase ϕ is pinned to the lattice. The pinning can be provided by impurities, commensurability between the CDW wave-length and the lattice, or by Coulomb interaction between adjacent chains. Oscillations of the CDW pinned mode are expected to lead to a large low frequency ac conductivity and to a giant dielectric constant. An applied dc electric field, however, can supply the CDW with an energy higher than the pinning one and above a threshold electric field, the CDW can slide and carry a current, but damping prevents superconductivity.

A number of inorganic linear compounds have recently been discovered which display a CDW ground state and strong electric field and frequency dependent conductivity.[31] The first such material to be studied was $NbSe_3$ synthesized in 1975. This compound initiated a rapidly growing field known as charge-density-wave transport phenomena. In addition, X-ray studies[32] have clearly demonstrated that the CDW is not destroyed by applied dc electric fields, confirming the postulated picture of a sliding mode. The current-carrying state also has other unusual transport properties, such as the absence of a Hall effect and zero thermoelectric power, both of which confirm that current is carried by a ground state system. Perhaps the most surprising observation is that of oscillating currents in the sliding CDW state, with the frequency of the oscillation proportional to the current carried by the condensate.[33,34]

Experimentally, a Peierls transition in a material can often be inferred from transport measurements, for example, from sharp changes in the dc electrical resistivity, anomalies in the static magnetic

susceptibility and specific heat. Direct evidence for CDW formation is provided by X-ray, electron or neutron scattering experiments.

C. Superconductivity and Charge Density Waves

Among the states of broken symmetry in a solid, charge density waves (CDW) and superconductivity (SC) are two prominent ones w ich require an effective attractive electron-electron interaction[7,35] mediated by phonons. It is therefore not surprising that systems in which CDW's have been observed[27] are also superconducting at very low temperature.[36-38] The tendencies toward the formation of SC and CDW are to a certain degree opposing one another. While the SC state has an infinite conductivity and a Meissner effect, the CDW state, for large enough interactions, produces a semiconductor gap in the spectrum and a nonconducting state. From the microscopic point of view on the other hand, the SC state arises from electron-electron coupling into Cooper pairs, while the CDW state comes from electron-hole coupling and charge redistribution, two effects which are in principle independent of one another.

According to the theoretical model proposed by Balseiro and Falicov,[39] the phonon-mediated attractive electron-electron interaction leads to both CDW and SC states. There are four possible states : (1) a normal paramagnetic state, (2) a SC state with uniform charge distribution, (3) a CDW state which may be either metallic or semiconducting, and (4) a metallic SC and CDW state, with a modulated charge distribution. The stability of each of these states depends

sensitively on the temperature, the strengths of the interactions, and the details of the electronic spectrum and Fermi surface.

In general the order parameters interfere destructively, with CDW tending to suppress SC and vice versa. A large enough CDW interaction which produces a semiconducting state may completely destroy SC, but all metallic CDW states become SC at sufficiently low temperature. If the CDW gap is small enough, smaller than an "ideal" SC gap, as the temperature decreases the system may make a transition from a nonuniform semiconductor to a nonuniform SC. This semiconducting-SC state shows persistent currents and a Meissner effect but the dependence of the SC parameters on the total currents is different and more pronounced than in the metallic SC state.

The correlation between the fall of the CDW transition temperature T_o and the increase of the SC transition temperature T_c under pressure was first discussed for the 2H-dichalcogenides.[40] The variation of T_c with pressure considers the pressure-temperature dependence of the electron-phonon coupling constant:[41]

$$\lambda = \frac{N(E_F) < I^2 >}{M \quad < \omega^2 >} \tag{2}$$

where $\langle I^2 \rangle$ is the Fermi surface average of the electron-phonon matrix element, $\langle \omega^2 \rangle$ an average of phonon frequencies, and $N(E_F)$ the density of electronic states at the Fermi level. The possibility for the enhancement of T_c is the increase of $N(E_F)$ under pressure by reducing the amplitudes of the gaps opened at the Fermi surface by the CDW.[42] Also, it may be possible to have phonon modes which soften under pressure was proposed by Testardi[43] to explain the pressure dependence

of T_c in A15 compounds. However, this soft-mode model predicts a maximum of T_c when $T_{CDW} \sim T_c$ which was never observed in layered compounds, although a T_c maximum at 6 kbar was observed in $NbSe_3$.

Impurities also have a profound effect on both CDW transitions and the dynamics of CDW formation. The presence of impurities in a CDW material may lead to a change in the transition temperature T_o and also to a possible smearing of the CDW transition itself. Since the disorder in the lattice smears the momentum space distribution for the electrons, it also reduces the enhanced susceptibility and hence lowers the T_o. As discussed by Bulaevskii[44] the influence of lattice disorder on the CDW transition and the influence of magnetic impurities on the SC transition are equivalent. In the dilute limit, T_o decreases linearly with increasing impurity concentration, and possibly enhances the T_c simultaneously. These effects have been observed in both $NbSe_3$ and TaS_3. For $NbSe_3$, low-field electrical resistivity studies[45] show that replacing 0.5% of the Nb atoms with isoelectronic Ta atoms results in a decrease of both CDW transition temperatures by approximately 10 K. At 5% Ta doping the lower transition is so depressed that it is no longer detectable, while a superconducting transition is observed at 1.5 K. Doping $NbSe_3$ with nonisoelectronic Ti atoms has a much more drastic effect. A 0.1% doping concentration leads to a decrease in T_o by nearly 20 K for both CDW transitions.

II. EXPERIMENTAL DETAILS

A. Sample Preparation

The samples used in this study were synthesized from high-purity (at least 99.9%) elements by arc-melting stoichiometric amounts in a Zr-gettered argon atmosphere on a water-cooled Cu hearth. The sources and purities of the starting materials are listed in the appendix. The resulting ingots were turned over and remelted several times to promote homogeneity. Weight losses during arc-melting were negligible (less than 0.3%) except for the Yb and Tm compounds, for which the boil-off of the rare earth element was compensated by adding an excess beforehand. The samples were then sealed in quartz ampoules with about 160 torr of argon and annealed at 1050°C for 7 days followed by a water quench to room temperature.

B. Sample Characterization

Powder X-ray diffration data were obtained using a microcomputer controlled Rigaku diffractometer with Cu K_α radiation and a diffracted beam graphite monochromator at a step scan rate of 0.01 °/sec over the 2θ angular range of 10 to 80 degrees. Lattice parameters were determined by the method of least-squares using 20 to 25 reflections incluing an internal silicon standard (a = 5.43083 Å).[46] In most cases these are in good agreement with those reported by Braun and Segre,[47] and Venturini et al.[48] In some samples, the X-ray patterns did show a

few peaks unindexible to the $Sc_5Co_4Si_{10}$-type structure (space group P4/mbm) which are attributed to small amounts of impurities.

Low temperature X-ray investigations were done for the $Lu_5Ir_4Si_{10}$ compound. Samples were mounted on the cold finger of a closed-cycle helium refrigerator and a pattern was taken at room temperature. The samples were then cooled to 70 K and held at this temperature while another pattern was taken. Finally, the samples were further cooled to 20~30 K (the low temperature limit of the refrigerator), and a third full pattern was taken.

C. Magnetic Susceptibility

The superconducting transition temperature T_c of the samples was determined from low frequency (~ 25 Hz) ac magnetic susceptibility measurements in a conventional He^4 dewar for the temperature range between 1.2 to 30 K. Most of the samples were measured in powdered form in order to eliminate the possibility of screening effects. The midpoint of the transition is taken as T_c, whereas the 10% and 90% values of the full transition were used to define the transition width.

The static magnetic susceptibility measurements were performed on a fully automated SQUID magnetometer sample property measurement system from Quantum Design Inc. This system had a temperature range from 2.1 to 400 K and an applied magnetic field up to 20 kOe. Temperatures were determined by a Pt thermometer in the range from 40 to 400 K, and a Carbon Glass thermometer in the range of 2.1 to 40 K, both calibrated against NBS traceable standards. The samples used here were irregular

pieces and had a mass on the order of 200 mg for superconducting materials and 50 mg for magnetic materials. In most cases, the samples were cooled down to the lowest temperature, the magnetic field applied, and the data taken as the temperature increased.

The upper critical field of the superconducting material for each temperature was taken by determining where each M vs H curve crossed H-axis (where M=0) measured below T_c.

D. Electrical Resistivity

A standard four-probe technique was used in electrical resistivity measurements. Fine platinum wires (0.002" diameter) were spot welded to the sample and served as the voltage and current leads. In most ambient pressure cases, the measurements were made with temperature control provided by the sample property measurement system in the range from 2.6 to 380 K. A programable dc constant current source and a nanovoltmeter (Keithley Inc.) were controlled and read by a personal computer (HP-85). The effects of thermoelectric voltages in the voltage circuit were eliminated by reversing the sample current at each temperature while data were taken. All samples used in this measurement were rectangular parallelpipeds having approximate dimension 1 x 1 x 7 mm^3.

For high pressure experiments, ac resistivity measurements were performed in a conventional dewar over the temperature range from 300 to 1.5 K. Low frequency (~ 25 Hz) current was applied in order to enhance the penetration capability such that the skin depth is much larger than the maximum cross-sectional dimension and to minimize the inductive

coupling between the driving current and voltage circuits. For irregular but flat pieces of samples, the method of van der Pauw[49] was utilized to calculate the resistivity from the resistance which was measured at room temperature.

A needle-like sample (0.1 x 0.1 x 3.5 mm^3) was used to measure the current dependence of resistivity for $Lu_5Ir_4Si_{10}$. Electrical contacts were bonded to the sample with silver paint. High pulsed (~ 1sec duration) current (up to 0.4 A) was used to generate the high electric field while minimizing the sample self-heating effect.

E. Hydrostatic High Pressure

The pressure dependence of T_c was determined for bulk pieces of the samples by a low frequency (~ 25 Hz) ac magnetic susceptibility technique using a piston-cylinder type hydrostatic pressure clamp.[50] A 1 : 1 mixture of isoamyl alcohol and n-pentane was used as the pressure transmitting fluid. Pressures were applied at room temperature and determined at low temperature by means of superconducting lead and tin manometers.[51] For each sample, the ambient pressure T_c was retaken after the series of high pressure measurements. In every instance, the original value was reproduced within experimental error indicating complete reversibility of the pressure effects on T_c.

Measurements of the electrical resistivity under hydrostatic pressure for the $Lu_5Ir_4Si_{10}$, $Lu_5Rh_4Si_{10}$, and $Tm_5Ir_4Si_{10}$ compounds were performed from room temperature down to just below the superconducting transition temperature. Kerosene was used as the pressure transmitting

fluid in this case. In every instance, T_c was measured resistively as well as inductively.

F. Heat Capacity

Heat capacity measurements were performed at temperatures ranging from 0.6 to 30 K on a heat pulse-type semi-adiabatic calorimeter. Designed details are given elsewhere.[52] Two advantages of this calorimeter are (1) a He^3 pot/bellows together with a mechanical heat switch serving to cool the sample without exchange gas, and (2) a continuous operating He^4 cold plate and circulating He^3 system. The cryostat was designed as an insert to an existing helium dewar and gas handling system. The mass of the magnetic sample investigated is about 0.8 g and about 200 data points were taken within the whole temperature range. A general heat capacity program was used to analyze data.

III. PRESSURE EFFECTS IN SUPERCONDUCTING $Sc_5Co_4Si_{10}$-TYPE COMPOUNDS

A. Introduction

The $R_5T_4X_{10}$ series was first reported[53,54] by Braun et al. in 1980 and further investigated[48] by Venturini et al. in 1984. The class of superconducting and magnetic compounds is constituted as follows: R = Gd-Yb, Sc and Y, T = Co, Rh, Ir, or Os, and X = Si or Ge. The system crystallizes in the $Sc_5Co_4Si_{10}$-type structure which is primitive tetragonal, space group P4/mbm, and has 38 atoms per unit cell. Fig. 2 indicates the structure of $Sc_5Co_4Si_{10}$ viewed approximately along the c-axis. Fig. 3 shows the basic building blocks comprising this structure.

The motivation to systematically study pressure effects in superconducting $Sc_5Co_4Si_{10}$-type compounds is as followed:

(1) This crystal structure is different from those of the extensively studied Chevrel phases[55] and ternary rhodium borides[56] in two aspects. The transition metal atoms form clusters in the Chevrel phases (Mo octahedral) and the rhodium borides (Rh tetrahedral) which are isolated from the rare earth site. The $Sc_5Co_4Si_{10}$-type compounds, have no transition metal-transition metal bonds and the transition metal and silicon atoms form a tightly bound three-dimensional network, in which the rare earth ions are imbedded. A further difference is the existence of three crystallographically independent lattice sites for the rare earth in the latter compounds, while in the former two classes all rare earth positions are equivalent. These crystal-chemical differences may bring about different superconducting or magnetic behaviors in the three classes of compounds.

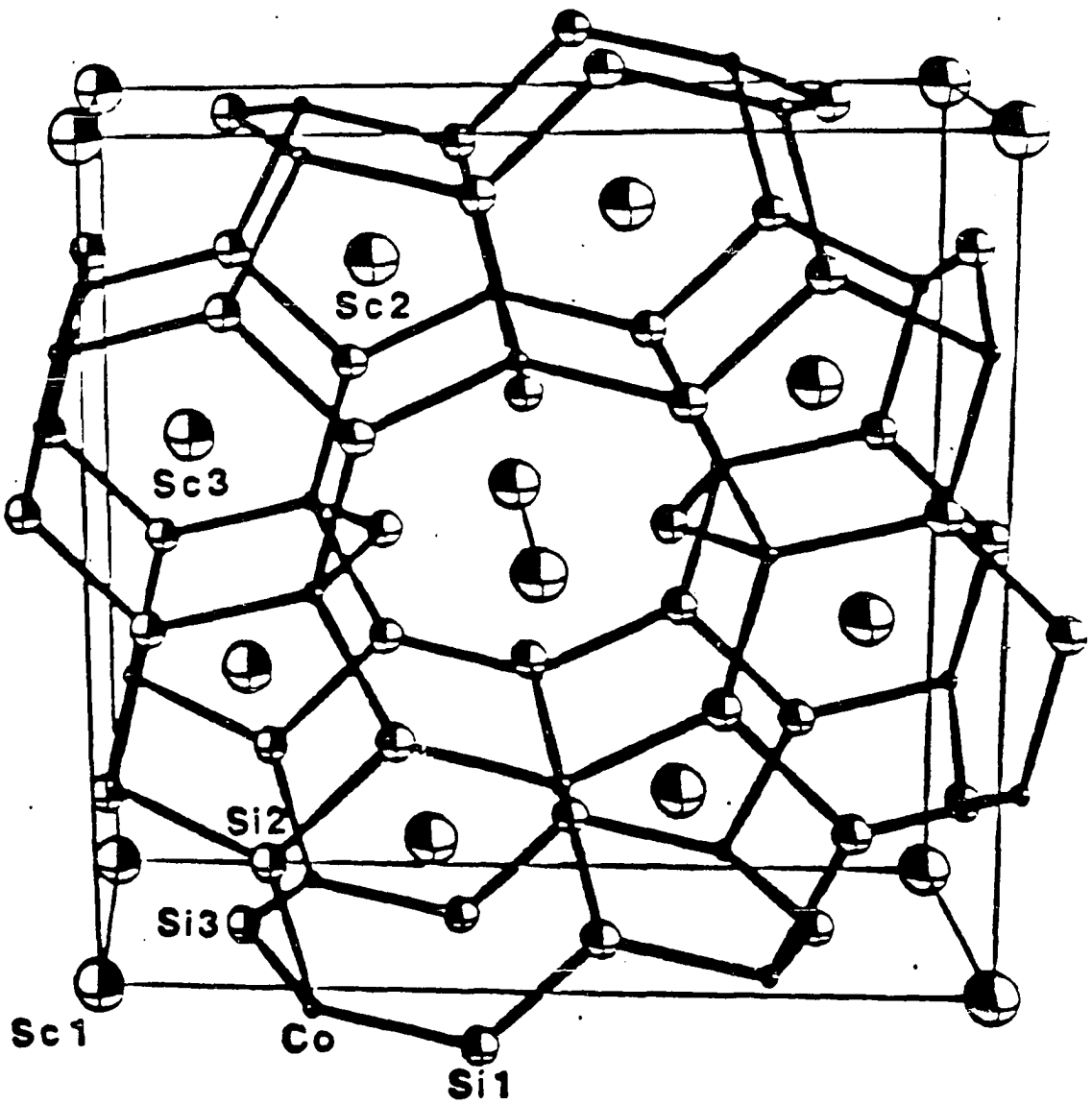

Fig. 2. $Sc_5Co_4Si_{10}$-type crystal structure looking approximately along the c-axis

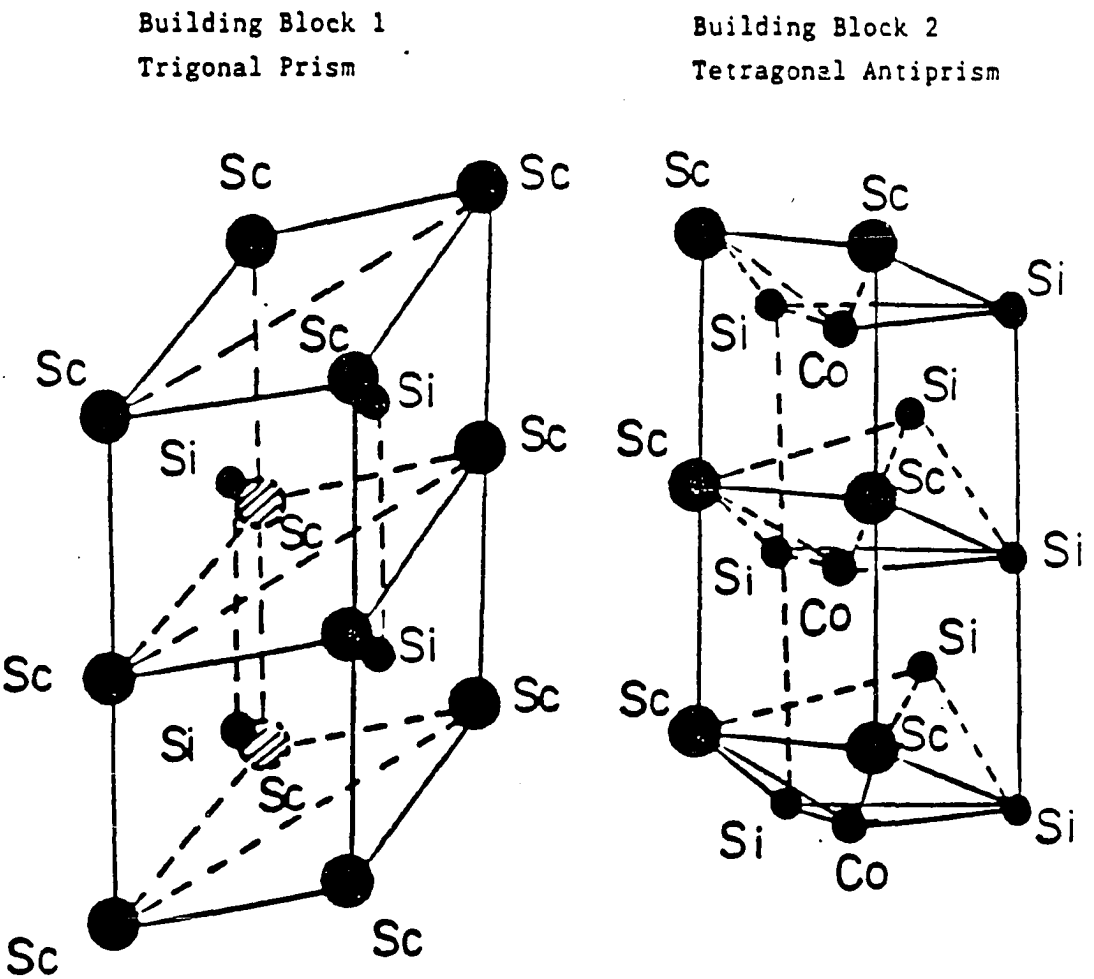

Fig. 3. The two basic building blocks in the $Sc_5Co_4Si_{10}$-type structure

(2) The occurrence of superconducting transition temperatures up to 8.3 K for $Sc_5Ir_4Si_{10}$ and $Sc_5Rh_4Si_{10}$, and up to 9 K for $Y_5Os_4Ge_{10}$ is remarkable in ternary silicides and germanides.

(3) The static magnetic susceptibility measurements indicate that the Co atoms in $Sc_5Co_4Si_{10}$ carry no magnetic moment.[47] In addition, $Sc_5Co_4Si_{10}$ becomes superconducting at T_c = 4.5 K and has one of the highest T_c's known for Co ternary compounds.

(4) There is an anomalous temperature dependence of susceptibility and resistivity[57,58,59] for some ternary silicides of this structure type.

(5) Coexistence of superconductivity and antiferromagnetic ordering was found in $(Sc_{1-x}Dy_x)_5Ir_4Si_{10}$ solid solutions.[60]

B. Results and Discussion

1. Superconductivity under high pressure

Superconductivity is interesting not only in its own right but also for the insights that one can get in using superconductivity as a probe into other physical phenomena. Pressure changes the inter-particle distance, and therefore the electromagnetic forces which are responsible for almost all interactions in solids. Thus, the high pressure technique has come to be recognized as a particularly valuable tool for studying the structure transformations, electronic instability, and magnetic properties in solids.[61] The effect of high pressure on T_c then plays an important role in the understanding of superconductivity. The common linear decrease in T_c with pressure observed in the non-

transition element superconductors has been generally attributed to the stiffening of lattice with applied pressure[62] while the distribution of positive and negative effects in the superconducting transition metals is generally attributed to electronic effects.[63] In those cases where non-linearities are observed in the elements (Re, U, and La), various effects such as crystallographic transformations, Fermi surface topology, and competitive phenomena, such as with charge density waves (CDW) or spin density waves (SDW), have been invoked as possible explanations.[63]

Results of hydrostatic pressure measurements of T_c for five ternary silicides and five ternary germanides are displayed in Fig. 4 and Fig. 5, respectively. Below 20 kbar, all ten compounds exhibit a linear dependence of T_c with pressure. Only $Lu_5Ir_4Ge_{10}$ shows a slight rise in T_c with pressure, while for all of the other samples T_c is depressed by the application of external pressure. Fig. 6 shows the pressure dependence of T_c for two samples of $Lu_5Ir_4Si_{10}$. Two distinct transitions are observed for the samples $Lu_5Ir_4Si_{10}$ at about 20 kbar. The more detailed description for this compound will be presented in next section.

The data for each of these ten compounds, as well as the linear portion of the data for the two samples of $Lu_5Ir_4Si_{10}$ shown in Fig. 6 were fitted by the method of least squares to obtain the values of dT_c/dp listed in Table 1. In the absence of any transformation, the effect of pressure on T_c is quite modest with values of dT_c/dp ranging from 0.21×10^{-5} K/bar to -3.42×10^{-5} K/bar. Crystallographic lattice parameters, ambient pressure T_c and computed volume dependences of the

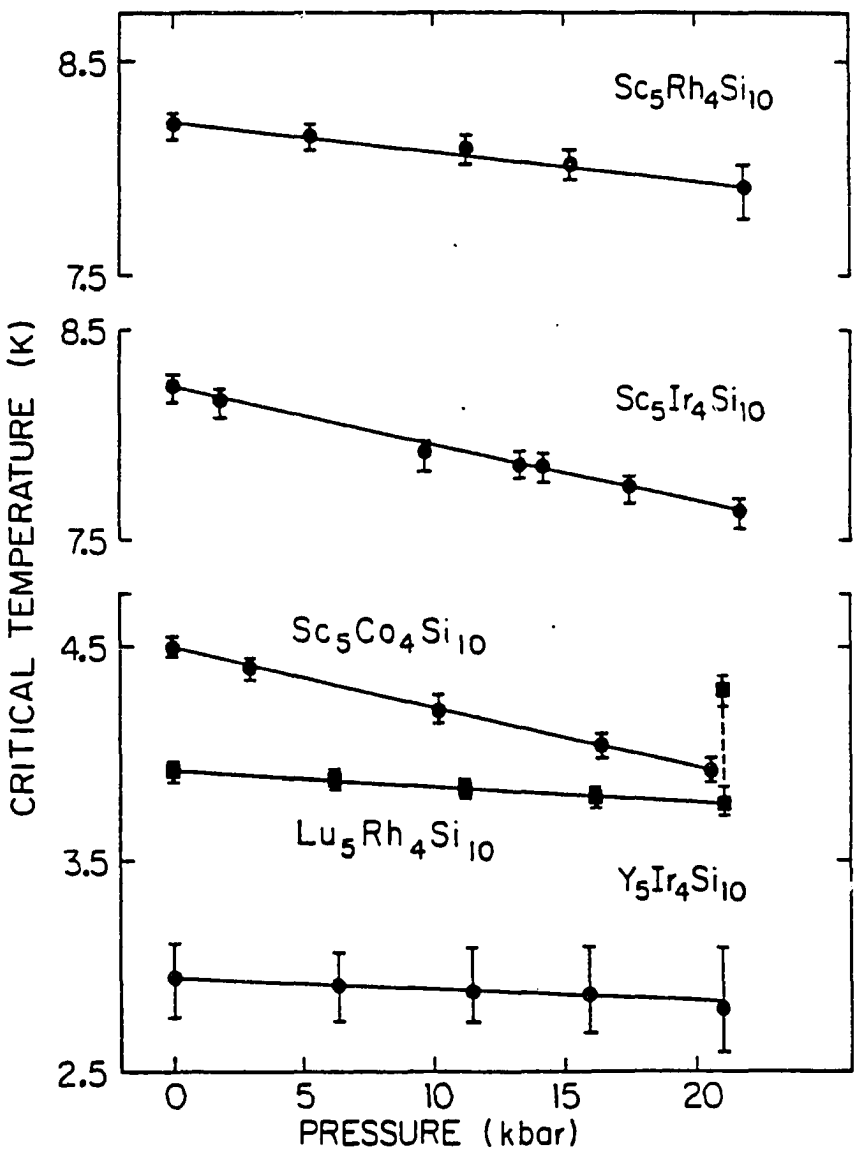

Fig. 4. Pressure dependence of the superconducting transition temperature for five ternary silicides with the $Sc_5Co_4Si_{10}$ -type structure. Error bars indicate 10%-90% transition widths. Lines are least squares fits to the data. $Lu_5Rh_4Si_{10}$ has undergone a partial transformation to a higher T_c at the highest pressure

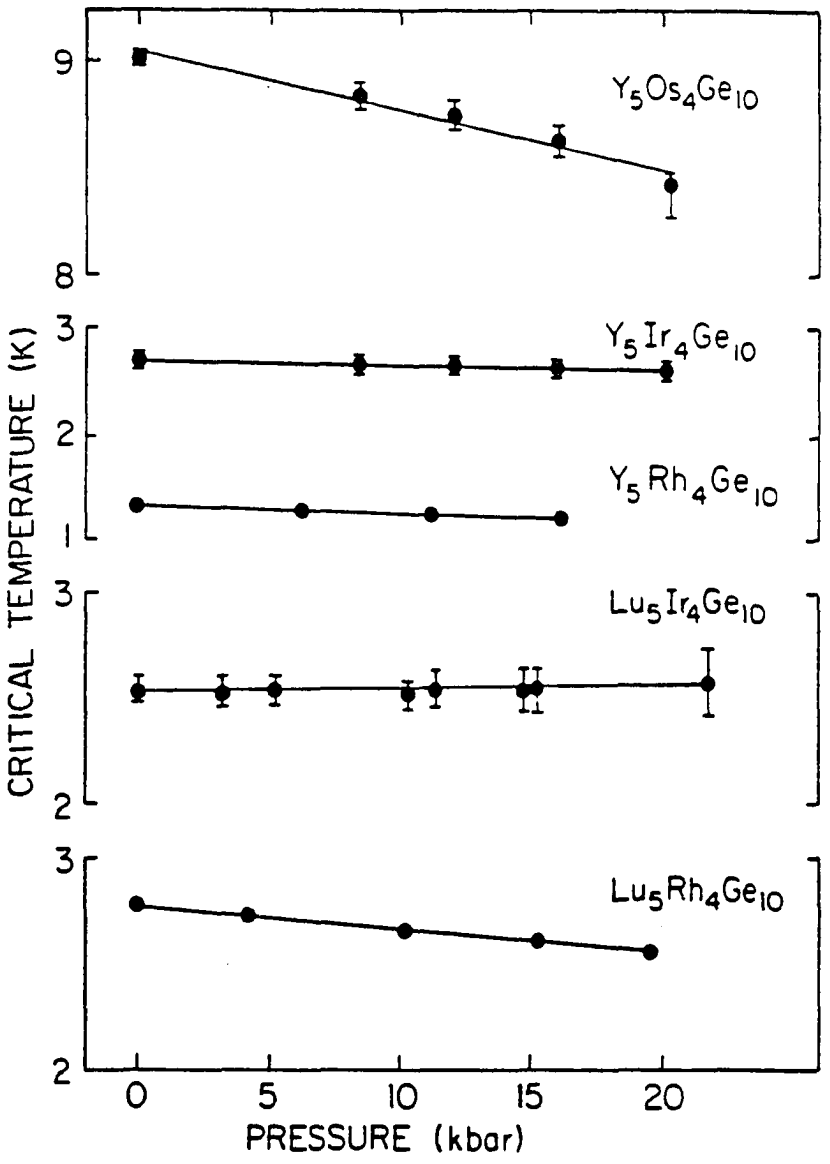

Fig. 5. Pressure dependence of the superconducting transition temperature for five ternary germanides with the $Sc_5Co_4Si_{10}$-type structure. Error bars indicate 10%-90% transition widths. Lines are least squares fits to the data

attractive electron-phonon interaction parameter are also presented in Table 1.

In order to examine the volume effect on T_c, we begin with an expression for T_c based on the standard electron-phonon interaction[7]

$$T_c = \Theta\, e^{-1/g} \tag{3}$$

where Θ is an average phonon frequency and g is the net attractive electron-electron interaction parameter which gives rise to superconductivity and depends on the repulsive Coulomb parameter μ^* and the attractive electron-phonon parameter λ. The general form of Eq. (3) has been retained in subsequent refinements of the BCS theory.[41,64,65] A successful specific form for Θ and g was given by McMillan[41] based on a solution at the Eliashberg equations for the spectrum of Nb and yields

$$\Theta = \Theta_D/1.45 \; ; \quad g = \frac{\lambda - \mu^*(1+0.62\lambda)}{1.04(1+\lambda)} \tag{4}$$

where Θ_D is the Debye temperature. Utilizing this form, the volume dependence of T_c may be written in terms of the Grüneisen parameter $\gamma_G = -\, d\ln\Theta_D/d\ln V$ and the volume dependence of λ by differentiating Eq. (3) and taking $d\mu^*/dV = 0$:

$$-\frac{B}{T_c}\frac{dT_c}{dp} = \frac{d\ln T_c}{d\ln V} = -\gamma + \ln\left(\frac{\Theta_D}{1.45T_c}\right)\left[\frac{\lambda(1+0.38\,\mu^*)}{(1+\lambda)[\lambda-\mu^*(1+0.62\lambda)]}\right]\frac{d\ln\lambda}{d\ln V}, \tag{5}$$

where B is the bulk modulus. We employ Eq. (5) to compute the values of $d\ln\lambda/d\ln V$ listed in Table 1. In addition to our measured values of dT_c/dp, we take the experimental bulk modulus of 1370 ± 70 kbar[57] for $Lu_5Ir_4Si_{10}$ below any pressure-induced transformation and typical transition metal values[66] for γ_G of 2±1 and for $\mu^* = 0.10$. Values for λ

Table 1. Pressure effects on the $Sc_5Co_4Si_{10}$-type superconductors

Compound	a (Å)	c (Å)	$T_c(0)$[a] (K)	dT_c/dp (10^{-5} K/bar)	Θ_D[b] (K)	$d\ln\lambda/d\ln V$
$Sc_5Co_4Si_{10}$	12.010(1)	3.936(5)	4.53-4.46	-2.70±0.04	580	2.3±0.3
$Sc_5Rh_4Si_{10}$	12.325(6)	4.032(3)	8.27-8.16	-1.53±0.04	450	1.5±0.3
$Sc_5Ir_4Si_{10}$	12.316(5)	4.076(3)	8.29-8.16	-2.56±0.04	400	2.2±0.3
$Y_5Ir_4Si_{10}$	12.599(8)	4.234(5)	3.10-2.76	-0.62±0.04	390	1.1±0.3
$Lu_5Rh_4Si_{10}$	12.502(2)	4.137(1)	3.95-3.87	-0.70±0.04	320	1.2±0.3
$Lu_5Ir_4Si_{10}$	12.475(8)	4.171(4)	3.91-3.84	-0.98±0.04	370	1.5±0.3
$Y_5Rh_4Ge_{10}$	12.953(3)	4.272(2)	1.35-1.34	-0.86±0.04	370	2.0±0.3
$Y_5Ir_4Ge_{10}$	12.927(5)	4.308(5)	2.76-2.71	-0.59±0.04	360	1.2±0.3
$Y_5Os_4Ge_{10}$	13.006(5)	4.297(5)	9.06-8.99	-3.42±0.04	270	2.9±0.3
$Lu_5Rh_4Ge_{10}$	12.850(8)	4.208(3)	2.79-2.76	-1.07±0.04	310	1.8±0.3
$Lu_5Ir_4Ge_{10}$	12.831(8)	4.252(3)	2.60-2.49	0.21±0.04	300	0.2±0.3

[a]Values represent 10% - 90% transition width.

[b]Data are taken from reference 58.

are obtained from Eqs. (3) and (4) using the experimental T_c's. Debye temperatures are known from low temperature heat capacity measurements.[67] Our calculated values of $d\ln\lambda/d\ln V$ fall between zero and three, with the majority in the range of 1.7 ± 0.6, while the corresponding values of $\phi = d\ln g/d\ln V$ lie between 0.2 and 2. These values of ϕ support the assumption that d-band electrons make an important contribution to the occurrence of superconductivity in this class of compounds.[68] This is true in spite of fact that the $Sc_5Co_4Si_{10}$-type structure does not contain any direct transition metal-transition metal bonds, in contrast to other well-studied ternary superconducting systems such as the Chevrel phases[55] and the rare earth transition metal borides.[56]

2. Superconductivity in the pseudoternary systems $(Lu_{1-x}R_x)_5Ir_4Si_{10}$ and $Lu_5(Ir_{1-x}T_x)_4Si_{10}$

The most remarkable effect of pressure on the superconducting state of these materials occurs for the compound $Lu_5Ir_4Si_{10}$ and is apparent in the data of Fig. 6. For two distinct samples, we observe a discontinuous, but reversible increase in T_c from a value of 3.7 K to a value in excess of 9 K. The complete reversibility of this transformation from low T_c to high T_c material is illustrated by the order in which the data were taken. For one sample at one specific pressure (point #7), there are two discrete transitions separated by more than 5 K indicating that only a portion of the sample has transformed. This is similar to the $Lu_5Rh_4Si_{10}$ sample shown in Fig. 4. The partial transformation to the high T_c phase may be attributed to a

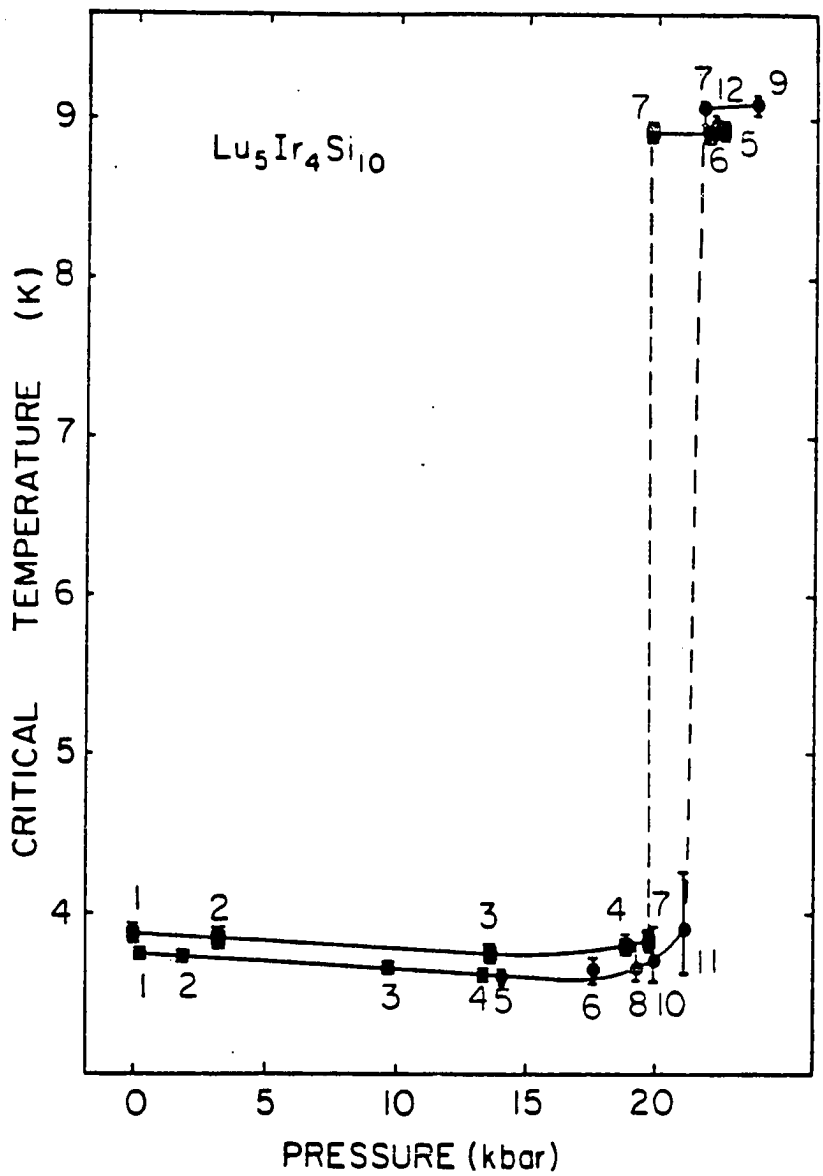

Fig. 6. Pressure dependence of the superconducting transition temperature for two samples of $Lu_5Ir_4Si_{10}$. Error bars indicate 10%-90% transition widths. Numbers next to the data points represent the order in which the data were taken for each sample and demonstrate the reversible nature of the pressure-induced transformation at approximately 21 kbar

small composition variations within a sample which are present in bulk samples, even following the annealing process. Assuming the critical pressure, p_c, varies with composition, there will be a small, but finite range of transformation pressures for each sample. The sharp transformation observed for each sample attests to its uniform composition, especially when compared to the difference (~ 1 kbar) in p_c between the two samples which is probably also due to a slight composition difference. A second factor which could broaden the transition into the high T_c phase is a pressure gradient within the high pressure cell estimated to be < 1 kbar.

The exact nature of this pressure-induced transformation and the reason for its dramatic effect on superconductivity are yet to be determined. Data for the compression of an indium-jacketed $Lu_5Ir_4Si_{10}$ sample at two temperatures are shown in Fig. 7. The total length of jacketed sample at p = 1 bar was 6.35 mm, while the equivalent length of the $Lu_5Ir_4Si_{10}$ sample was 2.44 mm for the 6.35 mm diameter sample holder. The change in sample length between 293 K and 14.3 K in Fig. 7 is due primarily to the thermal expansion of the indium jacket. The size of the data points which are shown corresponds to $\pm$ 5 x 10^{-4} V_o, where V_o is the volume of the $Lu_5Ir_4Si_{10}$ sample. The smoothness of the data suggests that if a transition occurs in this pressure region, the relative volume change, $\Delta V/V_o$, associated with it must be of the order of or smaller than 10^{-3} (0.1%). The isothermal bulk modulus determined in these measurements is 1370 $\pm$ 70 kbar, independent of temperature. Two additional sets of data taken at 201 K and 100 K are similarly featureless. We note that the lowest temperature of 14.3 K for these

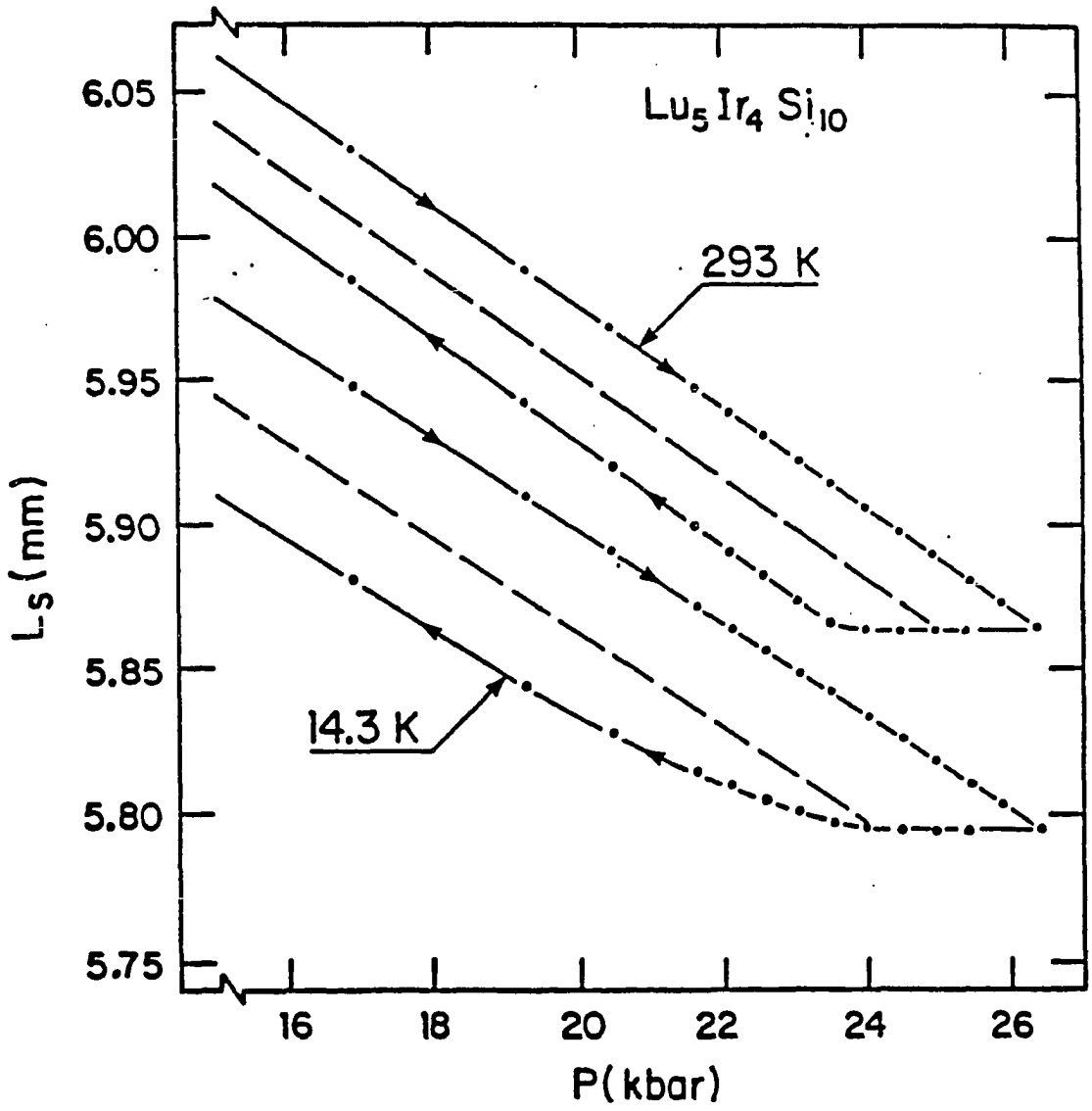

Fig. 7. Actual experimental data for the compressions of an indium-jacketed $Lu_5Ir_4Si_{10}$ sample at two temperatures in a piston-displacement experiment; the hysteresis loop is due primarily to friction effects in the apparatus

measurements is close to the high T_c of 9.1 K and that the maximum pressure of 26 kbar considerably exceeds p_c. Since the high sensitivity of this experiment would reveal a relative volume change of $\Delta V/V_o \sim 0.1\%$, these data provide strong evidence that the effect on T_c is electronically driven with no major change in the cohesive energy of the crystal.

Results of two alloy studies on $(Lu_{1-x}Sc_x)_5Ir_4Si_{10}$ and $Lu_5(Ir_{1-x}Rh_x)_4Si_{10}$ shown in Fig. 8 provide additional evidence as to the origin of this transfomation. A rapid initial increase in T_c occurs with the substitution of either Sc or Rh into $Lu_5Ir_4Si_{10}$, regardless of whether the other end member in the series has a higher T_c than $Lu_5Ir_4Si_{10}$. We have also observed a similar enhancement of T_c when Ir is replaced by Co. These data indicate that the ambient pressure T_c of $Lu_5Ir_4Si_{10}$ is depressed from an expected value based on its isostructural neighbor compounds. Powder X-ray diffraction experiments performed down to 21 K reveal no detectable deviation from the primitive tetragonal symmetry observed at room temperature, thus reducing the possibility of a crystallographic phase transformation. The non-linear behavior of T_c versus composition for both curves in Fig. 8 occurs while the room temperature lattice parameters and unit cell volume for the $(Lu_{1-x}Sc_x)_5Ir_4Si_{10}$ shown in Fig. 9 follow Vegard's law. The question remains: Why is the T_c of $Lu_5Ir_4Si_{10}$ so low?

A comparison between the volume dependence of T_c in these alloys and the volume dependence of T_c for $Lu_5Ir_4Si_{10}$ due to external pressures is shown in Fig. 10. The sharp jump in T_c due to pressure which occurs at critical volume of about $V_c \sim 639$ Å^3 is smeared into a broader curve

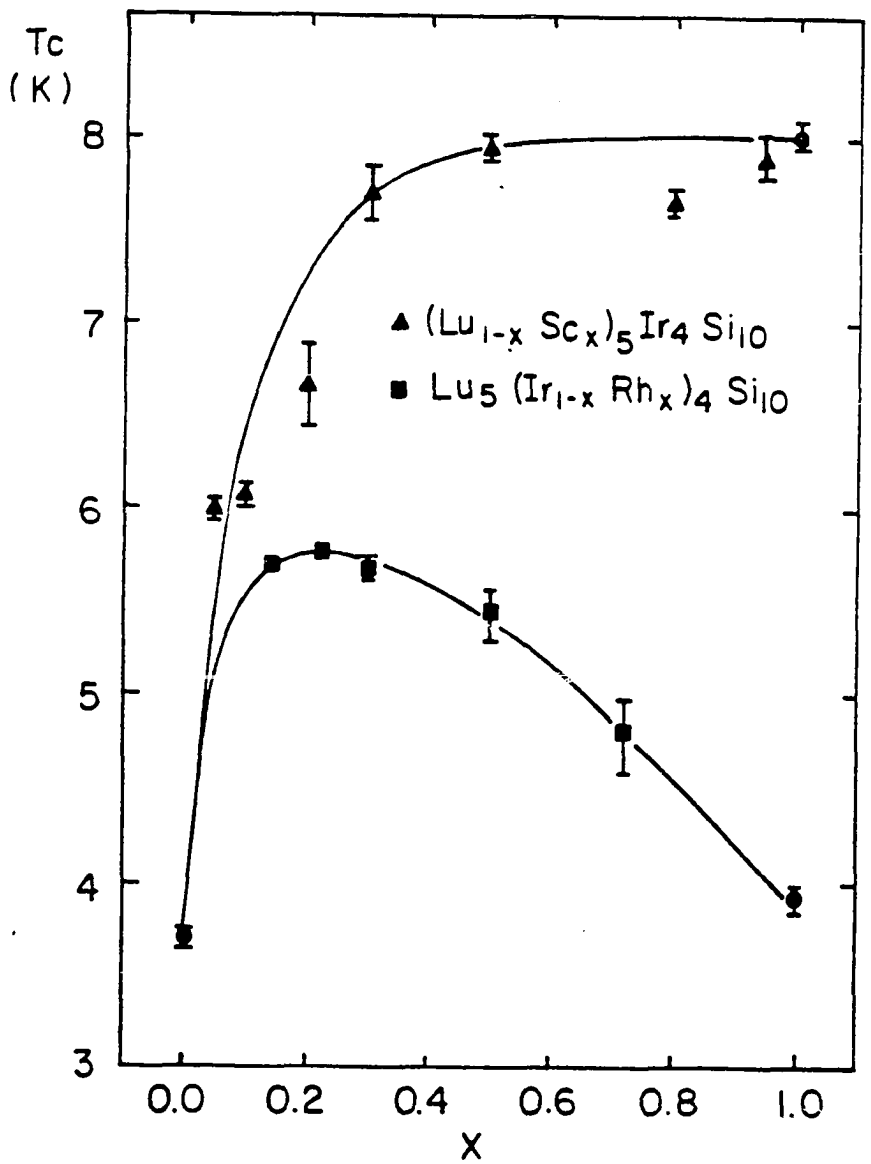

Fig. 8. Superconducting transition temperature versus alloy concentration for the pseudoternary systems: $(Lu_{1-x}Sc_x)_5Ir_4Si_{10}$ and $Lu_5(Ir_{1-x}Rh_x)_4Si_{10}$. Error bars indicate 10%-90% transition widths. Lines are drawn as a guide to the eye

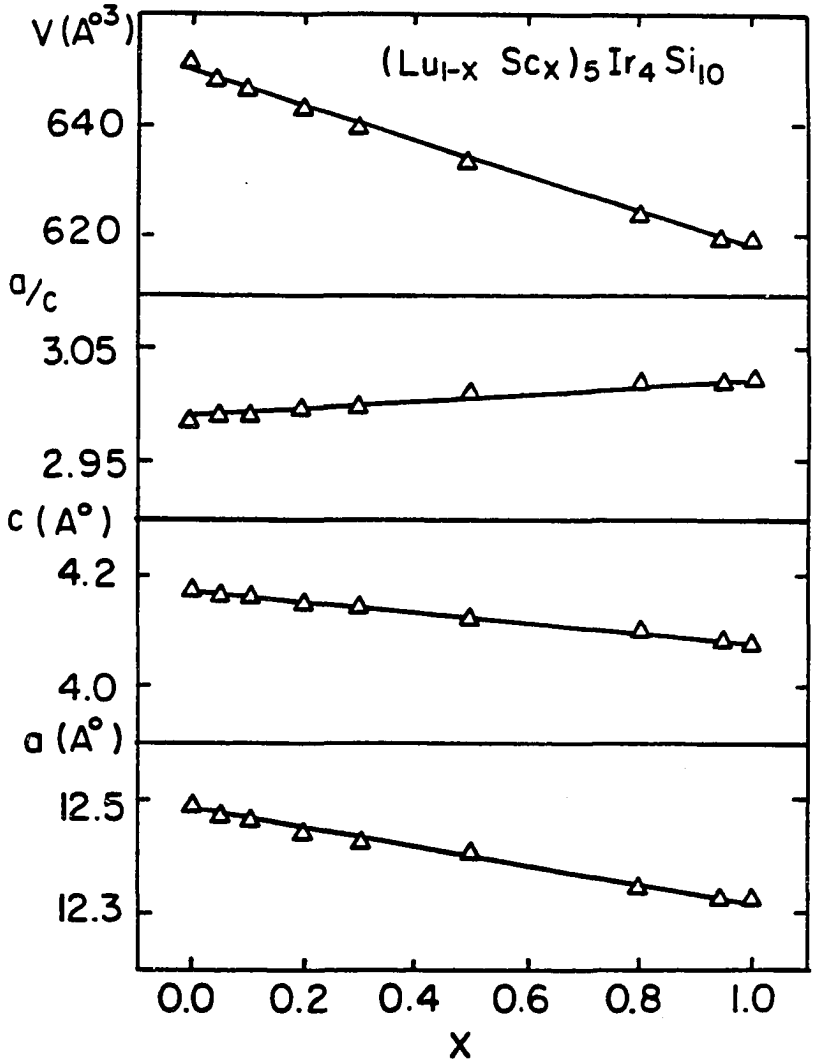

Fig. 9. Lattice parameters, a/c, and unit cell volume versus alloy concentration for the pseudoternary system $(Lu_{1-x}Sc_x)_5Ir_4Si_{10}$. Error bars are included in the symbols

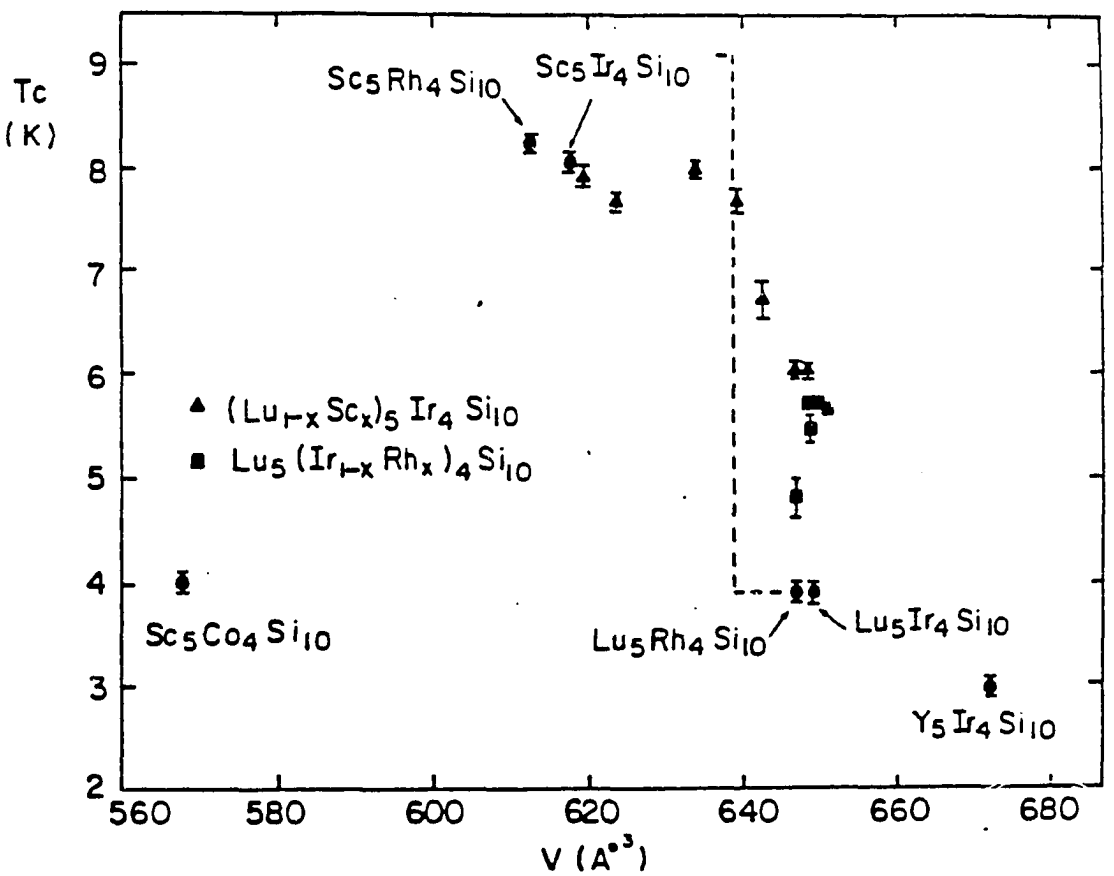

Fig. 10. Superconducting transition temperature versus unit cell volume for ternary silicides with the $Sc_5Co_4Si_{10}$-type structure. Error bars represent 10%-90% transition widths. Data for two pseudoternary series are given the same symbols as in Fig. 8. The dashed line indicates the behavior of T_c under pressure for the pure ternary $Lu_5Ir_4Si_{10}$ (see Fig. 6)

when volume changes are caused by alloying on the rare earth sublattice. Application of hydrostatic pressure is a particularly clean method of obtaining a volume reduction since no atomic disorder or chemical effects are introduced. In the case of the pseudoternary alloys, although T_c is ultimately limited by the values of the end member compounds ($Sc_5Ir_4Si_{10}$ and $Lu_5Rh_4Si_{10}$), the critical temperature does increase rapidly at low concentration, consistent with minimal disorder being favorable for higher T_c values. This broadening effect is evident by comparing the $(Lu_{1-x}Sc_x)_5Ir_4Si_{10}$ data to the pressure enhanced T_c of the pure $Lu_5Ir_4Si_{10}$ in Fig. 10. The sharp increase in $T_c(p)$ of $Lu_5Ir_4Si_{10}$ at V_c is smeared into a broader curve of T_c versus V in the alloy system. The difference in T_c at V_c between the pressure-induced high T_c state of $Lu_5Ir_4Si_{10}$ and alloy $(Lu_{0.7}Sc_{0.3})_5Ir_4Si_{10}$ is approximately 1.4 K and provides a rough measure of the effect of sublattice disorder on optimizing T_c.

The pressure dependence of T_c for $(Lu_{1-x}Sc_x)_5Ir_4Si_{10}$ system is shown in Fig. 11. A couple of facts from the graph can be pointed out.

(1) The compounds can be separated into two groups. At low concentration (x = 0.05, 0.1, 0.2) of Sc, the T_c's are lower and enhanced by external pressure. At high concentration (x = 0.3, 0.5, 0.95, 1.0) of Sc, the T_c's are higher and depressed by external pressure. However, there is a trend for T_c's to go to a certain limiting value of about 7 K at high pressure.

(2) $x \simeq 0.3$ is a critical value. Below this the phases exhibit an electronic intability and are sensitive to external pressure. This is consistent with data shown in Fig. 9, where the volume of x = 0.3

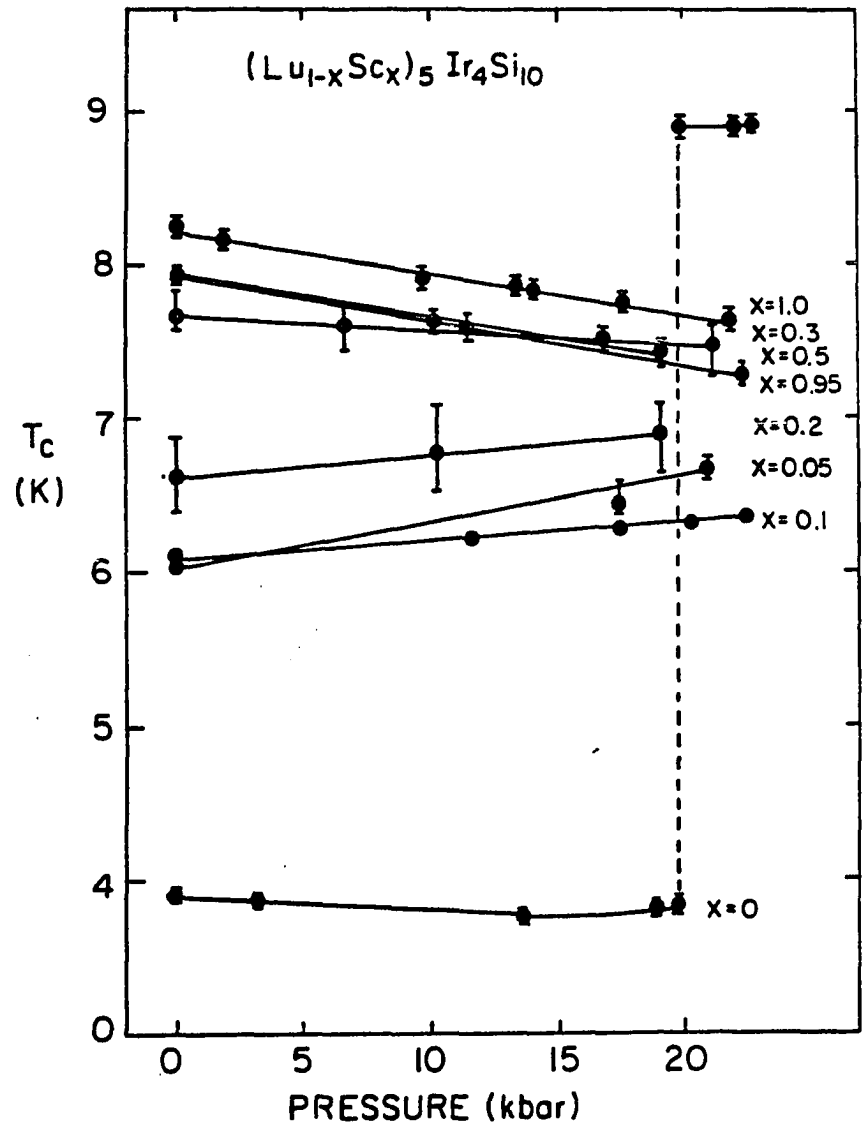

Fig. 11. Pressure dependence of superconducting transition temperature for the pseudoternary system $(Lu_{1-x}Sc_x)_5Ir_4Si_{10}$. Lines are least squares fits to the data. Error bars indicate 10%-90% transition widths

sample at ambient pressure is about the same as that of x = 0 sample at 20 kbar.

(3) It is surprising that no sudden jump in T_c is observed up to 21 kbar even at very low concentration (x = 0.05). This means that the nature of the pressure-induced phase transformation in $Lu_5Ir_4Si_{10}$ is more likely an electronic type and very easily destroyed by nn impurity effect.

The pressure effects on superconductivity for some alloys related to $Lu_5Ir_4Si_{10}$ are summarized in Table 2. We have to note that the T_c and pressure-induced effect of T_c are almost independent of stoichiometry of samples. The alloying of magnetic rare earths to the Lu site suppresses the T_c following the A-G theory[69] quite well, but pressure-induced T_c effects are still observed at around 20 ~ 22 kbar and T_c jumps (ΔT_c) are almost the same (about 5 K) even for the low T_c = 1 K in $(Lu_{.9}Dy_{.1})_5Ir_4Si_{10}$. Substituting 10% of Th for Lu, enhances T_c both at ambient and high pressures. This may be due to the different valence between Th (4^+) and Lu (3^+).

It will be interesting to understand the superconducting properties of $Lu_5Ir_4Si_{10}$ under high pressure compared with those at ambient pressure. Instead of measuring heat capacity and static magnetic susceptibility under high pressure, we take two pseudoternary samples $(Lu_{.98}Sc_{.02})_5Ir_4Si_{10}$ and $Lu_5(Ir_{.78}Rh_{.22})_4Si_{10}$ to study the upper critical field. The former is strongly enhanced in T_c (ΔT_c ~ 2 K) at a very low concentration of Sc, while the latter has the highest T_c in its pseudoternary system. The upper critical fields for $(Lu_{.98}Sc_{.02})_5Ir_4Si_{10}$ and $Lu_5(Ir_{.78}Rh_{.22})_4Si_{10}$ as well as those of the end members $Sc_5Ir_4Si_{10}$, $Lu_5Ir_4Si_{10}$, and $Lu_5Rh_4Si_{10}$[58] are shown in Fig.

Table 2. Pressure effects on pseudoternary superconductors

Material	$T_c(0)$ (K)	p_c (kbar)	ΔT_c (K)	dT_c/dp (10^{-5} K/bar)	T_o (K)
$Lu_{5.5}Ir_4Si_{10}$	3.72	20.5	5.4	-1.17	81
$Lu_{4.5}Ir_4Si_{10}$	4.00	-[a]	-[a]	-[a]	81
$Lu_5Ir_4(Si_{.9}C_{.1})_{10}$	3.74	20.8	5.4	-1.34	82
$(Lu_{.95}Sc_{.05})_5Ir_4Si_{10}$	6.06	-[b]	-[b]	3.14	-[b]
$(Lu_{.9}Sc_{.1})_5Ir_4Si_{10}$	6.09	-[b]	-[b]	1.23	-[b]
$(Lu_{.8}Sc_{.2})_5Ir_4Si_{10}$	6.54	-[b]	-[b]	1.76	-[b]
$(Lu_{.7}Sc_{.3})_5Ir_4Si_{10}$	7.64	-[b]	-[b]	-0.59	-[b]
$(Lu_{.5}Sc_{.5})_5Ir_4Si_{10}$	7.90	-[b]	-[b]	-2.60	-[b]
$(Lu_{.2}Sc_{.8})_5Ir_4Si_{10}$	7.68	-[b]	-[b]	-3.11	-[b]
$(Lu_{.05}Sc_{.95})_5Ir_4Si_{10}$	7.95	-[b]	-[b]	-2.91	-[b]
$(Lu_{.9}Y_{.1})_5Ir_4Si_{10}$	3.90	20.2	5.0	0.22	73&270
$(Lu_{.9}Th_{.1})_5Ir_4Si_{10}$	4.88	-[b]	-[b]	5.10	105
$(Lu_{.9}Tm_{.1})_5Ir_4Si_{10}$	2.84	23.4	5.0	-1.93	86
$(Lu_{.9}Er_{.1})_5Ir_4Si_{10}$	2.74	23.1	5.4	-1.34	82
$(Lu_{.9}Ho_{.1})_5Ir_4Si_{10}$	1.89	20.8	5.4	-1.34	82
$(Lu_{.9}Dy_{.1})_5Ir_4Si_{10}$	1.00	20.5	5.3	-0.52	78
$Lu_5(Ir_{.86}Rh_{.14})_4Si_{10}$	5.72	-[b]	-[b]	3.04	-[b]
$Lu_5(Ir_{.78}Rh_{.22})_4Si_{10}$	5.68	-[b]	-[b]	1.10	-[b]
$Lu_5(Ir_{.95}Co_{.05})_4Si_{10}$	5.52	-[b]	-[b]	3.38	-[b]

[a]Represents no datum.

[b]Not observed in the measurements.

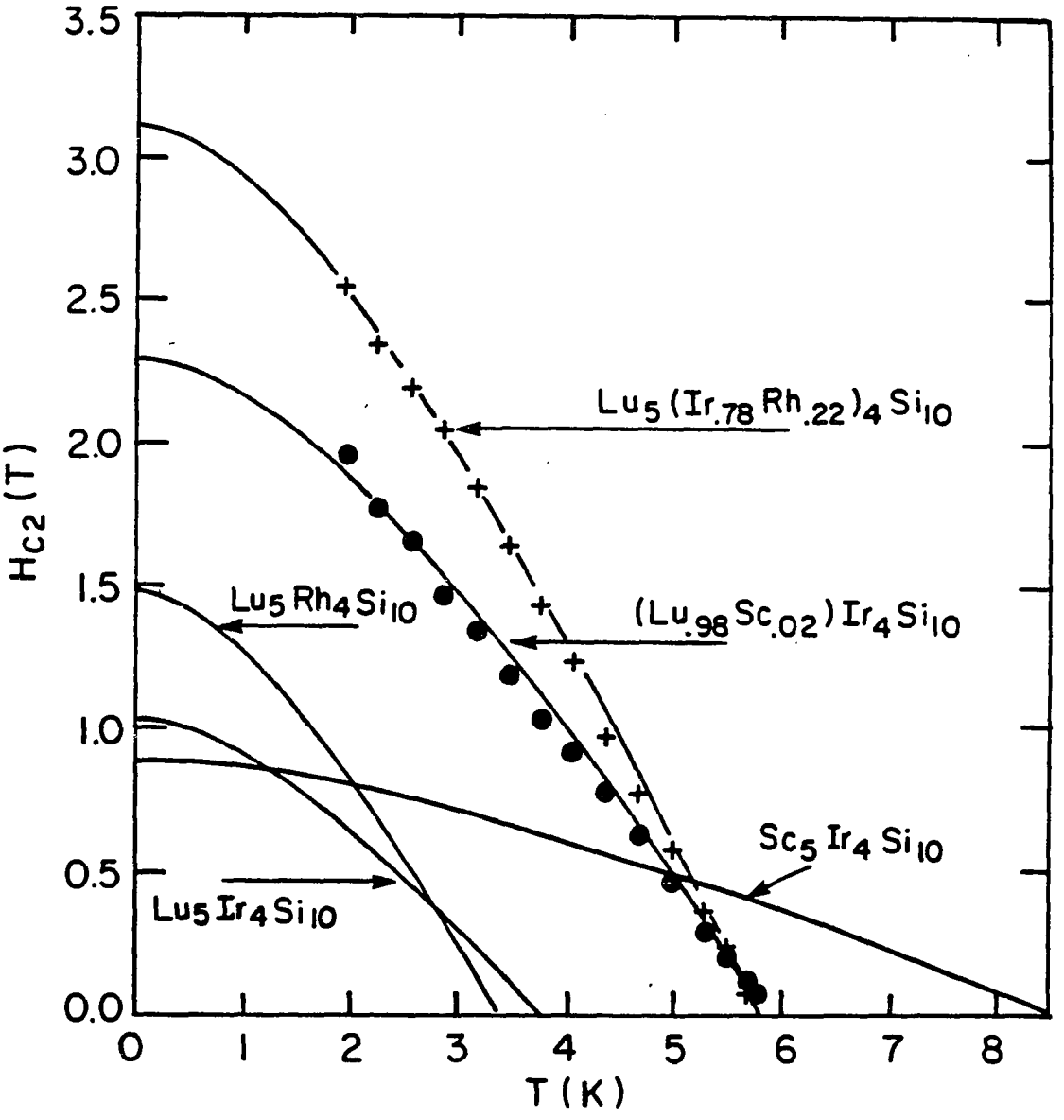

Fig. 12. Upper critical field for $Lu_5(Ir_{.78}Rh_{.22})_4Si_{10}$, $(Lu_{.98}Sc_{.02})_5Ir_4Si_{10}$, $Sc_5Ir_4Si_{10}$, $Lu_5Rh_4Si_{10}$, and $Lu_5Ir_4Si_{10}$. The last three data are taken from ref. 58. Solid lines are fit to the WHHM theory

12. The data were analyzed using the WHHM theory[70,71,72] in the dirty limit[73] (short mean free path).

$$\alpha = 5.28 \times 10^{-5} \left[- \frac{dH_{c2}}{dT} \right]_{T=T_c} \tag{6}$$

$$\left[- \frac{dH_{c2}}{dT} \right]_{T=T_c} = 4.48 \times 10^{4} \gamma_{cal} \rho_{res} \tag{7}$$

where the Maki parameter α is in units of Oe/K, γ_{cal} is the calculated electronic contribution to the normal state heat capacity with units of erg/cm^3-K^2, and ρ_{res} is the residual resistivity in Ω-cm. The values at T = 0 K of the Ginzburg-Landau (GL) coherence length ξ_{GL}, the GL penetration depth λ_{GL}, and GL parameter κ were calculated (in units of cm) by the following relations[71]

$$\xi_{GL} = 8.57 \times 10^{-7} (\gamma_{cal} \rho_{res} T_c)^{-1/2} (1-t)^{-1/2} \tag{8}$$

$$\lambda_{GL} = 6.42 \times 10^{-3} \left(\frac{\rho_{res}}{T_c}\right)^{-1/2} (1-t)^{-1/2} \tag{9}$$

$$\kappa_{GL} = 7.49 \times 10^{3} \gamma_{cal}^{1/2} \rho_{res} \tag{10}$$

where $t = T/T_c$. The results are listed in Table 3.

For $(Lu_{.98}Sc_{.02})_5Ir_4Si_{10}$, the $H_{c2}(0)$, $-(dH_{c2}/dT)_{T=T_c}$, and γ_{cal} are larger than those of two end members. Therefore, the enhancement of T_c is mainly due to the enhancement in the electronic density states at the Fermi level. For $Lu_5(Ir_{.78}Rh_{.22})_4Si_{10}$, even though T_c, $H_{c2}(0)$, and $(dH_{c2}/dT)_{T=T_c}$ are larger than those of two end members, γ_{cal} and ξ_{GL} are smaller than those of $Lu_5Rh_4Si_{10}$ due to the larger ρ_{res} caused by the comparable atomic disorder effects. Thus the enhancement of T_c may be caused by the enhancement of the electron-phonon interaction.

Table 3. Upper critical magnetic field parameters for some $R_5T_4Si_{10}$ compounds

Compound	T_c (K)	ρ_{res} ($\mu\Omega$-cm)	$H_{c2}(0)$ (Tesla)	α (Oe/K)	$-(dH_{c2}/dT)_{T=T_c}$[a] (T/K)	γ_{cal} (erg/cm^3-K^2)	γ_{cal} (mJ/mol-K^2)	ξ_{GL} (Å)	λ_{GL} (Å)	κ_{GL}
$Sc_5Ir_4Si_{10}$[b]	8.23	75	0.90	0.08	0.15	446.4	8.4	150	1920	11.9
$Lu_5Rh_4Si_{10}$[b]	3.91	160	1.48	0.34	0.64	892.9	17.4	115	4110	35.8
$Lu_5Ir_4Si_{10}$[b]	3.88	195	1.04	0.21	0.39	446.4	8.8	160	4550	30.9
$(Lu_{.98}Sc_{.02})_5Ir_4Si_{10}$	5.90	193	2.30	0.30	0.57	659.0	12.9	100	3670	37.1
$Lu_5(Ir_{.78}Rh_{.22})_4Si_{10}$	5.80	325	3.12	0.41	0.78	535.7	10.5	85	4810	56.3

[a]These values were obtained from a fit of the data to the WHHM theory.

[b]These data were derived from Ref. 58.

C. Conclusion

From the analysis of the pressure effects on T_c for eleven $Sc_5Co_4Si_{10}$-type superconducting compounds, we conclude that the d-band electrons make an important contribution to the occurrence of superconductivity in this class of compounds and that normal lattice stiffening effects are prominent for the linear depression of T_c with pressure. A dramatic and discontinuous increase in T_c at pressure around 20 kbar for $Lu_5Ir_4Si_{10}$ and $Lu_5Rh_4Si_{10}$ were observed. The mechanism responsible for this huge effect is not yet well-understood. A certain kind of electronic instability is indicated by alloy studies. Several questions remain unanswered. We believe that a crystal stucture determination at low temperature under high pressure and an electronic energy band structure calculation would be of great value in understanding the anomalous pressure effect on T_c in these two materials.

IV. ANOMALOUS ELECTRONIC PHASE TRANSITION IN $Lu_5Ir_4Si_{10}$ AND $Lu_5Rh_4Si_{10}$: POSSIBILITY OF NEW CDW SUPERCONDUCTORS

A. Introduction

Since the discovery[74] of a sudden striking enhancement of the superconducting transition temperature T_c from 3.8 to 9 K in $Lu_5Ir_4Si_{10}$ at a critical pressure of about 20 kbar, several efforts have also been made to try to answer the questions: What is the nature of this phase transition? What kind of mechanism should be responsible for this dramatic pressure effect on T_c? For instance, results of pressure effect and volume dependence on T_c in $(Lu_{1-x}Sc_x)_5Ir_4Si_{10}$, $Lu_5(Ir_{1-x}Rh_x)_4Si_{10}$, and $(Lu_{.9}R_{.1})_5Ir_4Si_{10}$ (R = Dy, Ho, Er, Tm, and Th) pseudoternaty systems, low temperature (down to 21 K) powder X-ray diffraction experiments[74], and isothermal bulk modulus measurement[57] (taken up to 26 kbar at four different temperatures ranging from 293 to 14 K) indicate that the tranformation responsible for this enormous pressure enhancement of T_c is probably electronic in nature with no major effect on the cohesive energy of the crystal.

With few exceptions, the pressure effect on the elements, binary compounds, and alloys are nearly linear and small (typical values are $dT_c/dp \sim 10^{-5}$ K/bar). In Table 4, we summarize the compounds with either an extremely large dT_c/dp value (at least 10 times larger than typical value) or an almost discontinuous increase in T_c under pressure for some selected binary and ternary systems. Even though some of them are still not well understood in nature, a couple of different kinds of

Table 4. T_c at p=0 and dT_c/dp for some selected compounds

Compound	$T_c(0)$ (K)	dT_c/dp (10^{-5} K/bar)	Ref.
La_3Se_4	7.6	30[a]	75
$Cu_2Mo_6Se_8$	1.7	1.7-6.4 K / 1-3 kbar[b]	76
$Cu_3Mo_6S_8$	6.4	6.5-10.5 K / 5-10 kbar[b]	77
$EuMo_6S_8$	-[c]	sudden jump to 12.2 K at 13 kbar	78
$AgMo_6Se_8$	5.8	150[a]	79
$AuGa_2$	1.2	1.4-2 K / at 6 kbar[b]	80,81
$NbSe_3$	-[c]	sudden jump to 2.5 K at 7 kbar	82
2H-$NbSe_2$	7.1	33[a]	83
$Y_2Fe_3Si_5$	2.3	33[a]	61
$Lu_5Ir_4Si_{10}$	3.8	3.8-9.1 K / at 20 kbar[b]	74
$Lu_5Rh_4Si_{10}$	3.4	3.3-4.3 K / at 18 kbar[b]	74

[a]Estimated from figure in Ref.

[b]Almost discontinuous increase in T_c at a certain pressure.

[c]Indicates that no T_c is observed to the lowest temperature.

transfomations are considered to be associated with the pressure effect in these materials.

A crystallographic transition was seen in La_3Se_4[75] (cubic to tetragonal at 60 K), $Cu_2Mo_6Se_8$[76] (lattice transformation at 166 K), $Cu_3Mo_6S_8$[77] (lattice transition at 60 K), and $EuMo_6S_8$[78] (rhombohedral to triclinic at 109 K). Application of pressure tends to suppress the structural instability and a higher T_c phase is stabilized at low temperature. The origins of the spectacular pressure enhancement of T_c in $AgMo_6S_8$ are not yet clear,[79] however, similar to the cases of $Cu_2Mo_6Se_8$ and $Cu_3MO_6S_8$, a lattice instability is suspected.

An electronic transition was thought to be the origin of the nearly discontinuous change in T_c of $AuGa_2$ near 6 kbar.[80] An abrupt change in the Fermi surface topology was suggested[81] as the cause of this behavior. That is to say, a high density-of-states peak is located immediately below the Fermi energy at normal volume. Application of pressure results in moving the Fermi level into the sharp peak of density-of-states thus raising the T_c.

The pressure enhancement of T_c in $NbSe_3$[82] and 2H-$NbSe_2$[83] is mainly due to the progressive removal of the charge density waves (CDW), which lower the T_c when present in the crystal.

$Y_2Fe_3Si_5$[61] shows a dramatic initial increase of T_c which doubles its value at 15 kbar before it decreases at higher pressure. The variation of resistivity with pressure for this compound shows no evidence for any crystallographic transformation. A detailed low temperature X-ray study is needed to investigate the possible origin for this pressure effect of this material.

Preliminary data indicate that the pressure-induced phase transition in $Lu_5Ir_4Si_{10}$ and $Lu_5Rh_4Si_{10}$ is probably due to the formation of charge density waves in the solids. Measurements of static magnetic susceptibility and electical resistivity as a function of temperature exhibit a remarkable anomaly in $Lu_5Ir_4Si_{10}$ at 83 K and $Lu_5Rh_4Si_{10}$ at 155 K. Doping, pressure, as well as electrical field effects have been carried out on the polycrystalline samples of these compounds to support our hypothesis.

B. Results and Discussion

1. Electrical resistivity and static magnetic susceptibility

The normalized resistivity as a function of temperature between 2.6 and 300 K for $Sc_5Ir_4Si_{10}$, $Y_5Ir_4Si_{10}$, $Lu_5Rh_4Si_{10}$, and $Lu_5Ir_4Si_{10}$ is shown in Fig. 13. $Sc_5Ir_4Si_{10}$ shows a normal metallic behavior through the whole temperature region with a residual resistivity ratio (RRR) $\rho(300\ K)/\rho(4.2\ K) \sim 20$. The other three compounds exhibit an anomaly at $T_o = 250$ K for $Y_5Ir_4Si_{10}$, at 155 K for $Lu_5Rh_4Si_{10}$, and at 83 K for $Lu_5Ir_4Si_{10}$, but with a much smaller RRRs. These anomalies are reproducible by independent samples. In the $Lu_5Ir_4Si_{10}$ compound, the resistivity decreases when the temperature is lowered from 300 K, showing a metallic behavior, but increases sharply at 83 K and reaches a maximum at 78 K before resuming a metallic-type temperature variation. The amplitude of this peak $\Delta\rho$ is about 21% of the room temperature resistivity $\rho(300\ K)$. No obvious thermal hysteresis is detected when we vary the temperature across the transition temperature. A similar

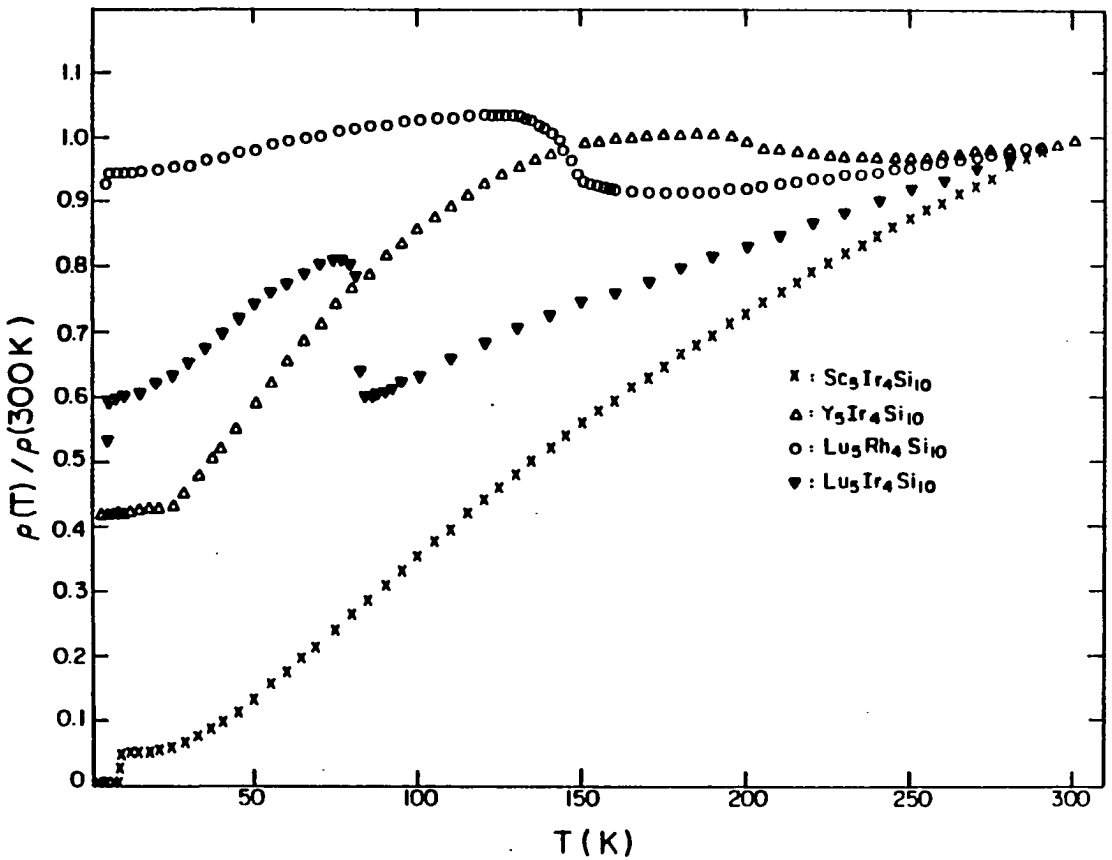

Fig. 13. Normalized resistivity as a function of temperature between 2.6 and 300 K for $Sc_5Ir_4Si_{10}$, $Y_5Ir_4Si_{10}$, $Lu_5Rh_4Si_{10}$, and $Lu_5Ir_4Si_{10}$

behavior is also seen in $Y_5Ir_4Si_{10}$ and $Lu_5Rh_4Si_{10}$ compounds but with a broader, less pronounced (the value of $\Delta\rho/\rho(300\ K)$ is 5% for $Y_5Ir_4Si_{10}$ and 13% for $Lu_5Rh_4Si_{10}$), and higher temperature anomaly. This feature is characteristic of a phase transition associated with an increase in conduction-electron scattering, or the loss of a portion of the Fermi surface. It resembles the type of anomaly one expects from the formation of a CDW or SDW or perhaps a crystallographic transformation. The latter possibility is remote considering the lack of volume discontinuity in the isothermal bulk-modulus measurements. However, as a further check, we performed powder X-ray diffraction experiments down to 21 K which revealed no detectable deviation from the primitive tetragonal symmetry observed at room temperature. In addition, this anomaly in the resistivity is insensitive to applied magnetic fields, showing no measurable shift in a field of 20 kOe.

The effect of this phase transition is also evident in the molar magnetic susceptibility shown in Fig. 14. The size, width, and transition temperature of the anomaly for these four compounds are mutually consistent in magnetic susceptibility and electrical resistivity measurements. For $Lu_5Ir_4Si_{10}$, the data are essentially temperature-independent from 300 K to T_o = 83 K, with a value of $\chi(85\ K) = 0.732 \times 10^{-4}$ emu/mole. At T_o, χ decreases sufficiently over a narrow temperature range to become diamagnetic. The magnetic susceptibility maintains a relatively constant value of $\chi(35\ K) = -0.468 \times 10^{-4}$ emu/mole until an increase at the lowest temperatures causes χ to become positive again. This low-temperature upturn is probably due to the presence of a few ppm of paramagnetic impurity in the sample which is undetectable by our other experiments.

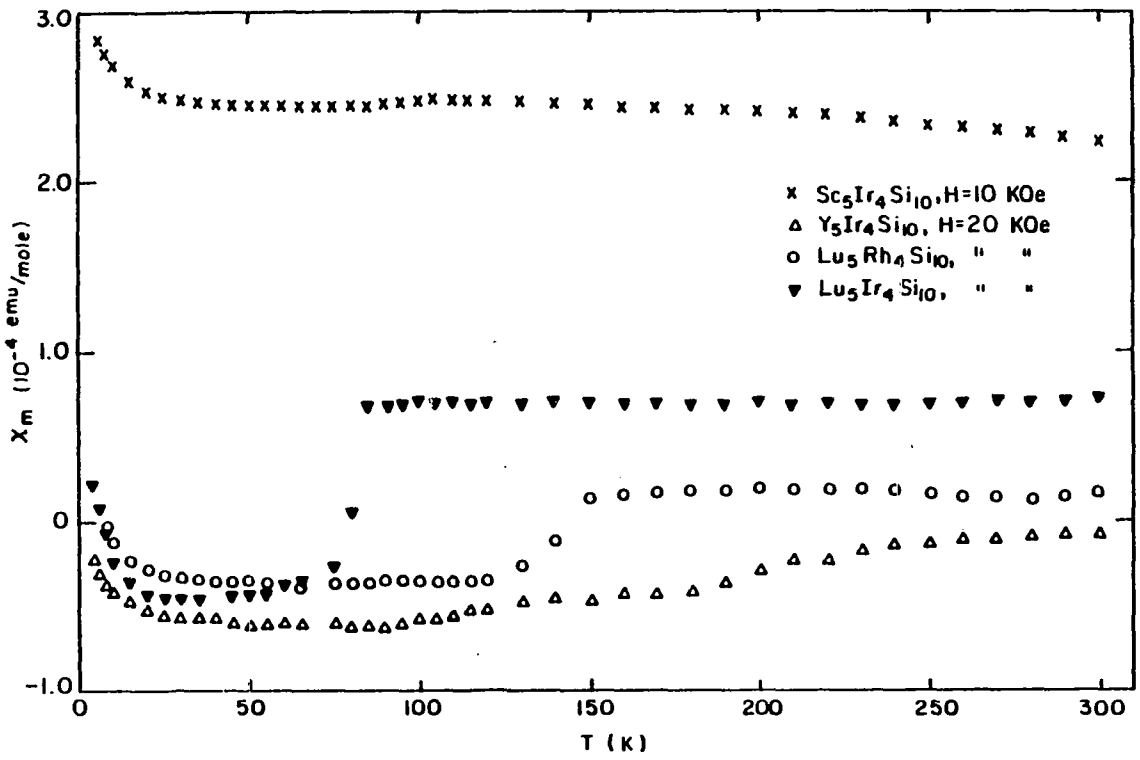

Fig. 14. Molar magnetic susceptibility as a function of temperature between 4 and 300 K for $Sc_5Ir_4Si_{10}$, $Y_5Ir_4Si_{10}$, $Lu_5Rh_4Si_{10}$, and $Lu_5Ir_4Si_{10}$

We analyze this susceptibility data by writing the total temperature- independent part of the susceptibility as,

$$\chi_o = \chi^{core} + \chi^{Pauli} + \chi^{Landau} \qquad (11)$$

where χ^{core} is the core diamagnetism term, χ^{Pauli} is the Pauli paramagnetism due to the conduction electrons and χ^{Landau} is the diamagnetic orbital contribution due to the conduction electrons. The core diamagnetism may be estimated from the tabulated value[84] using Ir^{3+} which yields a value of $\chi^{core} = -2.35 \times 10^{-4}$ emu/mole. Representing the conduction electron band effects by an effective mass, m^*, permits one to relate χ^{Pauli} to χ^{Landau} (ref. 85)

$$\chi^{Landau} = -\frac{1}{3}\left[\frac{m}{m^*}\right]\chi^{Pauli} \qquad (12)$$

$$\chi^{Pauli} = 2\,\mu_B^2\,N_b(0) \qquad (13)$$

where μ_B is the Bohr magneton and $N_b(0)$ is the bare density of states at the Fermi level per spin direction. Combining equations 11, 12, and 13 yields an expression involving the effective mass and density of states; namely,

$$\chi_o - \chi^{core} = \left[\frac{r}{1.545\times10^4}\right]\left[1 - \frac{1}{3}\left(\frac{m}{m^*}\right)^2\right]N_b(0) \qquad (14)$$

In this equation, r is the number of atoms per molecule (r = 19), susceptibilities are expressed in units of emu/mole and the density of states, $N_b(0)$, is given in terms of states/eV-atom-spin. The left side of the equation is known from our experimental data and tabulated values of χ^{core}, while the right side of the equation involves two unknowns

that characterize the electronic state of the compound; namely, m^*/m and $N_b(0)$. Below the phase transformation temperature, T_o = 83 K, we obtain an independent experimental determination of the enhanced density of electronic states at the Fermi level $N^*(0) = N_b(0)[1+\lambda] = N_b(0)[m^*/m]$ from low temperature heat capacity measurements.

The heat capacity data of $Lu_5Ir_4Si_{10}$ were fit to an equation of the form $C = \gamma T + \beta T^3 + \alpha T^5$, where γT is the usual electronic contribution, β is the lattice specific heat coefficient and the αT^5 term accounts for any anharmonicity of the lattice. Utilizing the coefficients γ, we calculate $N^*(0)$, the enhanced density of electronic states at Fermi level, $N^*(0) = 3\gamma/2\pi^2 N_A r k_B^2$, where N_A is the Avogardro number and k_B is the Boltzmann constant. The experimental value of $N^*(0)$ = 0.26 states/eV-atom-spin[58] is used in the analysis below.

The combination of magnetic susceptibility and heat capacity data provides an experimental determination of $N_b(0)$ and $m^*/m = 1+\lambda$ at temperatures below the phase transition. Specifically, we use equation 14 with $\chi_o = \chi(35\ K)$ and heat capacity data that give $N_b(0)[m^*/m]$ = 0.26 states/eV-atom-spin to obtain m^*/m = 1.43 and $N_b(0)$ = 0.18 states/eV-atom-spin for $T < T_o$. This results in a value for the electron-phonon coupling parameter, λ, of 0.43. As a check on this result, we use the formalism of McMillan[41] with μ^* = 0.10 and calculate λ = 0.50 based on calorimetric T_c of 3.77 K. These two values of λ are in reasonable agreement.

As the system goes through the phase transition at T_o = 83 K, we attribute the change in susceptibility at T_o to an increase in $N_b(0)$ and thus an enhanced Pauli susceptibility. We can estimate the new

effective electron mass by noting that the superconducting transition temperature is T_c = 9.1 K when this phase transition is prevented from occurring. Using this value for T_c in the McMillan equation yields $\lambda = 0.66$, or a mass enhancement of $m^*/m = 1.66$ for $Lu_5Ir_4Si_{10}$ when no phase transition occurs. Taking this ratio of m^*/m and using $\chi_o = \chi(85\ K)$ as the experimental value on the left side of equation 14 yields a value of $N_b(0) = 0.28$ states/eV-atom-spin. Therefore, the electronic phase transition which occurs at 83 K is responsible for a 36% reduction in $N_b(0)$ as the sample cools through the transition. This is consistent with the occurrence of a CDW or SDW transition at T_o which opens an energy gap over about 36% of the Fermi surface.

For $Lu_5Rh_4Si_{10}$ and $Y_5Ir_4Si_{10}$, a small decrease in the density of states at the transition would be anticipated because of their much smaller anomalies in resistivity and magnetic susceptibility than that of $Lu_5Ir_4Si_{10}$.

2. Electrical resistivity under high pressure

The resistivity, normalized to its room temperature value, for $Lu_5Ir_4Si_{10}$ at nine distinct pressures is shown in Fig. 15. The pressure was fixed at room temperature and the data were taken as the sample cooled slowly to below the superconducting transition. Each isobaric sequence was followed by an increase in pressure until the highest pressure sequence at 21.42 kbar was completed. At this point, the pressure was released and the ambient pressure resistivity remeasured. This second set of data at ambient pressure was identical to initial one, confirming the complete reversibility of the phase transition. Absolute values for ρ(300 K) and ρ(7 K) at ambient pressure are 85.6

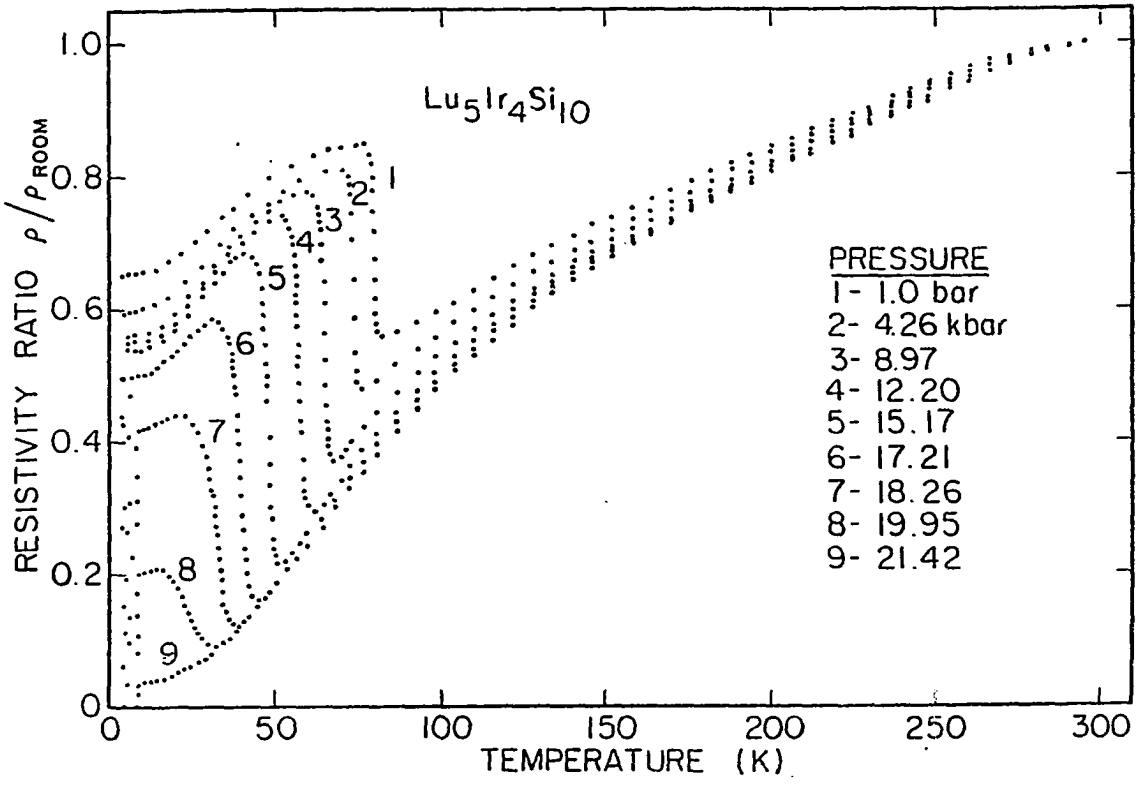

Fig. 15. Electrical resistivity normalized to the value at 300 K versus temperature for $Lu_5Ir_4Si_{10}$ at nine distinct pressures. Some data points are omitted for clarity.

μΩ-cm and 56.2 μΩ-cm, respectively, while the corresponding numbers at 21.42 kbar are: ρ(300 K) = 94.4 μΩ-cm and ρ(10 K) = 3.52 μΩ-cm. At ambient pressure the resistivity shows a clear and sharp jump at T_o = 83 K. From the Fig. 15, T_o is depressed monotonically by the application of pressure. We compute the initial pressure dependence of T_o to be $(dT_o/dp)_{p=0}$ = -1.4 K/kbar. This slope increases in magnitude with increasing pressure, resulting in a phase boundary with negative curvature in a T_o versus pressure graph. In addition to lowering T_o, the size of the anomaly is also suppressed as p_c is approached (e.g., see curve 8). When the pressure exceeds p_c, this resistivity anomaly is destroyed completely and the resistivity goes to zero simultaneously at 9 K. These data demonstrate conclusively that the complete suppression of this phase transition correlates with the stablization of the the high-T_c superconducting state.

Normalized resistivity as a fuction of temperature for $Lu_5Rh_4Si_{10}$ at five different pressures is presented in Fig. 16. At ambient pressure the resistivity shows an anomaly at T_o = 155 K. Application of pressure at 8.6 and 14.4 kbar depresses T_o severely down to about 125 and 110 K respectively. The anomaly is much broader and the RRR is smaller than those at ambient pressure. As the pressure increase to 17.9 kbar, the transition becomes very sluggish and more than one relative maximum seems to exist in the curve. Further application of pressure at 18.3 kbar yields only one clear maximum in resistivity at 64 K, but with a different shaped anomaly from that at ambient pressure. At this point we note that the superconducting transition temperature T_c is 4.3 K at pressures of 17.9 and 18.3 kbar compared to a T_c of 3.4 K at

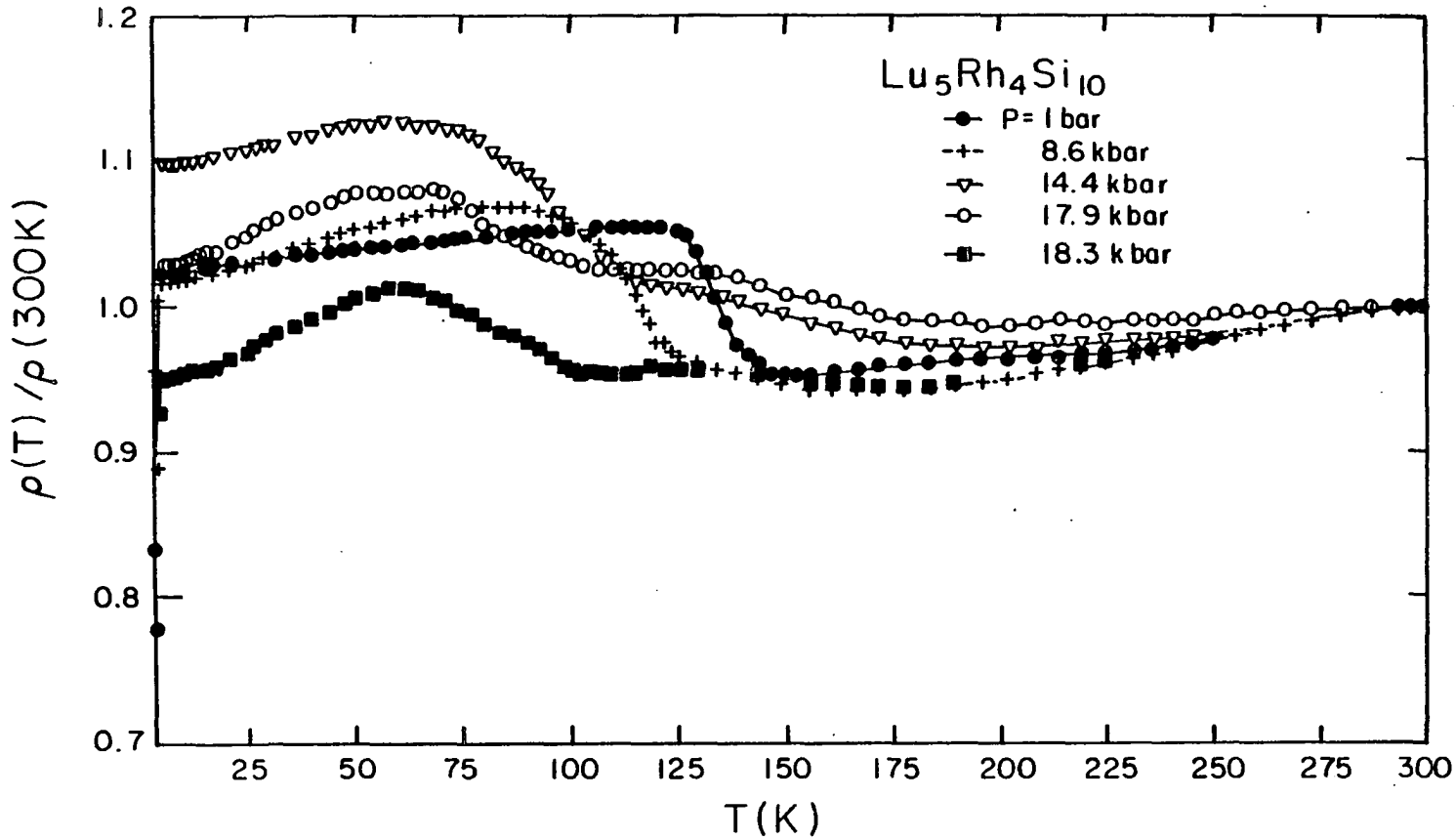

Fig. 16. Normalized resistivity as a function of temperature for $Lu_5Rh_4Si_{10}$ at five distinct pressures

pressures of 1bar, 8.6 kbar, and 14.4 kbar. This indicates specific differences between $Lu_5Rh_4Si_{10}$ and $Lu_5Ir_4Si_{10}$. In the latter case, the anomaly in resistivity is totally suppressed at 21.42 kbar and T_c jumps from 3.8 to 9.1 K at the same time, while in the former case, the T_c jumps from 3.4 to 4.3 K at 17.9 kbar but the resistivity anomaly is still partially retained. One could anticipate that at higher pressures the anomaly could be suppressed completely for $Lu_5Rh_4Si_{10}$, resulting in another jump in T_c to a higher value.

The electrical resistivity of $Lu_5Ir_4Si_{10}$ and $Lu_5Rh_4Si_{10}$ can be consistently explained by assuming the formation of charge density waves. When a CDW forms, gaps open at the Fermi surface at those portions that satisfy the nesting condition. The increase in resistivity at T_o for these two compounds can be attributed to the decrease in area of the Fermi surface resulting from the opening of the gaps. The formation of a CDW is determined by the competition between two terms in the free energy of the system: the strain energy, which increases with the formation of superlattice disorder, and the gain in electronic energy resulting from the opening of the gaps. The gain in electronic energy increases with decreasing temperature because the Fermi surface is sharper at low temperature. By applying pressure, we expect a stiffening of the lattice which increases the strain energy. To offset this increase in energy, the electronic energy gain must be larger to stablize the CDW state. Consequently, the transition temperature T_o is lowered. We have shown that the T_o of these two compounds decreases with the application of pressure. This is similar to the pressure dependence of the CDW transition temperature in the

layered compound 2H-$NbSe_2$,[83] quasi-one-dimensional transition metal trichalcogenide $NbSe_3$,[86] and even the three dimensional cubic spinel compound CuV_2S_4.[87]

Now, we briefly discuss the correlation between T_o and T_c with the parameter of pressure. A supplementary contribution to the decrease of T_o with pressure can be expected from the stiffening of the lattice, since the distortion associated with CDW will then cost more strain energy. This stiffening should also cause a decrease of T_c[41] at the same time. The onset of the CDW will open a gap at the Fermi surface, reduce the density of states at the Fermi level $N(E_F)$ and then decrease the T_c. When pressure is applied, both the area where the gap opens and the amplitude of the gap decrease; therefore, the reduction of $N(E_F)$ will be smaller and T_c will increase.[88] However, the soft-mode model which was proposed by Testardi[43] for the explanation of the variation of T_c with pressure in A15 superconductors cannot be ruled out. The soft-mode associated with the structure distortion may decrease $\langle\omega^2\rangle$ as long as $T_o > T_c$ and should be more efficient when $T_o \sim T_c$. From this point of view, the absence of a jump[74] in T_c at 21 kbar for $Y_5Ir_4Si_{10}$ can be explained by assuming that the applied pressure is not high enough to suppress the anomaly which appears in resistivity and static magnetic susceptibility at about 250 K.

The P-T phase diagram for $Lu_5Ir_4Si_{10}$ shown in Fig. 17 was generated by the pressure dependence of resistivity and ac magnetic susceptibility data, where T_o's are taken as the temperatures where the resistivity starts to behave with a nonmetallic-type variation. According to the resistivity and ac magnetic susceptibility measurements of $Lu_5Rh_4Si_{10}$

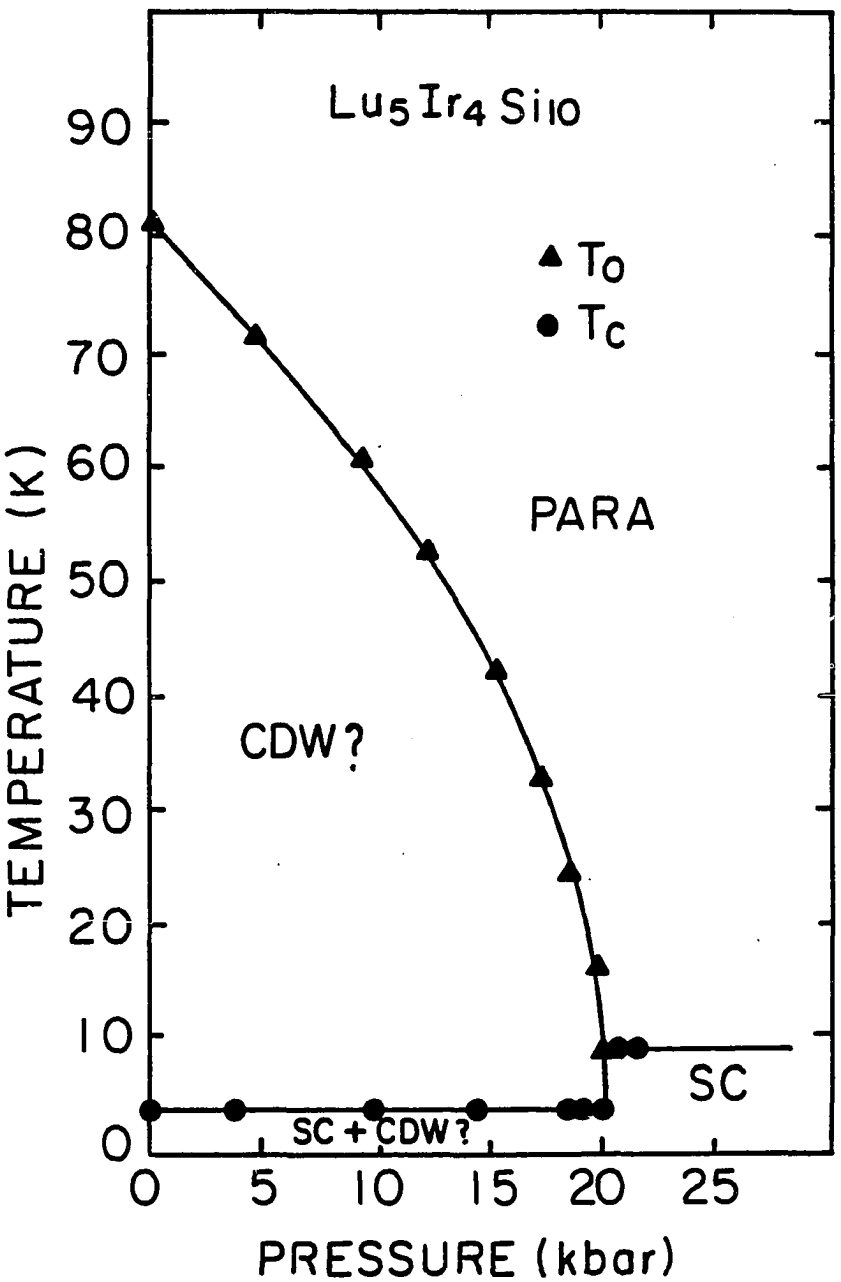

Fig. 17. P-T phase diagram of $Lu_5Ir_4Si_{10}$. PARA: paramagnetism, CDW: charge density waves, SC: superconducting, T_c: superconducting transition temperature, T_o: temperature taken where the resistivity starts to behave with a non-metallic-type variation

under pressure ($p < 18.3$ kbar), we postulate a more complicated CDW structure in this compound. The changing shape of the resistive anomaly as the pressure increases may reflect that the type of CDW is pressure dependent or that the coupled CDW's are separated by a application of pressure.

3. Alloying and doping effects

Before going into this section, we give a brief comparison among $Sc_5Ir_4Si_{10}$, $Lu_5Rh_4Si_{10}$, and $Lu_5Ir_4Si_{10}$ with different points of view.

(1) They are all isostructrual with the $Sc_5Co_4Si_{10}$-type structure. The lattice parameters of $Lu_5Ir_4Si_{10}$ and $Lu_5Rh_4Si_{10}$ are about the same, but are about 1.5% larger than those of $Sc_5Ir_4Si_{10}$.

(2) $Sc_5Ir_4Si_{10}$ undergoes a superconducting transition at $T_c = 8.5$ K with a fairly linear depression under pressure up to 21 kbar. In contrast, there is a remarkable discontinuous jump in T_c for $Lu_5Ir_4Si_{10}$ and $Lu_5Rh_4Si_{10}$ by the application of pressure at about 20 kbar.

(3) $Sc_5Ir_4Si_{10}$ shows a paramagnetic metal-type temperature variation in the resistivity and static magnetic susceptibility between 2.6 and 300 K. However, $Lu_5Ir_4Si_{10}$ and $Lu_5Rh_4Si_{10}$ exhibit an anomaly in the temperature dependence of the resistivity and static magnetic susceptibility.

In order to study the effects of atomic size and electronic configuration on the anomaly in resistivity of $Lu_5Ir_4Si_{10}$, we have tried to alloy on both the Lu and Ir sites with different elements.

Normalized resistivity as a fuction of temperature for the pseudoternary system $(Lu_{1-x}Sc_x)_5Ir_4Si_{10}$ is shown in Fig. 18. The reason

to choose Sc to substitute for Lu is to chemically "squeeze" the lattice since Sc has smaller metallic radius. So, an unnegligible size effect should be seen in the alloying process. At x = 0.05, the resistivity is almost identical to that of x = 0 for the high temperature (T > 250 K) region, and then starts to deviate as temperature is lowered. No noticeable anomaly appears and the curve ends with a smaller residual resistivity ratio. With a further increase of x, for intance, x = 0.1, the resistivity curve becomes flatter with an even smaller RRR. For x = 0.3, the RRR is larger than that of the x = 0 sample. Combining the results of resistivity under pressure with the value of bulk modulus 1370±70 kbar for $Lu_5Ir_4Si_{10}$, we determine that the unit cell volume of x = 0.05 at ambient pressure approximately equals that of x = 0 at 3.3 kbar. As we have seen in Fig. 18, with 5% of Sc substitution, the anomaly in resistivity is totally suppressed. Contrasting this to pressure data of pure $Lu_5Ir_4Si_{10}$ shown in Fig. 15, we conclude that the substitution of Sc not only gives rise to a size effect but induces an atomic disorder to suppress the anomaly in resistivity for $Lu_5Ir_4Si_{10}$ which is considered indicative of a CDW.

Figure 19 shows the normalized resistivity as a function of temperature for the pseudoternary system $Lu_5(Ir_{1-x}Rh_x)_4Si_{10}$. In this case, there exists an anomaly in resistivity for both end members, but no anomaly exists for the intermediate composition $0.13 \leqslant x \leqslant 0.72$. Because the unit cell volumes of $Lu_5Ir_4Si_{10}$ and $Lu_5Rh_4Si_{10}$ are about the same (0.7% difference), the atomic disorder or chemical effects in the pseudoternary system are the dominant factors in suppressing the anomaly in the resistivity. Results of lattice parameters, a/c, and unit cell

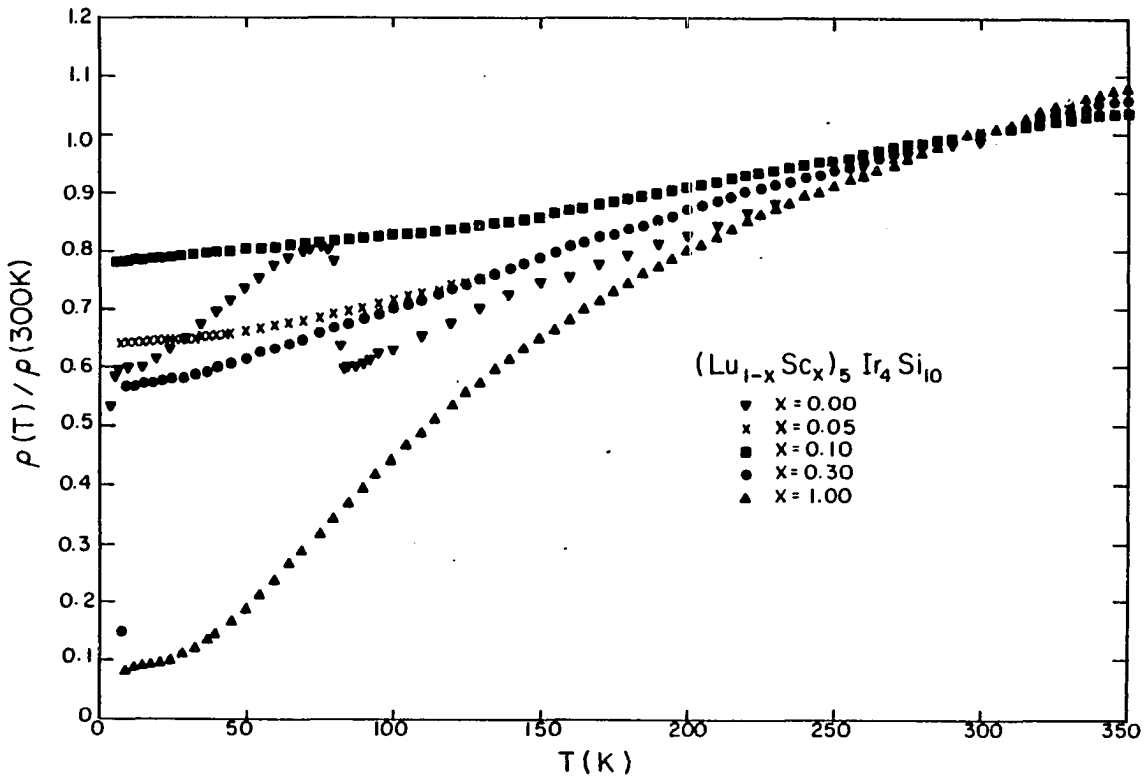

Fig. 18. Normalized resistivity as a function of temperature for the pseudoternary system $(Lu_{1-x}Sc_x)_5Ir_4Si_{10}$ (x= 0, 0.05, 0.1, 0.3, and 1.0)

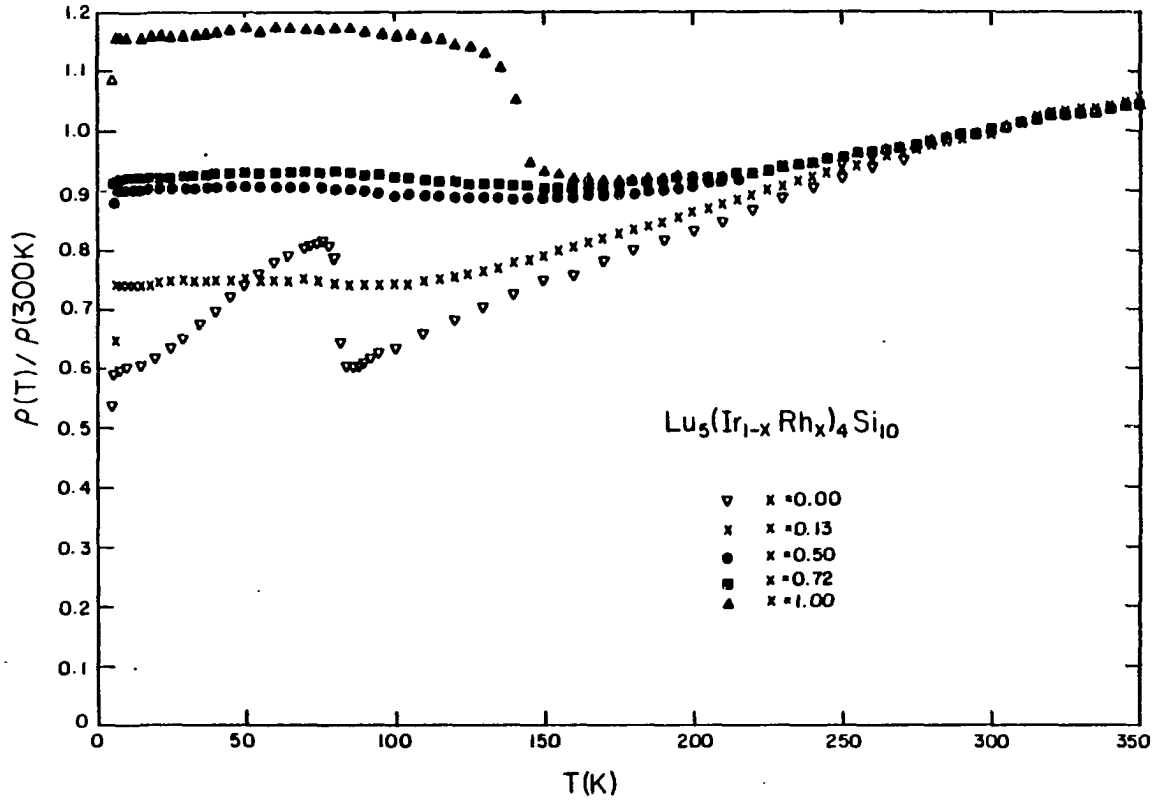

Fig. 19. Normalized resistivity as a function of temperature for the pseudoternary system $Lu_5(Ir_{1-x}Rh_x)_4Si_{10}$ (x= 0, 0.13, 0.5, 0.72, and 1.0)

volume for the pseudoternary system $Lu_5(Ir_{1-x}Rh_x)_4Si_{10}$ are shown in Fig. 20 provide additional evidence for this point. A detectable chemical contraction is clearly seen in the a and c axes and unit cell volume as x varies between 0.2 and 0.7; however, the ratio a/c follows Vegard's law through the whole composition range. It should be noted that the chemical contraction is equivalent to the application of pressure which will suppress the anomaly in resistivity. We think this is the main reason why no anomaly in resistivity is seen in the range of $0.13 \leqslant x \leqslant 0.72$.

Figure 21 shows the normalized resistivity as a function of temperature for the pseudoternary systems $(Lu_{0.9}R_{0.1})_5Ir_4Si_{10}$ (R = Dy, Ho, Er, Tm, Sc, Y, and Th). An anomaly is still seen for R = Dy-Tm and Y, is smeared out for R = Th, and disappears completely for R = Sc. These results are consistent with the data which are presented in Table 2; namely, that an anomaly in resistivity is always associated with a jump in T_c at high pressure. Because the atomic volume of these atoms (except Sc) is larger than that of Lu, no alloying compression comes into the system to suppress the anomaly. On the other hand, all pure ternaries $R_5Ir_4Si_{10}$ (R = Dy-Tm and Y) have an anomaly in resistivity (see Fig. 30 in chap. V). Thus, the presence of the anomaly in the $R_5Ir_4Si_{10}$ compounds results in a reduced effect in the $(Lu_{0.9}R_{0.1})_5Ir_4Si_{10}$ systems. The $(Lu_{0.9}Th_{0.1})_5Ir_4Si_{10}$ compound shows a slightly different feature. The anomaly in the resistivity is much less pronounced than that of the others. This result correlates with the pressure data where the T_c jump is absent, but with a bigger positive value of dT_c/dp. It is probably due to the tetravalent nature of Th as distinct from the trivalent rare earths.

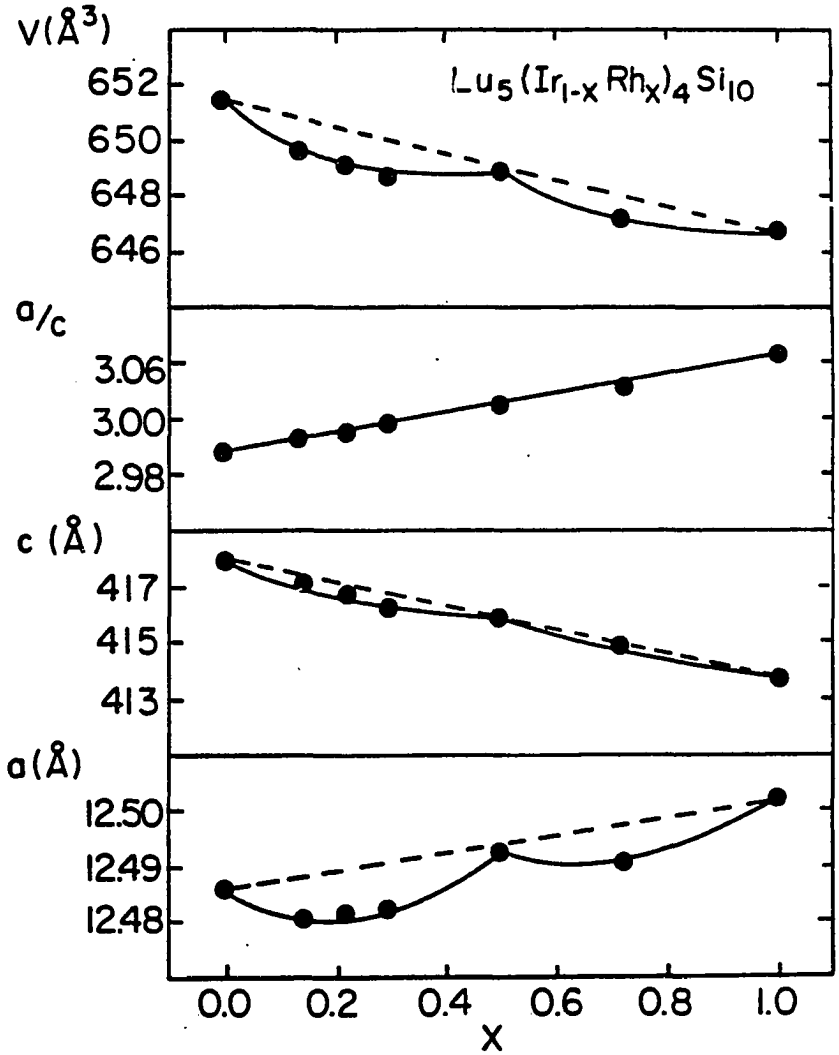

Fig. 20. Lattice parameters, a/c, and unit cell volume versus alloy concentration for the pseudoternary system $Lu_5(Ir_{1-x}Rh_x)_4Si_{10}$. Error bars are included in the symbols

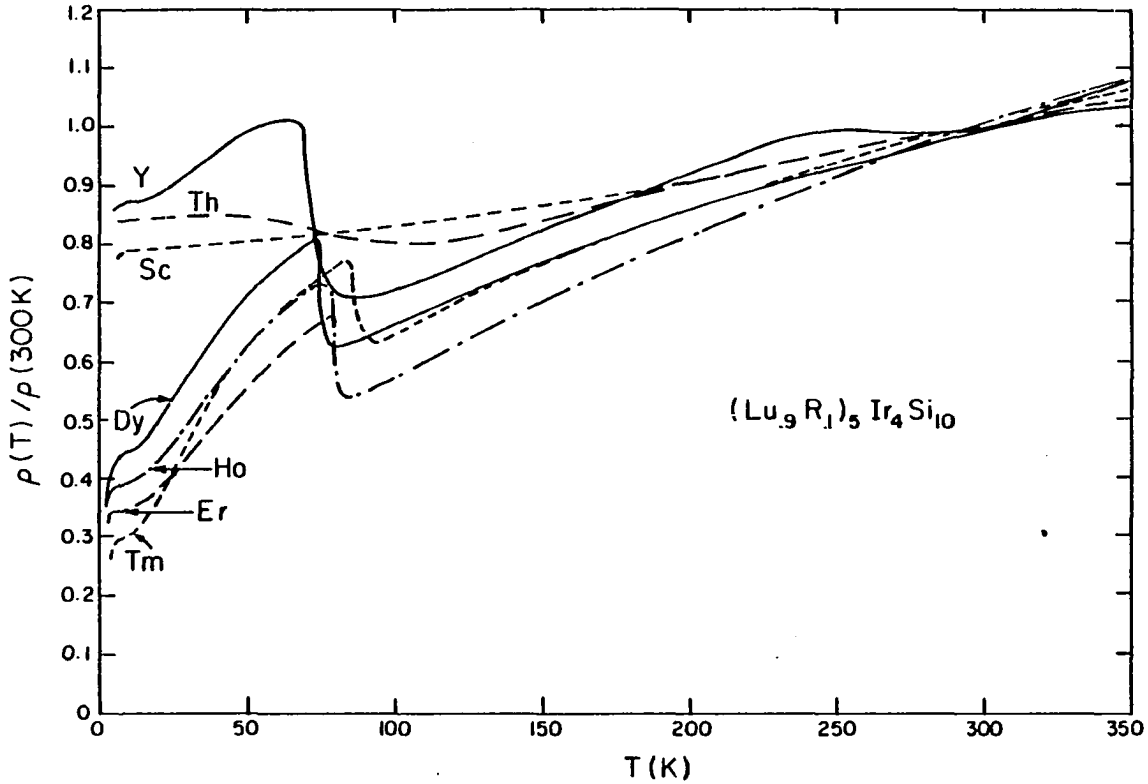

Fig. 21. Normalized resistivity as a function of temperature for the pseudoternary system $(Lu_{.9}R_{.1})_5Ir_4Si_{10}$ (R= Dy, Ho, Er, Tm, Sc, Y, and Th)

It has been suggested[89] that CDW formation and superconductivity are antagonistic, both competing for states near the Fermi surface. In the last section, we have shown a suppression of CDW and an increase of superconducting transition temperature by the application of pressure. At present, we use a quite separate way to study the interplay between superconductivity and CDW in $Lu_5Ir_4Si_{10}$ by doping with the impurity Sc on Lu sites. The presence of an impurity in a CDW material may lead to a change of the CDW transition temperature T_o and also to a possible smearing of the CDW transition itself. The mathematical analogy between the theories describing a (BCS) superconductor and CDW state suggests[90] that magnetic impurities in a superconductor play a role equivalent to non-magnetic impurities in a CDW system. In analogy to superconductors, the critical mean free path $l_{cr} = v_F b_{cr}$ for the electrons, in a CDW system[91,92] is $l_{cr} \propto 1.14\ v_F/T_o$. Where v_F is the Fermi velocity, $1/b_{cr}$ is the critical pair-breaking parameter for a BCS superconductor, and T_o is the CDW transition temperature in the absence of impurities. The quantity l_{cr} may be associated with an effective localization length applicable to any disorder. Consequently, in the dilute impurity limit, T_o decreases linearly with increasing impurity concentration. In addition to scattering electrons and inducing a finite electron life time, an impurity may also induce Friedel oscillations in the electron charge distribution, leading to a static lattice distortion. A direct result of this effect is a smearing of the CDW transition.

Normalized resistivity as a function of temperature between 30 and 90 K for pure and doped samples is shown in Fig 22. It shows that replacing 0.5% of the Lu atoms by Sc atoms results in a decrease of the

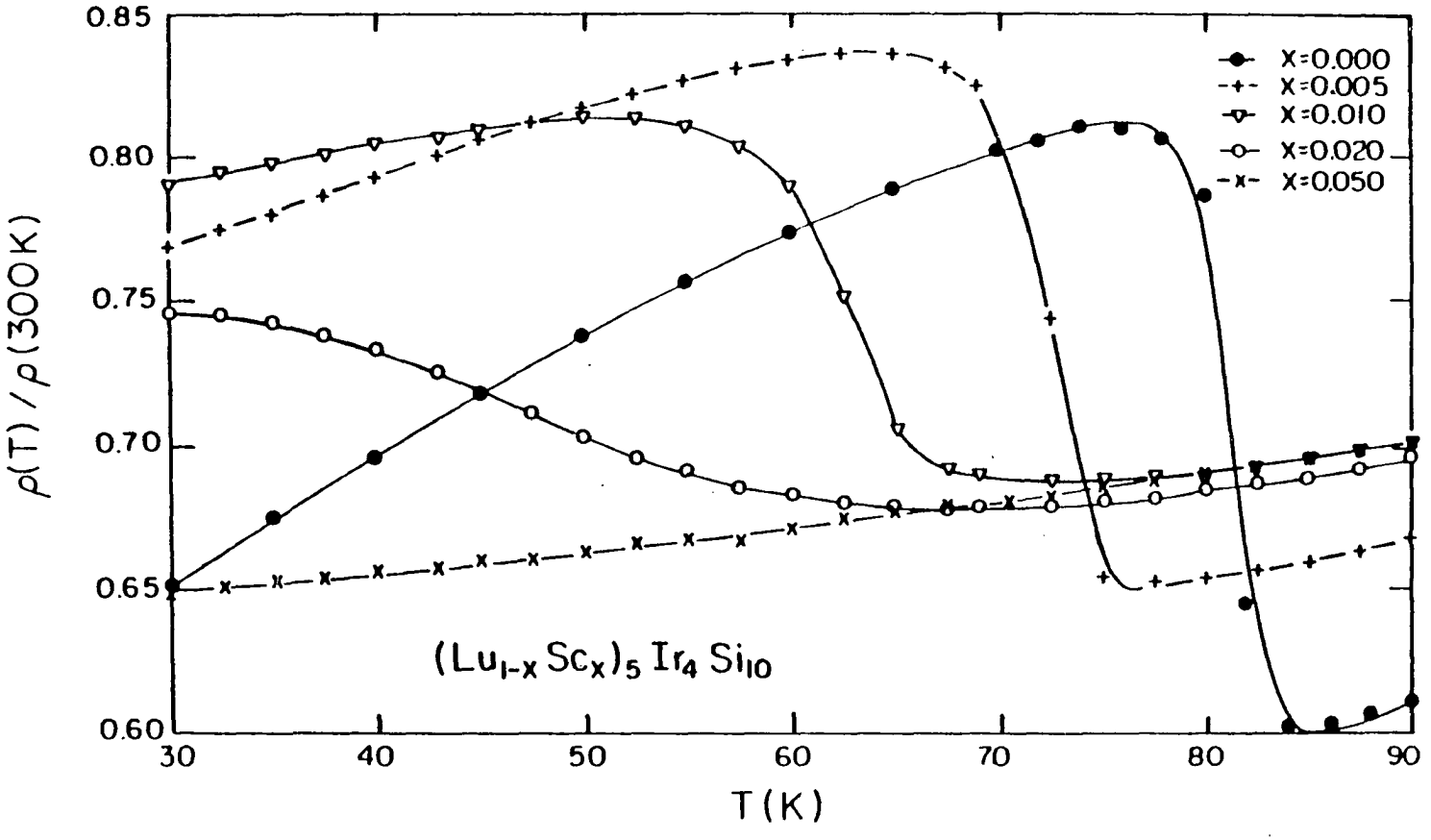

Fig. 22. Normalized resistivity as a function of temperature between 30 and 90 K for the pseudoternary system $(Lu_{1-x}Sc_x)_5Ir_4Si_{10}$ (x= 0, 0.005, 0.01, 0.02, 0.05)

CDW transition temperature by approximately 9 K. At 5% of Sc doping, the transition is so depressed that it is no longer detectable. The concentration dependence of the CDW temperature T_o, the amplitude of the anomaly in resistivity $\Delta\rho/\rho(300\ K)$, and the superconducting transition temperature T_c for the pseudoternary system $(Lu_{1-x}Sc_x)_5Ir_4Si_{10}$ (x= 0.0, 0.005, 0.01, and 0.02) are presented in Fig. 23. It is shown that the impurities lower the T_o, broaden and smear the CDW transition, while increasing T_c just as one would expect in this system. We calculate the initial concentration dependence of T_o and T_c to be $(dT_o/dx)_{x=0}$ = -18.5 K/at % and $(dT_c/dx)_{x=0}$ = 0.5 K/at %. These values are consistent with the lack of observation of an anomaly and the enhancement of T_c to 5.8 K for 5% of Sc substitution for Lu. Thus, from the view of volume change, the effect of impurity is at least 6 times more sensitive than that of pressure for suppressing the CDW transition in this system. This also provides information that the impurity may induce a change in the band structure or density of states near Fermi surface.

To investigate the electronic density of states near the Fermi level in $Lu_5Ir_4Si_{10}$, we vary the Fermi level slightly by the impurity doping and measure the temperature dependence of the resistivity. Os and Pt, which are different from Ir by only one in the atomic number, are chosen as dopants in order to minimize the lattice distortion due to the substitutional disorder. We also use Co as a dopant that is isoelectronic to Ir. Normalized resistivity as a function of temperature between 60 and 90 K for pure $Lu_5Ir_4Si_{10}$ and 0.5% of Co, Os, and Pt doped $Lu_5Ir_4Si_{10}$ is shown in Fig. 24. It is found that Os doping is more effective than Pt doping in suppressing the anomaly for both the

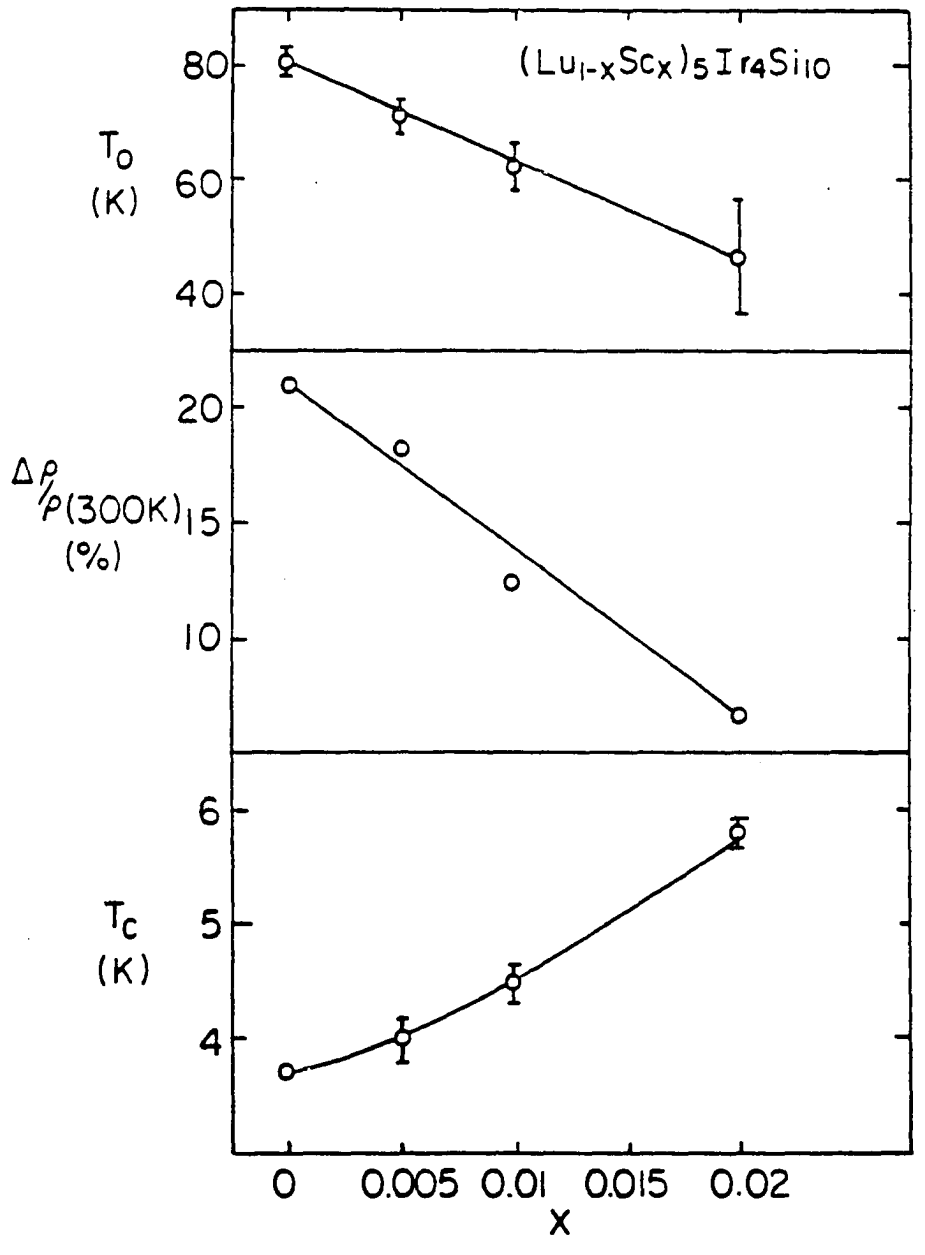

Fig. 23. Alloy concentration dependence of CDW transition temperature T_o, amplitude of anomaly $\Delta\rho/\rho(300\ K)$, and superconducting transition temperature T_c for the pseudoternary system $(Lu_{1-x}Sc_x)_5Ir_4Si_{10}$ (x= 0, 0.005, 0.01, and 0.02)

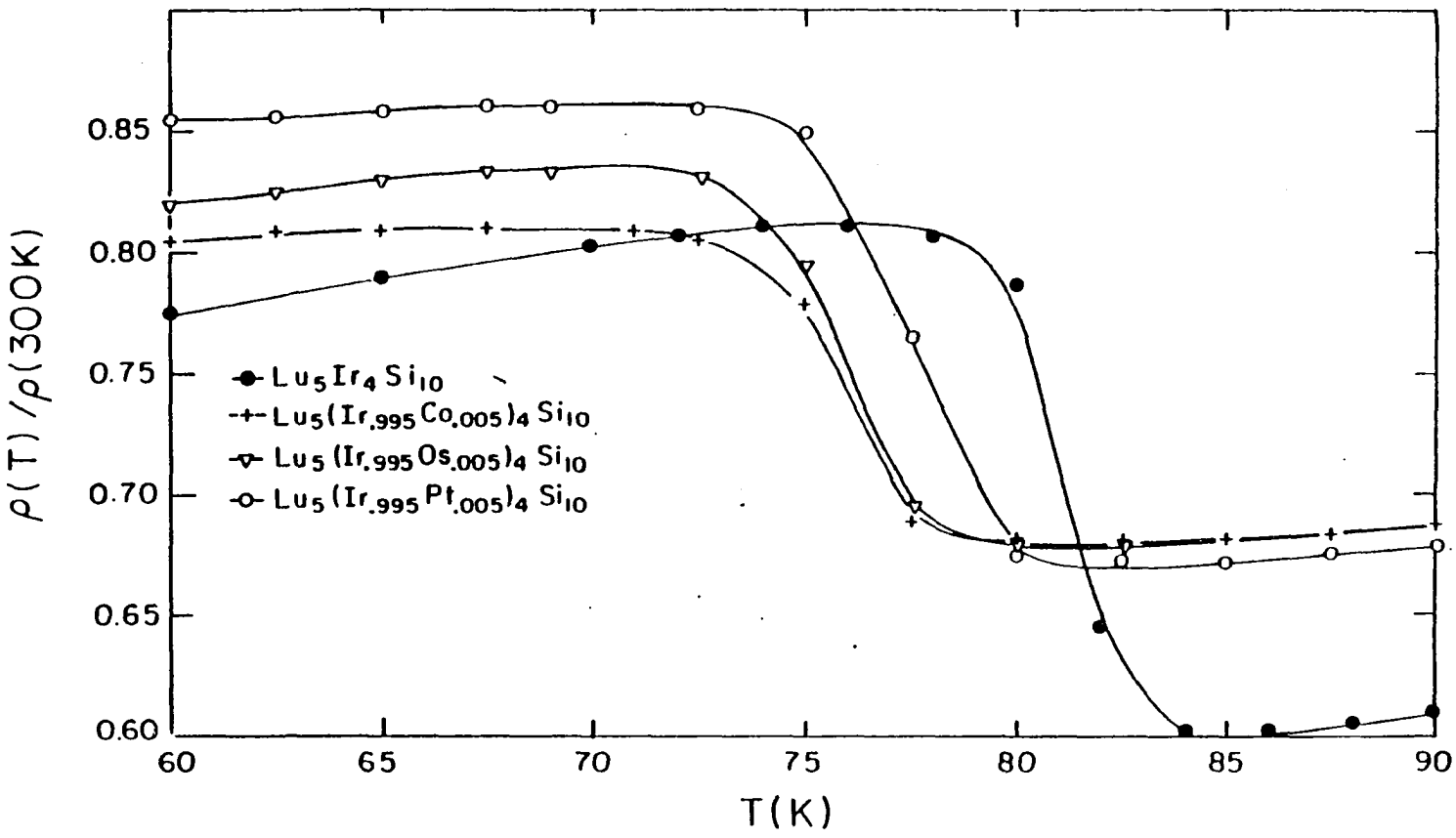

Fig. 24. Normalized resistivity as a function of a temperature between 60 and 90 K for pure and 5% Co, Os, and Pt doped $Lu_5Ir_4Si_{10}$

transition temperature and the ampliture in the resistivity. However, the superconducting transition does not change in a complementary manner. For both the Os and Pt doped samples, T_c increases as T_o decreases which is expected. While T_c increases more for the Pt-containing compound, this is not consistent with what we observe in $(Lu_{1-x}Sc_x)_5Ir_4Si_{10}$ system. This inconsistency indicates that atomic size effects which also occur during doping may be as important as the electronic effects. The reduction of T_o when isoelectronic Co is substituted for Ir is larger than that for Os or Pt and confirms the importance of the atomic size effects.

4. Electric field effects

One of the most fascinating characteristics of charge density waves is the nonlinear resistivity behavior[93,94] below the phase transition temperature. The resistive anomalies associated with the CDW formation are strongly reduced by a weak electric field (0.1 ~ 1 V/cm). This behavior was interpreted as evidence that the CDW can be depinned easily and move freely under the influence of a small electric field,[90,95,96] carrying a current as was suggested by Fröhlich[28]. Evidence for this type of conductivity has been observed in the one-dimensional $NbSe_3$ system.[93]

The polycrystalline sample of $Lu_5Ir_4Si_{10}$ used was 3.56 x 0.13 x 0.09 mm^3 in size. Platinum leads were attached to the sample with silver paint. The measurements were performed by a standard four-probe technique. Temperature control was provided by a sample property measurement system (from Quantum Design Inc.) in the range from 2.6 to

300 K. The programable dc constant current source and nanovoltmeter (from Keithley Inc.) were controlled and read by a personal computer (HP-85). The current direction was reversed to eliminate the thermoelectric effects which might form in the circuit. In order to reduce the self-heating on the sample, the current was controlled to flow across the sample for only two seconds, and the voltage acoss the sample was read just before the current was turned off.

Results of the normalized resistivity as a function of temperature between 20 and 100 K for $Lu_5Ir_4Si_{10}$ are shown in Fig. 25. At the lower currents (J = 0.86 and 4.3 A/mm^2), the curves are basically consistent with our previous low field measurements. As the current increases, the anomaly starts to move toward lower temperatures but retains approximately the same amplitude. The contacts were damaged when the current density exceeded 34.2 A/mm^2.

We also made another measurement with the temperature held constant while we swept the current. Fig. 26 shows the normalized resistivity as a function of current density at eight different temperatures. The results are similar to those derived directly from Fig. 25.

After careful analysis of these data, we cannot eliminate the possibility that the decrease in the transition temperature with increasing current might be due to the local heating on the sample itself. In Fig. 26, the slopes of the linear portion (lower and higher than transition) are roughly the same as that in Fig. 25 with J = 0.86 A/mm^2. This strongly indicates that the sample temperature was higher than the thermometer during the high current measurement. For example, the sample temperature, determined by the thermometer, is 70 K before

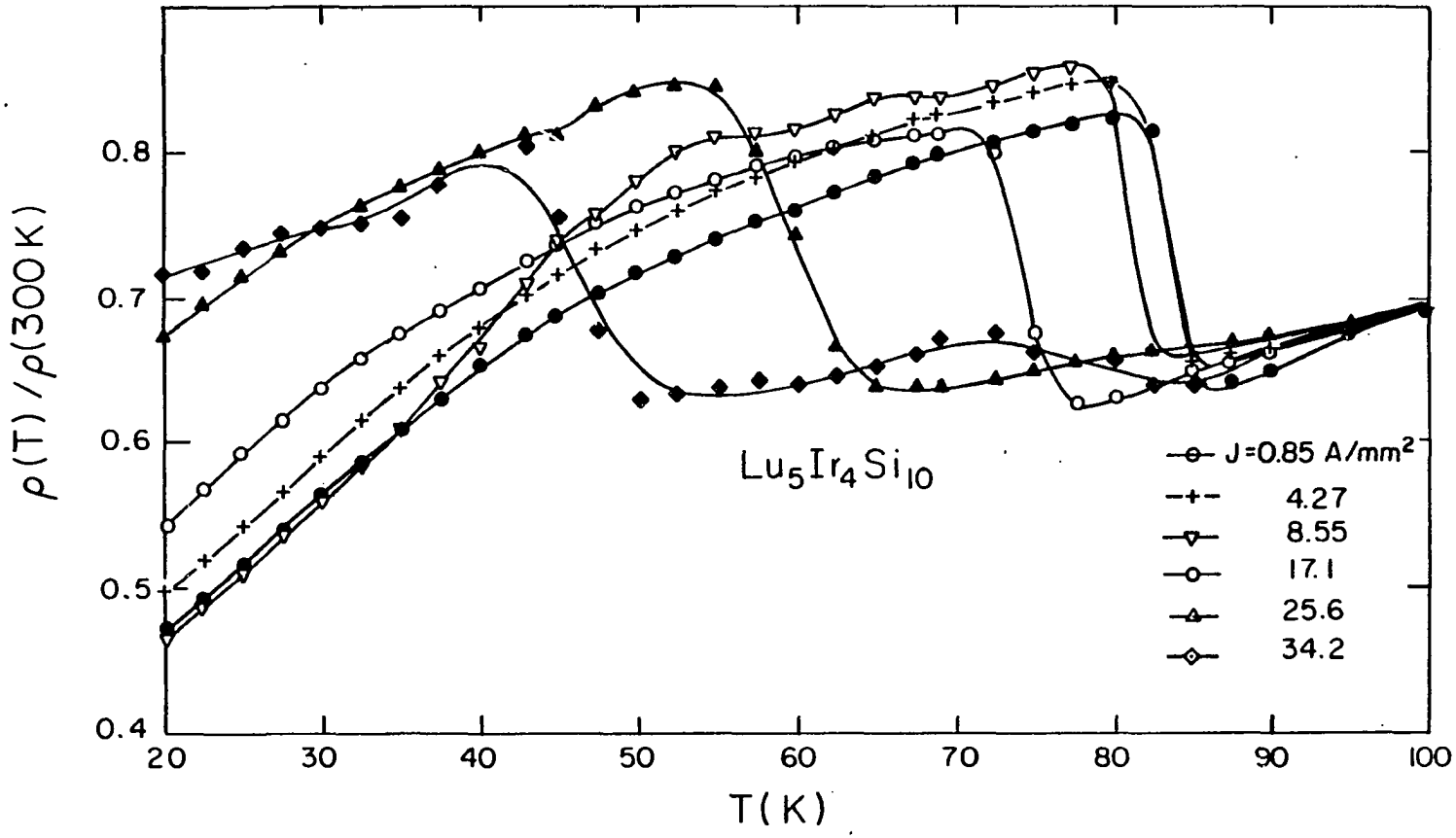

Fig. 25. Normalized resistivity as a function of temperature between 20 and 100 K with six different currents for $Lu_5Ir_4Si_{10}$

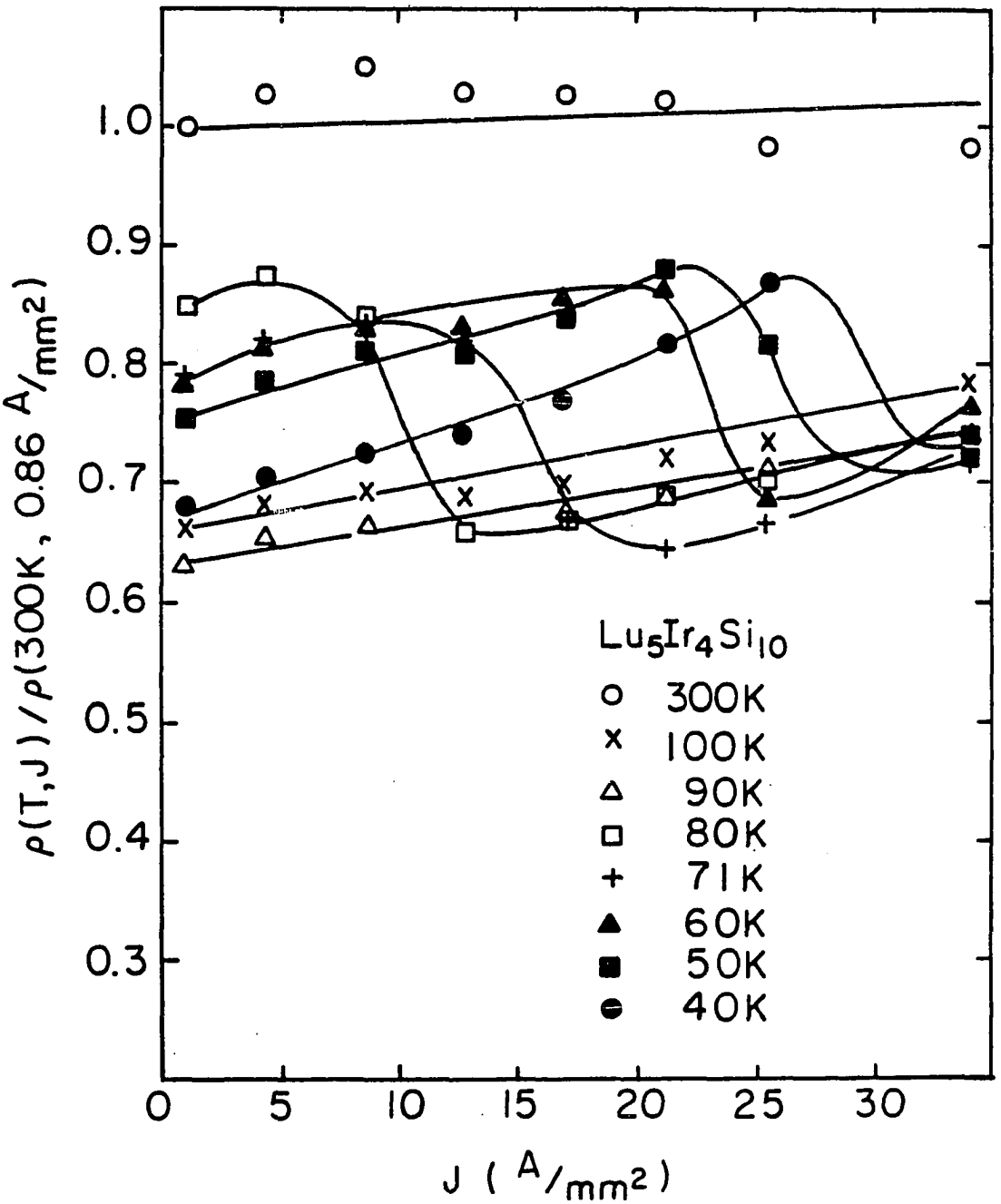

Fig. 26. Electrical resistivity normalized to the value of T=300 K, J=0.86 a/mm^2, as a function of current density at eight diffent temperatures for $Lu_5Ir_4Si_{10}$

the current is turned on. The sample may be heated up to 90 K after the high current (> 20 A/mm^2) is turned on for 2 seconds, but the thermometer may remain at 70 K at that moment. This picture would account for the results we observed.

Several questions still remain.

(1) We also tried to let the current flow only for 1 second (this is the shortest time we can finish reading the voltage) across the sample. The results are very similar to those done for 2 seconds. Does this mean that the local heating on the sample is not as severe as we thought?

(2) We believe that the thermal contact was quite good between the sample and the copper probe in our experimental set-up. According to our estimation from the relation of $C\ \Delta T = I^2\ R\ \Delta t$ and assuming the Joule heat was totally absorbed by the sample without any diffusion or conduction, the temperature of the sample could only increase about 2 K. This calculation indicates that the depression of T_o with increasing current density (electric field) is real. However, contact resistance between the two current leads and the sample could be as high as 0.5 Ω. If this is the case, the Joule heating at these contact points could result in a temperature increase of as much as 20 K.

C. Conclusion

We have presented electric resistivity and static magnetic susceptibility data for the isostructural compounds $Lu_5Ir_4Si_{10}$, $Lu_5Rh_4Si_{10}$, $Y_5Ir_4Si_{10}$, and $Sc_5Ir_4Si_{10}$. These experiments document the

presence of an ambient pressure phase transition at T_o = 83 K, 155 K and 250 K for the first three compounds respectively, while $Sc_5Ir_4Si_{10}$ shows a common metallic behavior over the temperature range from 2.6 to 300 K.

High pressure electrical resistivity experiments for $Lu_5Ir_4Si_{10}$ show that T_o decreases with pressure, resulting in the complete suppression of this phase transition at a critical pressure p_c = 21 kbar. Thus the removal of the electronic phase transition by pressure results in the large and discontinuous enhancement of the superconducting critical temperature from 3.8 to 9.1 K. For $Lu_5Rh_4Si_{10}$, the anomaly in resistivity is partially suppressed and the T_o is enhanced discontinuously from 3.4 to 4.3 K by the application of pressure at 18 kbar. A complete suppression of the transition and at the same time another jump in T_c are expected if the pressure is high enough.

We have given a quantitative estimate of a 36% loss in electronic density of states at the Fermi level due to this phase transition for $Lu_5Ir_4Si_{10}$. All of these experimental data indicate this electronic phase transition may involve the development of a charge-density-wave (CDW) that opens an energy gap over a portion of the Fermi surface. The formation of CDW has been observed and well documented for two-dimensional compounds such as the transition metal dichalcogenides,[27,97] anisotropic metals such as the one-dimensional conductors,[98] and the spinel compound CuV_2S_4 where the underlying crystal lattice is certainly three-dimensional.[87,99]

Results of the quite sensitive atomic disorder effect and the correlation between superconducting transition temperature and CDW

transition temperature by doping effects in the pseudoternary systems $(Lu_{1-x}Sc_x)_5Ir_4Si_{10}$ and $Lu_5(Ir_{1-x}Rh_x)_4Si_{10}$ are very similar to those observed in 1T-TaS_2,[100] $(Ti_{1-x}V_x)Se_2$,[101] $(Ta_{1-x}Nb_x)S_3$,[102] and 4H-TaS_2.[103]

Unfortunately, we obtained no definite conclusion from studying the density of states near the Fermi level in $Lu_5(Ir_{.995}T_{.005})_4Si_{10}$ (T = Os, Pt, and Co), since atomic disorder and size effects dominated any electronic effects. The electric field dependence of resistivity in $Lu_5Ir_4Si_{10}$ was masked by local heating of the sample.

A crucial experiment to be performed in the future is a low temperature single crystal X-ray or electron diffraction measurement to look for specific evidence of a CDW superlattice in $Lu_5Ir_4Si_{10}$. In addition, band structure calculation would provide great insight to understand why the CDW is observed in $Lu_5Ir_4Si_{10}$, $Lu_5Rh_4Si_{10}$, and $Y_5Ir_4Si_{10}$, but not in $Sc_5Ir_4Si_{10}$ and the other isostructural superconductors. These conclusions might also clarify the effective dimensionality (or anisotropy) of $Lu_5Ir_4Si_{10}$.

V. LOW TEMPERATURE PHYSICAL PROPERTIES IN $R_5Ir_4Si_{10}$ (R = Dy, Ho, Er, Tm, and Yb) COMPOUNDS

A. Introduction

The rare earth transition metal ternary compounds exhibit a great variety of unusual phenomena.[15] In particular, the rhombohedral rare earth molybdenum chalcogenides RMo_6S_8[55] and the tetragonal rare earth rhodium borides RRh_4B_4[56] have been extensively studied for the interplay between superconductivity and long range magnetic order. More recently, three rare earth transition metal silicides, $R_2Fe_3Si_5$,[104,105] $R_5Co_4Si_{10}$,[53] and RCu_2Si_2[106] have also received much attention due to the high superconducting transition temperatures ($Lu_2Fe_3Si_5$, T_c = 6.2 K; $Sc_5Co_4Si_{10}$, T_c = 4.9 K) observed even in the presence of 3d transition elements 30% iron and 21% Co for the first two systems and superconductivity involving by the enormous effective mass electrons ($CeCu_2Si_2$, $m^*/m \sim 200$, T_c = 0.5 K) for the last system.

Reports of large pressure effects on T_c in $Y_2Fe_3Si_5$,[61] reentrant[107] and pressure-induced superconductivity destroyed by long-range antiferromagnetic order in $Tm_2Fe_3Si_5$[108], complicated multiple magnetic phase transitions in $Sm_2Fe_3Si_5$, $Tb_2Fe_3Si_5$, and $Er_2Fe_3Si_5$ shown in heat capacity measurements,[109] anomalous pressure effect on T_c[74] and temperature dependence of resistivity and magnetic susceptibility in $Lu_5Ir_4Si_{10}$[57] all provide motivation for our present study of the low temperature physical properties of the $R_5Ir_4Si_{10}$ system as a means of better understanding the nature of superconductivity, magnetic order, and electronic phase transition in these materials.

The rare earth iridium silicides $R_5Ir_4Si_{10}$ (R = Dy, Ho, Er, and Tm) are formed in the $Sc_5Co_4Si_{10}$-type structure and magnetic ordering temperatures, T_N = 5.0 K (Dy), 1.5 K (Ho), 2.3 K (Er), and 1.0 K (Tm) were reported.[47] In this work, we investigate the static magnetic susceptibility and electrical resistivity for $R_5Ir_4Si_{10}$ including $Yb_5Ir_4Si_{10}$, as well as resistivity and ac susceptibility under high pressure and heat capacity for $Tm_5Ir_4Si_{10}$ to search for any possibility of mixed valence, reentrant superconductivity, or coexistence of superconductivity and magnetic order phenomena in these compounds.

B. Results and Discussion

1. Crystallography and magnetic properties

The lattice parameters and unit cell volumes of $R_5Ir_4Si_{10}$ (R = Dy, Ho, Er, Tm, Yb, and Lu) are listed in Table 5, which are basically in agreement with those in the literature.[47] It should be noted that $Yb_5Ir_4Si_{10}$ is first reported here. The variation in the lattice parameters and unit cell volumes with rare earth are shown in Fig. 27. The plot indicates that all the rare earth ions in these compounds are trivalent at room temperature. In fact, the a and c values decrease on going from Dy to Lu by approximately 0.8% and 1.6% respectively. These contractions are about the same order of magnitude as those found for the $R_2Fe_3Si_5$ series. These also reflect the feature of this type of stucture that the c parameter is equal to the height of the R_6Si trigonal prism and is thus directly coupled to the rare earth radius. The a parameter does not vary as rapidly as c since it is determined by

Table 5. Crystallographic and magnetic parameters for the ternary silicides $R_5Ir_4Si_{10}$

Compound	a (Å)	c (Å)	a/c	V (Å^3)	$\mu_{eff}(\mu_B)$ exp.	$\mu_{eff}(\mu_B)$ theo.	θ (K)	T_N (K)
$Yb_5Ir_4Si_{10}$	12.503(3)	4.182(2)	2.990	653.74	4.53	4.54	-58.8	-[a]
$Tm_5Ir_4Si_{10}$	12.513(2)	4.197(1)	2.982	657.14	8.05	7.55	-27.1	1.9
$Er_5Ir_4Si_{10}$	12.540(2)	4.208(1)	2.981	661.80	9.79	9.59	0.6	3.0
$Ho_5Ir_4Si_{10}$	12.558(2)	4.218(1)	2.977	665.10	11.27	10.58	-13.2	2.0
$Dy_5Ir_4Si_{10}$	12.577(2)	4.237(1)	2.968	670.16	10.69	10.63	-5.9	5.0

[a]Not observed down to 52 mK.

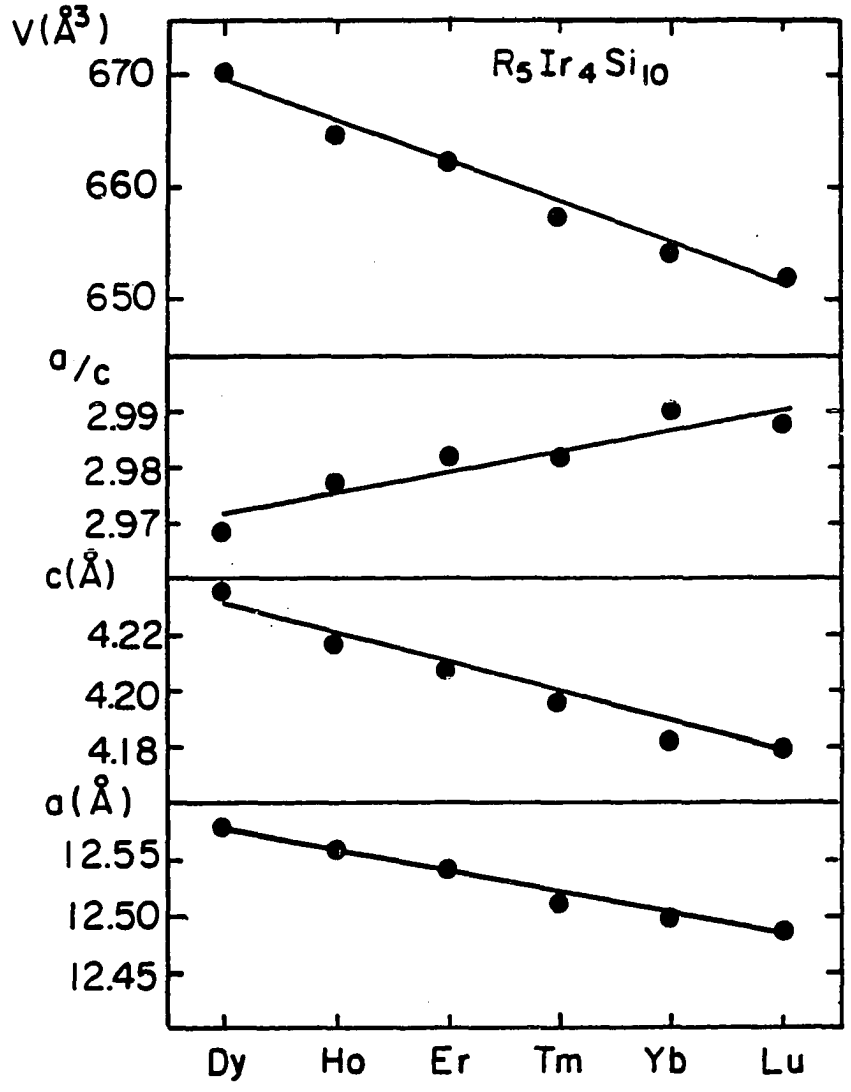

Fig. 27. The variation in the lattice parameters, a/c, and unit cell volume for $R_5Ir_4Si_{10}$ with rare earths (R= Dy-Lu). Lines are guided to the eye. Error bars are included in the symbols

both the rare earth radius and size of the transition metal atom. This correlates with the fact that this structure forms only with rare earths with size equal to or less than Dy.

The results of magnetic measurements of $R_5Ir_4Si_{10}$ (R = Dy, Ho, Er, Tm, and Yb) silicides are presented in Table 5. The reciprocal molar magnetic susceptibility as a fuction of temperature taken from 2.6 to 300 K is shown in Fig. 28. The paramagnetic susceptibility of these compounds closely obeys the Curie-Weiss law at high temperatures (T > 50 K) and the magnetic parameters are obtained from a least squares fit to the general equation:

$$\chi_m = \frac{N_A (\mu_{eff})^2}{3 k_B (T - \theta)} + \chi_o \qquad (15)$$

where N_A is the Avogadro number, k_B is the Boltzmann constant, θ is the asymptotic Curie temperature, and χ_o corresponds to the temperature independent term including the diamagnetic core term χ_{dia}, the Pauli susceptibility of the conduction electrons χ_{Pauli} and the diamagnetic orbital contribution due to the conduction electrons χ_{Landau}. The calculated effective magnetic moments are slightly larger than those expected for R^{3+} free ions. This observation has also been made for the $R_2Fe_3Si_5$ compounds and indicates that there may be a small contribution from the transition element sublattice or a little amount of impurities. A slight deviation of the magnetic susceptibility (more noticeable in $Yb_5Ir_4Si_{10}$) from Curie-Weiss Law below 50 K suggests the presence of crystal field effects. The magnetic ordering temperatures T_N of these compounds (R = Dy-Tm) which are defined as the temperature corresponding to a cusp-like anomaly in a χ_{ac} - T plot are also given in Table 5. The

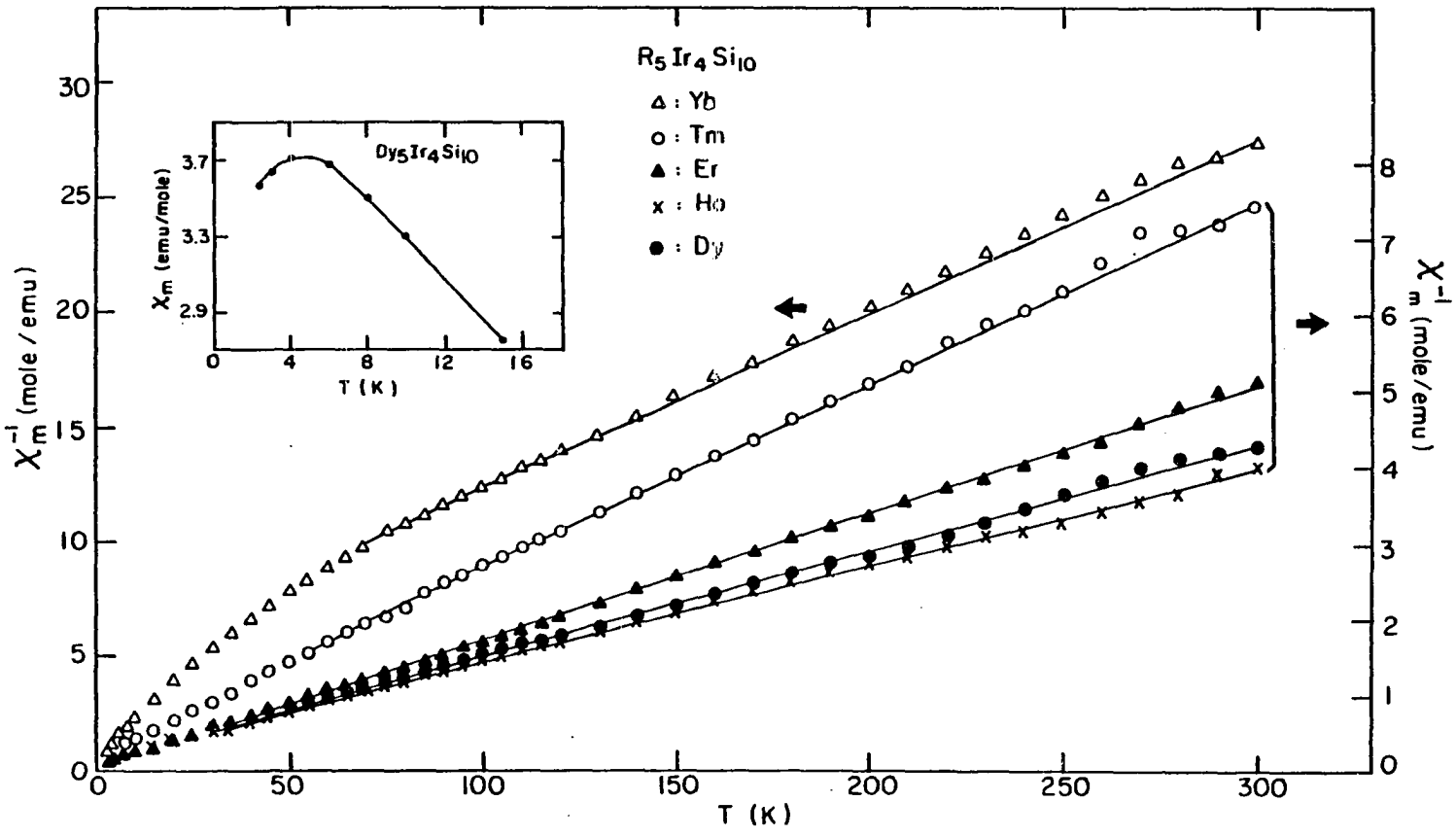

Fig. 28. Reciprocal molar magnetic susceptibility as a function of temperature for (R= Dy-Yb). Inset shows the magnetic susceptibility of $Dy_5Ir_4Si_{10}$ at low temperature

anomaly is not very pronounced in all of these compounds as temperature goes down to 1.2 K. This anomaly is also seen in the χ_{dc} - T plot for $Dy_5Ir_4Si_{10}$ shown in the inset of Fig. 28. Therefore, we would expect these materials to order antiferromagnetically below these temperatures. This is supported by the small negative value of Θ and coexistence of superconductivity and magnetic order in $(Sc_{1-x}Dy_x)_5Ir_4Si_{10}$ solid solutions.[58] Whereas, surprisingly, no anomaly is observed as the temperature decreases to 52 mK at ambient pressure and to 1.2 K at the pressure of 18 kbar for $Yb_5Ir_4Si_{10}$. Valence fluctuations at low temperatures may be important for $Yb_5Ir_4Si_{10}$ because its magnetic susceptibility deviates so much from the Curie-Weiss law at temperature below 70 K.

2. Electrical Resistivity

Results of normalized resistivity as a function of temperature between 2.6 and 300 K for $R_5Ir_4Si_{10}$ (R = Dy-Yb) are presented in Fig. 29. One cusp for $Dy_5Ir_4Si_{10}$, $Ho_5Ir_4Si_{10}$, and $Yb_5Ir_4Si_{10}$; and two distinct cusps for $Er_5Ir_4Si_{10}$ and $Tm_5Ir_4Si_{10}$ are observed. It is important to note that the resistivity increases at least twice as fast as the average between 60 and 70 K for $Er_5Ir_4Si_{10}$ and between 25 and 40 K for $Tm_5Ir_4Si_{10}$.

The temperature T_o which the cusp occurs for each rare earth compound is plotted in Fig. 30. The anomalies in these compounds have the same nature as that in $Lu_5Ir_4Si_{10}$ for the following reasons.

(1) Except for $Yb_5Ir_4Si_{10}$, T_o decreases just like the volume contraction seen in Fig. 27. This is also consistent with the pressure

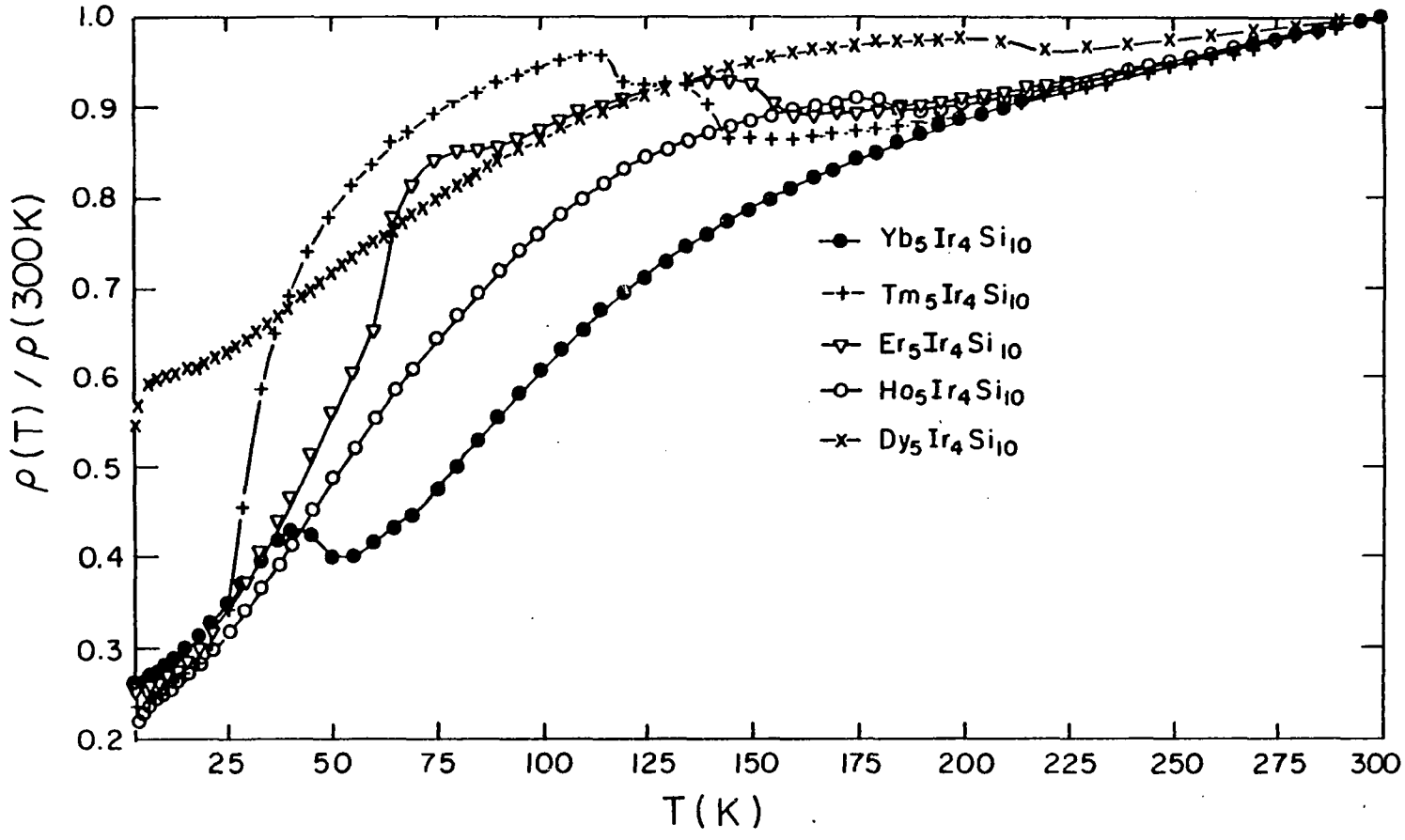

Fig. 29. Normalized resistivity as a function of temperature between 2.6 and 300 K $R_5Ir_4Si_{10}$ (R= Dy-Yb)

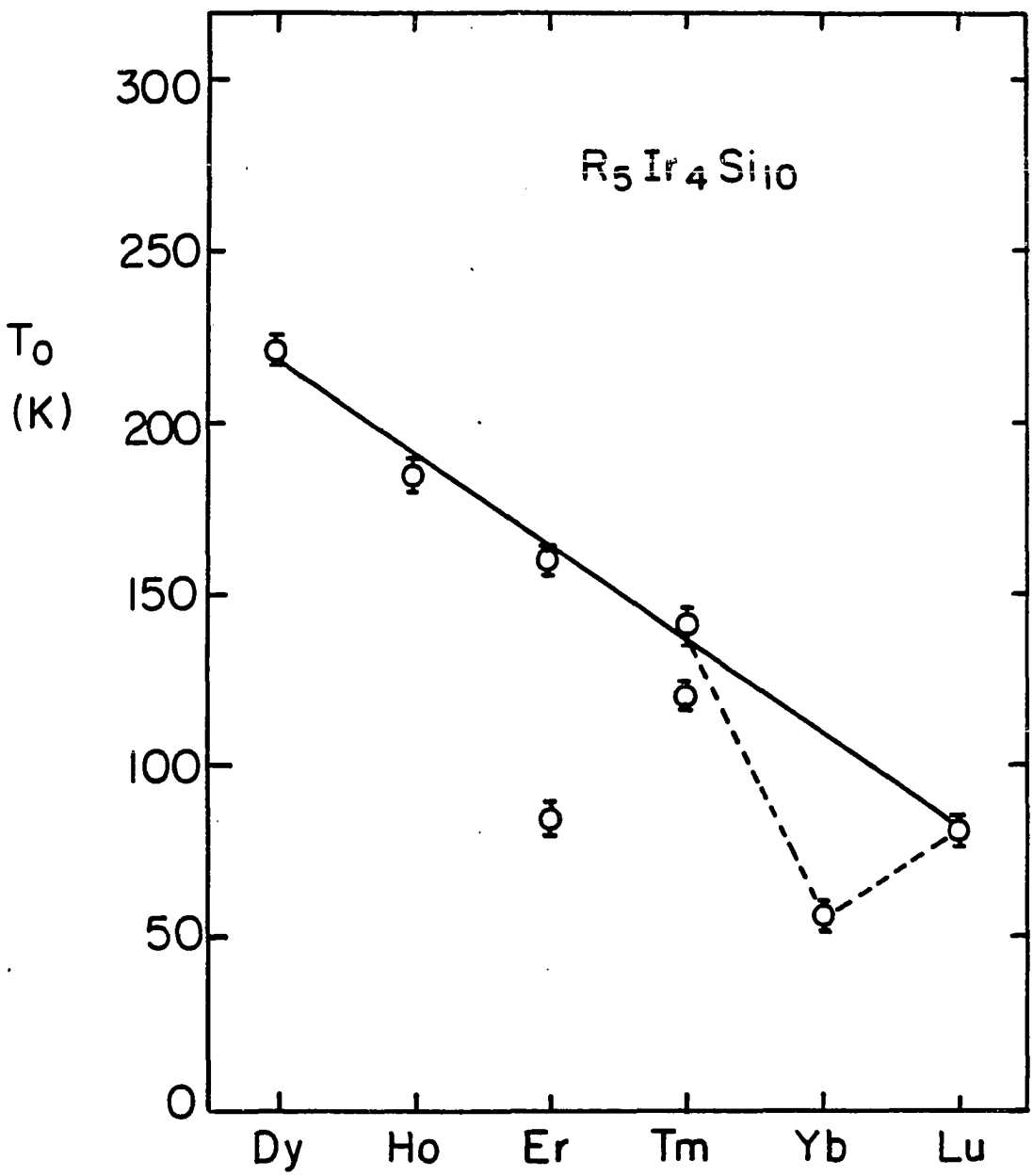

Fig. 30. The resistive anomaly temperature T_o for $R_5Ir_4Si_{10}$ (R= Dy-Lu)

effect on this kind of electronic phase transition which has been studied for $Lu_5Ir_4Si_{10}$.

(2) In Fig. 31, we see the change of T_o across the $(Lu_{1-x}Er_x)_5Ir_4Si_{10}$ system without losing the anomaly.

(3) In Chapter III, the sudden jump in T_c at high pressure retained in the $(Lu_{0.9}R_{0.1})_5Ir_4Si_{10}$ (R = Dy-Tm) series, provides a strong argument that this mechanism was not destroyed by these magnetic rare earth substitutions. We can ascribe this to the same type of phase transition also formed in the pure ternary compounds $R_5Ir_4Si_{10}$ (R = Dy-Yb).

In Fig. 30, the T_o = 56 K for $Yb_5Ir_4Si_{10}$ lies significantly below the line which is drawn on T_o's between $Dy_5Ir_4Si_{10}$ and $Lu_5Ir_4Si_{10}$. This deviation may be due to the valence fluctuation of Yb at low temperatures. From this point of view, we conclude that the volume change is not as dominant an influence on the anomaly as the electronic configuration difference. This change in electronic configuration is caused by the valence of Yb from 3^+ to an intermediate value between 2^+ and 3^+.

Two anomalies in resistivity for $Er_5Ir_4Si_{10}$ and $Tm_5Ir_4Si_{10}$ reflect the presence of more complex electronic phase transitions. This kind of phenomena was seen in the quasi-1D compound $NbSe_3$[86] and layered compound dichalcogenide TaS_2.[27,110]

3. Pressure effects in $Tm_5Ir_4Si_{10}$

For $Tm_5Ir_4Si_{10}$, the χ_{ac} - T plot at different applied pressures is shown in Fig. 32. The temperature of the cusp at 1.86 K increases only

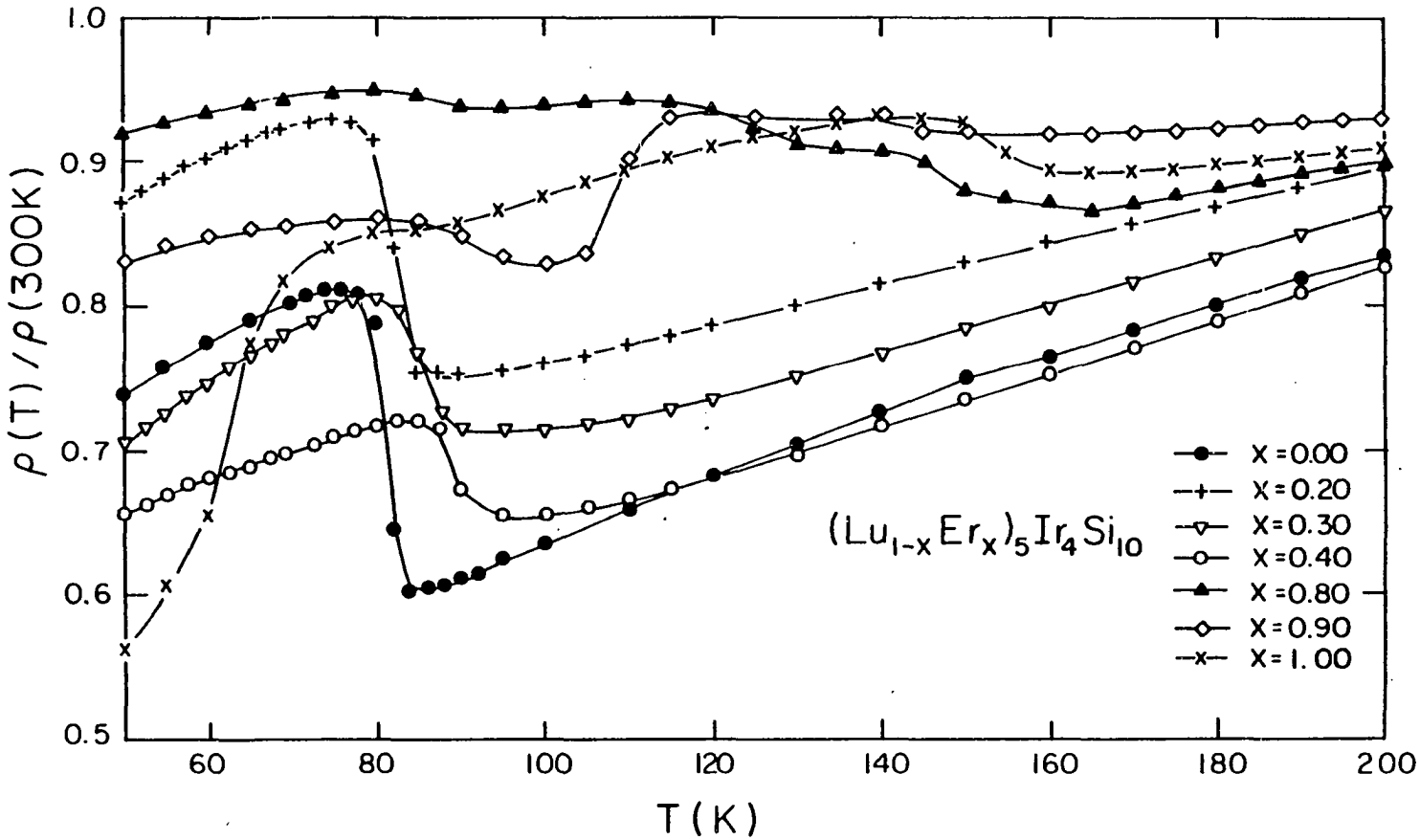

Fig. 31. Normalized resistivity as a function of temperature between 50 and 200 K for the pseudoternary system $(Lu_{1-x}Er_x)_5Ir_4Si_{10}$ (x= 0, 0.2, 0.3, 0.4, 0.8, 0.9, 1.0)

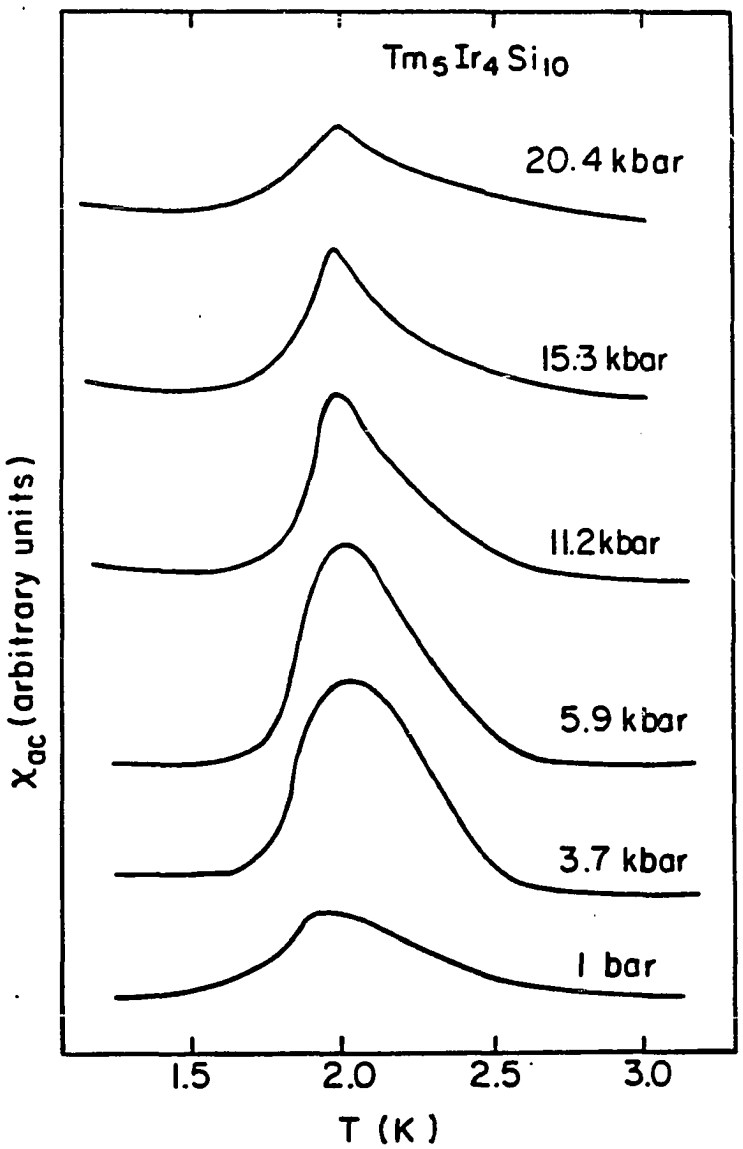

Fig. 32. χ_{ac} as a function of temperature between 1.2 and 3.2 K at six different pressures for $Tm_5Ir_4Si_{10}$

slightly with pressure, however the slope and magnitude of the χ_{ac} signal depend strongly on the pressure. The cusp is not as pronounced at ambient and high pressures (20 kbar) as at middle pressures (14 ~ 15 kbar). This may indicate that the strength or the type of the magnetic transition are different under various pressures. In fact, as the temperature is cooled further at ambient pressure in a dilution refrigerator, another sharper cusp is found at 0.82 K. Comparing these two anomalies by shape and amplitude, we speculate that this compound orders antiferromagnetically at 1.8 K and then ferromagnetically at 0.82 K. This idea is supported generally by the heat capacity data (see next section), and should be confirmed by other experiments such as neutron diffraction.

Normalized resistivity versus temperature between 4 K and 300 K at four different pressures for $Tm_5Ir_4Si_{10}$ is presented in Fig. 33. Two anomalies decrease monotonically by the application of pressure at the rate $(dT_o/dp)_{p=0}$ = -1.2 K/kbar for the higher and -1.4 K/kbar for the lower. The anomalies are also depressed in height and become broader in shape with pressure. The correlation between the electronic phase transition temperature T_o and the magnetic ordering temperature T_N in $Tm_5Ir_4Si_{10}$ shown in Fig. 32 and Fig. 33 is not as strong as that between the electronic phase transition temperature T_o and the superconducting transition temperature T_c observed in $Lu_5Ir_4Si_{10}$.[59]

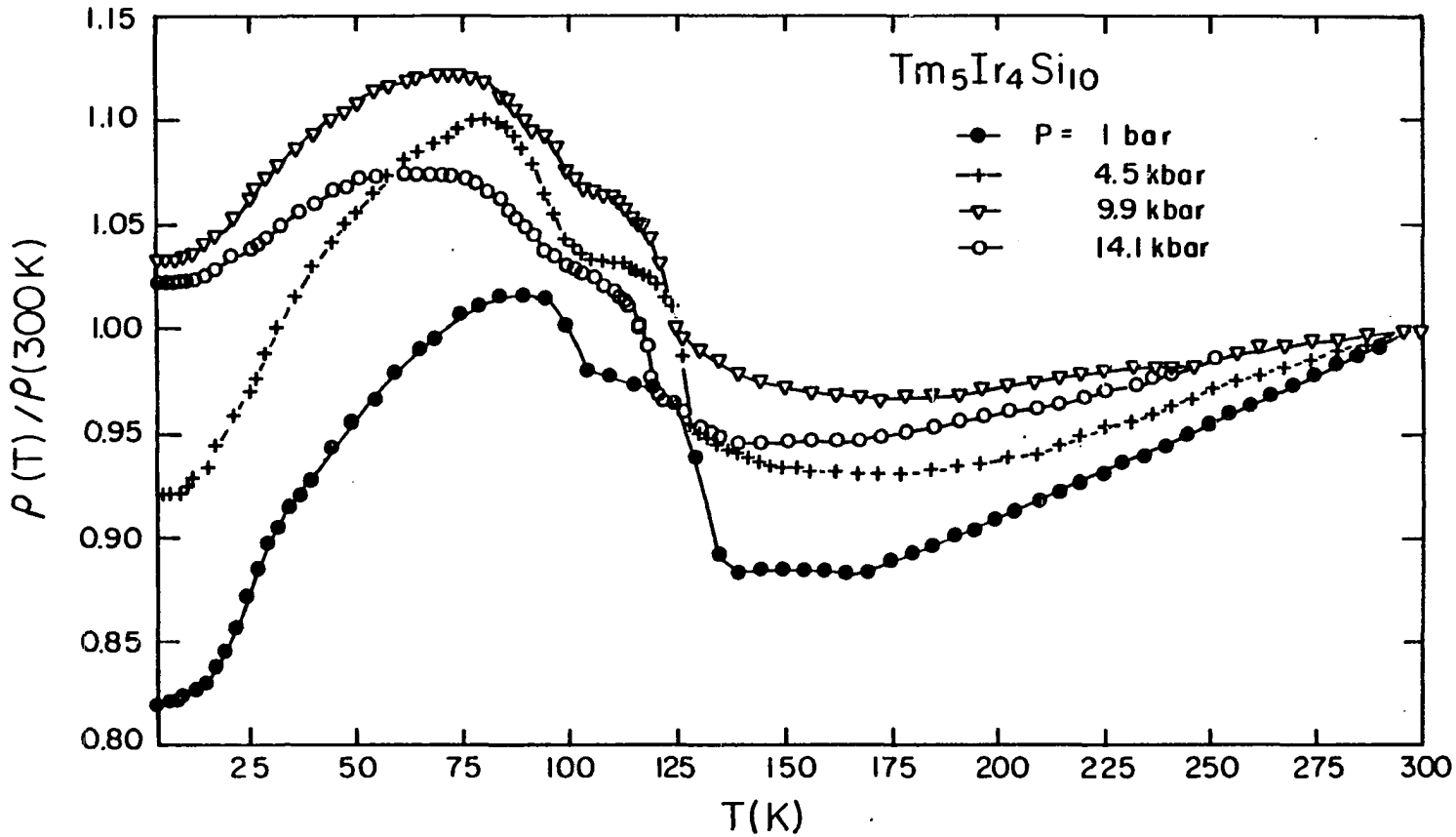

Fig. 33. Normalized resistivity as a function of temperature between 4 and 300 K at four distinct pressures for $Tm_5Ir_4Si_{10}$

4. Heat capacity for $Tm_5Ir_4Si_{10}$

The low temperature heat capacity from 0.6 to 30 K for $Tm_5Ir_4Si_{10}$ is presented in Fig. 34. Two distinct maxima at 0.86 and 1.91 K shown in the inset of Fig. 34 indicate two magnetic phase transitions. This is consistent with the magnetic susceptibility measurement as determined by low frequency (~25 Hz) ac inductance measurements. We note that the sizes and the shapes of the maxima shown in the inset of Fig. 34 are completely different. This may reflect two different types of magnetic transitions as predicted by ac magnetic susceptibility.

The heat capacity can be expressed as[111]

$$C = C_n + C_m + C_e + C_l \tag{16}$$

where C_n is the nuclear contribution. This nuclear Schottky anomaly arising from the interaction of the nucleus with the effective magnetic field at the nucleus can be written as[111]

$$C_n = A/T^2 \tag{17}$$

at temperatures well above the maximum. C_m is the magnetic contribution arising from the electrons in the unfilled 4f shell of the rare earth ions. C_e is the usual electronic contribution, and C_l is the lattice contribution. In Fig. 35, we show the heat capacity data for $Tm_5Ir_4Si_{10}$ from 1 to 10 K where the solid line is fitted by the equation

$$C/R = A/T^2 + BT + DT^3 \tag{18}$$

in the range from 4 to 10 K, where R is the universal gas constant with the value of 8.343 J/mole-K, A = 9.43 K^2, B = 0.11 1/K, and D = 9.9 x

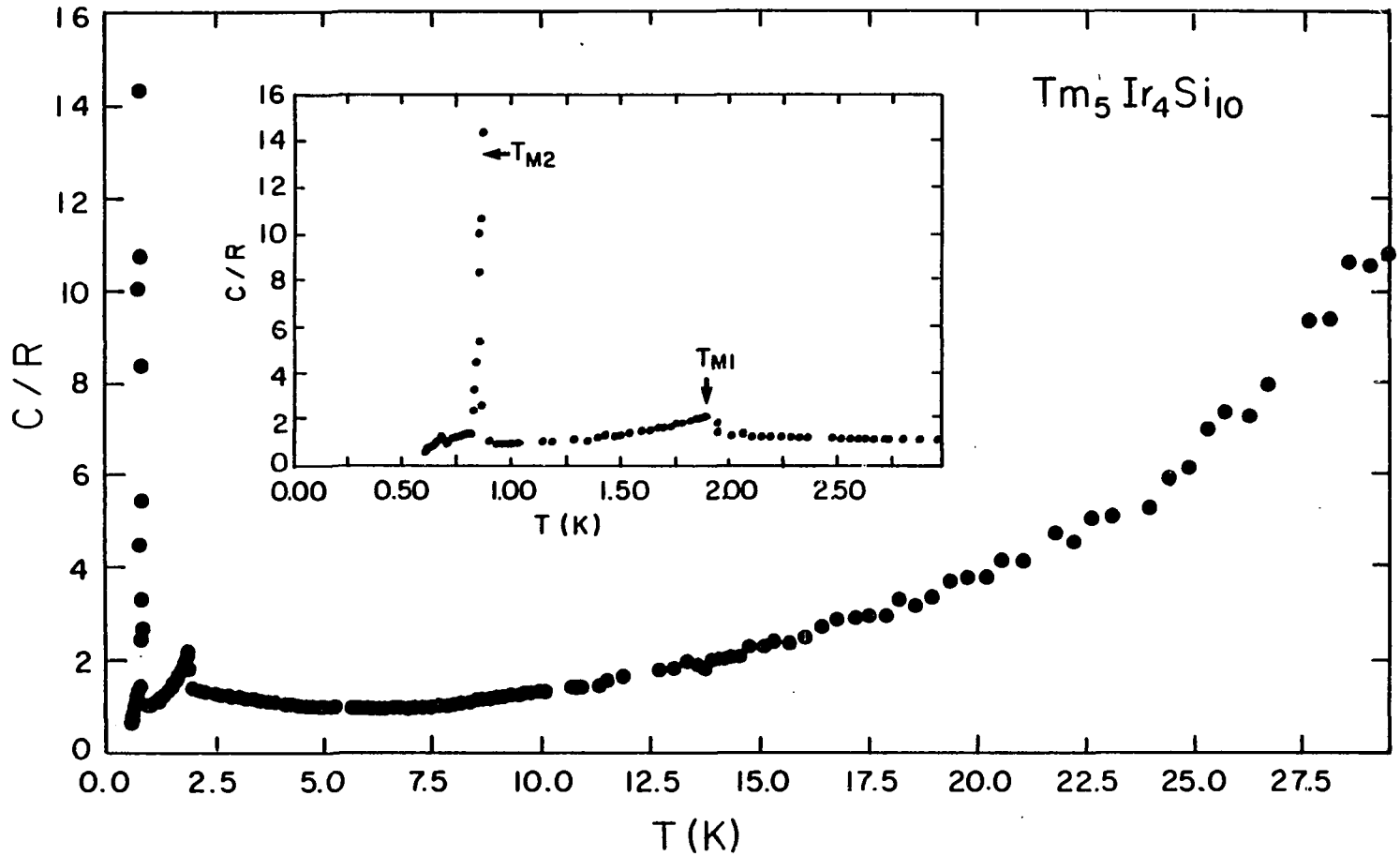

Fig. 34. Low temperature heat capacity for $Tm_5Ir_4Si_{10}$ from 0.6 to 30 K. Inset shows that of temperature range from 0.6 to 3 K

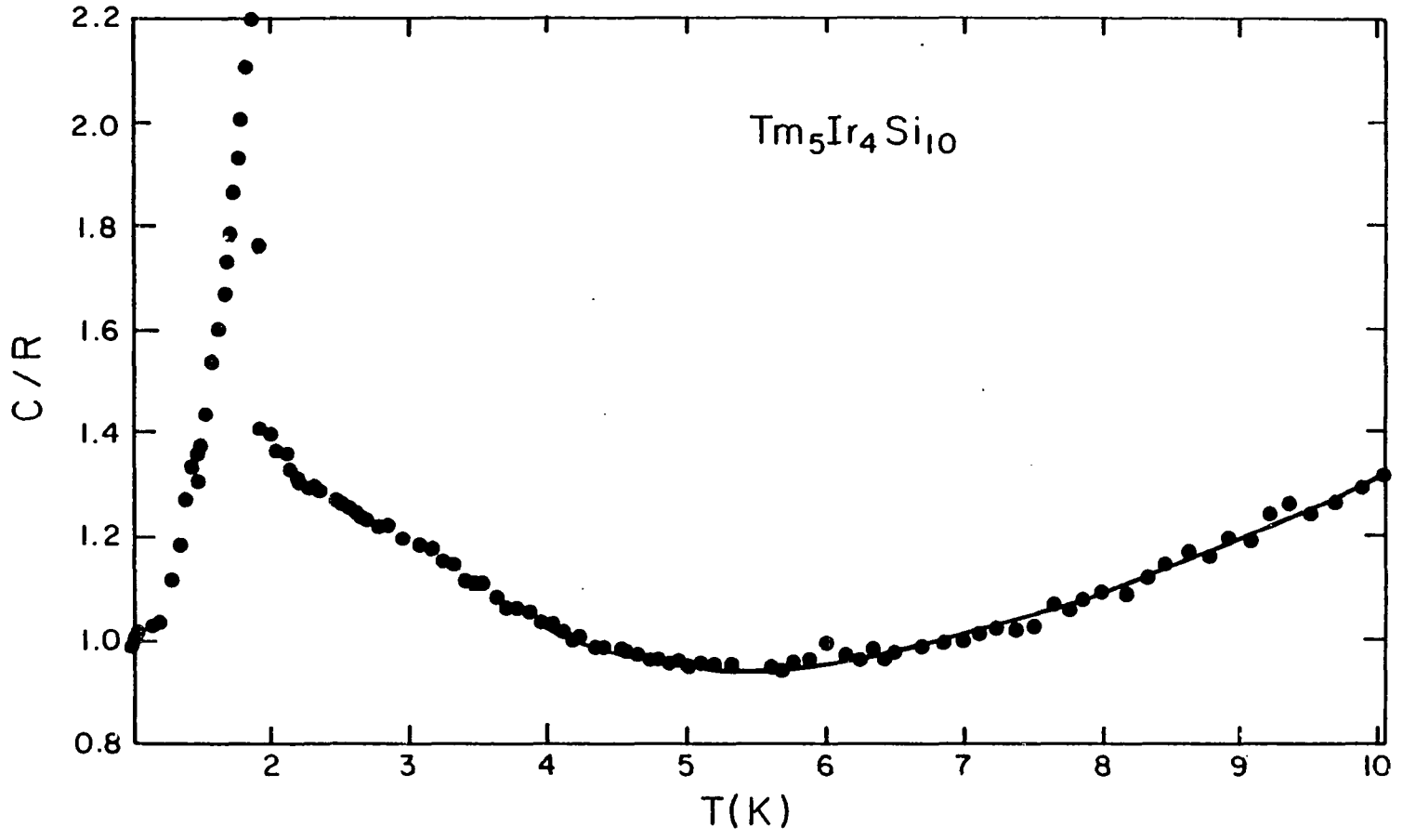

Fig. 35. Low temperature heat capacity for $Tm_5Ir_4Si_{10}$ from 1 to 10 K. Solid line is fit to $C/R = A/T^2 + BT + DT^3$ in the range from 4 to 10 K

10^{-5} $1/K^3$ are obtained from the fit. The unnegligible nuclear Schottky contribution to the heat capacity is also seen in $Sm_2Fe_3Si_5$ and $Ho_2Fe_3Si_5$ ternary silicides.[109] Combining the results of $Lu_5Ir_4Si_{10}$,[58] γ_n = 23.1 mJ/mole-K^2, β_n = 0.752 mJ/mole-K^4, and α_n = 3.95 x 10^{-3} mJ/mole-K^6 fitted by

$$C = \gamma_n T + \beta_n T^3 + \alpha_n T^5 \qquad (19)$$

and assuming the electronic and lattice contributions to the heat capacity of $Tm_5Ir_4Si_{10}$ are identical to those of $Lu_5Ir_4Si_{10}$, we can write the form of the magnetic contribution as

$$C_m/R = B'T + D'T^3. \qquad (20)$$

Then B'= 0.107 1/K and D'= 9 x 10^{-6} $1/K^3$ are obtained in the range of 4 to 10 K.

C. Conclusion

Measurements of the ac and dc magnetic susceptibility as a fuction of temperature have been performed for the ternary silicides $R_5Ir_4Si_{10}$ (R = Dy-Yb). All compounds, except $Yb_5Ir_4Si_{10}$ which is neither magnetic nor superconducting down to 52 mK, undergo magnetic transitions at very low temperature (the highest 5 K). Two magnetic transitions are found at 0.86 and 1.91 K in $Tm_5Ir_4Si_{10}$. Probably, one is antiferromagnetic and the other is ferromagnetic according to the ac magnetic susceptibility and heat capacity data for this compound. Strong crystal field effects or valence fluctuations are expected for $Yb_5Ir_4Si_{10}$ at low

temperatures ($T < 70$ K) because of the large deviation of the static magnetic susceptibility from Curie-Weiss law.

All compounds also exhibit an anomaly in the measurement of the resistivity versus temperature. Charge density wave formation, which was considered to occur in $Lu_5Ir_4Si_{10}$, is again thought to be the key reason giving rise to this anomaly.

For more information about the magnetic transition and resistivity anomaly in these materials, low temperature neutron scattering and low temperature single crystal X-ray diffraction are needed for further investigation.

VI. SUMMARY

The variation of the superconducting transition temperature T_c with hydrostatic pressure up to 23.7 kbar is reported for eleven ternary silicides and germanides with the $Sc_5Co_4Si_{10}$-type structure. Most of these compounds display a modest linear depression of T_c with pressure ($dT_c/dp \sim 10^{-5}$ K/bar); however, two materials, $Lu_5Ir_4Si_{10}$ and $Lu_5Rh_4Si_{10}$, undergo a discontinuous transformation to a state with a significantly higher T_c above a critical pressure of about 20 kbar. For $Lu_5Ir_4Si_{10}$, the pressure enhanced T_c of 9.12 K is the highest transition temperature for this class of compounds. We determine that the linear depression of T_c with pressure may be attributed mostly to the normal stiffening of the lattice with pressure and that d-band electrons make an important contribution to the occurrence of superconductivity in these materials.

Non-linear and enhanced T_c's are seen in T_c as a function of concentration x for $(Lu_{1-x}Sc_x)_5Ir_4Si_{10}$ system, while the room temperature lattice parameters and unit cell volume follow Vegard's law, and no jump in T_c is seen for pressures up to 21 kbar as $x \geq 0.05$. Even though the atomic volume of Ir is about the same as that of Rh and T_c jumps are seen in both pure $Lu_5Ir_4Si_{10}$ and $Lu_5Rh_4Si_{10}$ under a pressure of about 21 kbar, no T_c jump is seen in the $Lu_5(Ir_{1-x}Rh_x)_4Si_{10}$ system in the composition range $0.13 \leq x \leq 0.72$ up to the highest pressure. This indicates that the size (chemical contraction) and atomic disorder effects play a key role in suppressing the anomalous pressure effect on T_c in $Lu_5Ir_4Si_{10}$ and $Lu_5Rh_4Si_{10}$.

From the study of the superconducting transition temperature versus unit cell volume for materials with the $Sc_5Co_4Si_{10}$-type structure, we find that there exists a critical volume V_c=639 $Å^3$. Samples with a unit cell volume smaller than V_c show high T_c (8 ~ 9 K) and $(dT_c/dp)_{p=0} < 0$. Samples with a unit cell volume greater than V_c show low T_c (3 ~ 6 K) and $(dT_c/dp)_{p=0} > 0$. This relation holds for both pure ternary and pseudoternary compounds.

Combining the pressure and alloy data with the low temperature powder X-ray diffraction and isothermal bulk modulus measurements, we conclude that the enormous pressure effect on T_c in $Lu_5Ir_4Si_{10}$ and $Lu_5Rh_4Si_{10}$ is due to an electronic phase transition rather than a crystallographic transformation.

Two pseudoternary systems $(Lu_{0.98}Sc_{0.02})_5Ir_4Si_{10}$ and $Lu_5(Ir_{0.78}Rh_{0.22})_4Si_{10}$ in which T_c's are 2 K higher than $Lu_5Ir_4Si_{10}$ are used to study the enhanced superconducting state by upper critical field measurements. It is found that the enhanced T_c is mainly due to an increase in the electronic density of states at the Fermi surface for the former, and an increase of the electron-phonon interaction for the latter.

The electrical resistivity and static magnetic susceptibility show an anomaly in $Lu_5Ir_4Si_{10}$, $Lu_5Rh_4Si_{10}$, and $Y_5Ir_4Si_{10}$ compounds at 83 K, 155 K, and 250 K respectively, while $Sc_5Ir_4Si_{10}$ shows a common metallic behavior. Combining the magnetic susceptibility and heat capacity data, we give a quantitative estimate that this transition results in a 36% loss in the electronic density of states at the Fermi level in $Lu_5Ir_4Si_{10}$. This is consistent with the hypothesis that the electronic

phase transition involves the development of a charge density wave that opens an energy gap over a portion of the Fermi surface.

The general tendency of pressure to suppress the formation of CDW is observed in $Lu_5Ir_4Si_{10}$ with $(dT_o/dp)_{p=0}$ = -1.4 K/kbar. The complete suppression of the transition at 21 kbar results in the large, discontinuous enhancement of superconducting critical temperature from 3.8 to 9.1 K. For $Lu_5Rh_4Si_{10}$, the application of pressure at 18 kbar only partially suppress the anomaly in resistivity, but the T_c is also enhanced discontinuously from 3.4 to 4.3 K. This may be due to the sample homogeneity or a more complicated structure of CDW in $Lu_5Rh_4Si_{10}$. A complete suppression of the transition and simultaneously another jump in T_c are expected if the applied pressure is high enough.

The P-T phase diagram for $Lu_5Ir_4Si_{10}$ is given to demonstrate the correlation between T_o (CDW transition temperature) and T_c (superconducting transition temperature) via a parameter of pressure provides clear evidence that the pressure enhancement of T_c is due to a progressive removal of the CDW in the crystal.

The pseudoternary system $(Lu_{1-x}Sc_x)_5Ir_4Si_{10}$, $0 \leqslant x \leqslant 0.05$, is used to study the doping (impurity) effect on CDW and the competition between T_o and T_c in $Lu_5Ir_4Si_{10}$. $(dT_o/dx)_{x=0}$ = -18.5 K/at % and $(dT_c/dx)_{x=0}$ = 0.5 K/at % are obtained from data. These values are comparable to other CDW system such as $(Ta_{1-x}Nb_x)S_3$.[102]

According to the Ehrenfest equation for a second order phase transition

$$\Delta C_p = V\, T_o\, (\Delta\beta) \left[\frac{dT_o}{dp}\right]^{-1}_{p=0} \qquad (21)$$

where C_p is the heat capacity at constant pressure, V the volume, and β the volume thermal expansion coefficient, we take $(dT_o/dp)_{p=0}$ = -1.4 (K/kbar) and $\Delta\beta = -4.95 \times 10^{-4}$ (1/K),[112] and estimate $(\Delta C_p/C_p)_{T = 80\ K}$ = 5.8%. Therefore one should be able to observe a thermal anomaly at T_o in the heat capacity measurement.

The magnetic rare earth iridium silicides $R_5Ir_4Si_{10}$ (R=Dy,Ho,Er) show magnetic transitions at very low temperatures (the highest 5 K). Two magnetic transitions are seen by ac susceptibility and heat capacity measurements in $Tm_5Ir_4Si_{10}$, which might have different magnetic structures. Neither a magnetic nor superconducting transition is seen in $Yb_5Ir_4Si_{10}$ down to 52 mK, but a noticeable deviation from Curie-Weiss Law below 70 K in static magnetic susceptibility suggests the strong crystal field effects or valence fluctuations occur in this compound. All of these magnetic compounds (Dy-Yb) exhibit an anomaly (two in Er and Tm) in the resistivity. We attribute this anomaly is due to the formation of CDW, which is the same origin as that in $Lu_5Ir_4Si_{10}$.

Finally, we would like to make a survey of unit cell volume for 33 compounds, which form the $Sc_5Co_4Si_{10}$-type structure. The resistive anomaly only occurs in 8 compounds in which the unit cell volume lies between 647 and 671 $Å^3$. At this point, energy band calculation for this type of structure could explore the crystal or electronic instability versus lattice constants. As we know, with the exception of CuV_2S_4, CDW's form in the highly anisotropic and low-dimensional materials, while the $Sc_5Co_4Si_{10}$-type stucture looks three-dimensional. The anisotropy and effective dimensionality for these materials deserve further investigating. Future work should focus on low temperature

single crystal x-ray or electron diffraction experiments to determine the details of the CDW superlattice formed in $Lu_5Ir_4Si_{10}$.

VII. REFERENCES

1. H. Kamerlingh Onnes, Leiden Comm. 120b, 122b, 124c, (1911).

2. H. Kamerlingh Onnes, Leiden Comm. Suppl 34, (1913).

3. W. Meissner and R. Ochsenfeld, Naturwissenschaften 21, 787 (1933).

4. F. London and H. London, Proc. Roy. Soc. (London) A419, 71 (1935).

5. V. L. Ginzburg and L. D. Landau, Zh. Eksp. i. Teor. Fiz. 20, 1064 (1950).

6. A. B. Pippard, Proc. Roy. Soc. (London) A216, 547 (1953).

7. J. Bardeen, L. N. Cooper, and J. R. Schrieffer, Phys. Rev. 108, 1175 (1957).

8. C. A. Reynolds, B. Serin, W. H. Wright, and L. B. Nesbitt, Phys. Rev. 78, 487 (1950).

9. E. Maxwell, Phys. Rev. 78, 477 (1950).

10. A. A. Abrikosov, Zh. Eksp. i. Teor. Fiz. 32, 1442 (1957) [Soviet Phys.— JEPT 5, 1174 (1957)].

11. L. P. Gor'kov, Zh. Eksp. i. Teor. Fiz. 36, 1918 (1959) [Soviet Phys.— JEPT 9, 1364 (1959)]; 37, 1407 (1959) [10, 998 (1960)].

12. S. V. Vonsovosky, Yu. A. Izyumov, and E. Z. Kurmaev, **Superconductivity of Transition metals: Their Alloys and Compounds**, P. Fulde, ed. Springer Series in Solid State Science 27 (Springer-Verlag, Berlin, 1982).

13. a)See papers in "**Superconductivity in d- and f- Band Medals**", D. H. Douglass, ed. (Plenum, New York (1972).
b)See papers in "**Superconductivity in d- and f- Band Metals**", D. H. Douglass, ed. (plenum, New York, 1976).

14. J. Friedel, Nuovo Cimento Suppl. 12, 1861 (1958).

15. **Superconductivity in Ternary Compounds** I and II, Ø. Fischer and M. B. Maple, ed. (Springer, New York, 1982).

16. W. A. Fertig, D. C. Johnston, L. E. Delong, R. W. McCallum, M. B. Maple, and B. T. Matthias, Phys. Rev. Lett. 38, 987 (1977).

17. J. W. Lynn, G. Shirane, W. Thomlinson, and R. N. Shelton, Phys. Rev. Lett. 46, 368 (1981).

18. G. R. Stewart, **Heavy Fermion Systems in Perspective**, Rev. Mod. Phys. 56, 755 (1984).

19. a)L. F. Mattheiss and D. R. Hamann, **Superconductivity in d- and f-Band Metals**, ed. by W. Buckel and W. Weber (Kernforschungszentrum Karlsruhe, FRG., 1982), p. 405p.
b)C. Methfessel and S. Methfessel, **Superconductivity in d- and f-Band Metals**, ed. by W. Buckel and W. Weber (Kernforschungszentrum Karlsruhe, FRG., 1982), P. 393.
c)B. Batlogg, J. P. Remeika, R. C. Dynes, H. Barz, A. S. Cooper, and J. P. Garno, **Superconductivity in d- and f- Band Metals**, ed. by W. Buckel and W. Weber (Kernforschungszentrum Karlsruhe, FRG., 1982), p. 401.

20. See papers in "**Charge Density Waves in Solids**", ed. by G. Hutiray and J. Solyon, Lecture notes in Physics, Vol. 217 (Springer-Verlag, New York, 1985).

21. J. G. Bednorz and K. A. Müller, Z. Phys. B 64, 189 (1986).

22. M. K. Wu, J. R. Ashburn, C. J. Torng, P. H. Hor, R. L. Meng, L. Gao, Z. J. Huang, Y. Q. Wang, and C. W. Chu, Phys. Rev. Lett. 58, 908 (1987).

23. A. R. Moodenbaugh, M. Suenaga, T. Asnao, R. N. Shelton, H. C. Ku, R. W. McCallum, and P. Klavins (to be published).

24. R. E. Peierls, **Quantum Theory of Solids** (Oxford Univ. Press, New York 1955) p. 108.

25. R. Comes, M. Lambert, H. Launois, and H. R. Zeller, Phys. Rev. B 8, 571 (1973).

26. See for example, **Highly Conducting One-Dimensional Solids**, eds. J. T. Devreese, R. P. Evnard, and V. E. van Doren (Plenum Press, New York and London, 1975).

27. J. A. Wilson, F. J. DiSalvo, and S. Mahajen, Adv. Phys. 24, 117 (1975).

28. H. Fröhlich, Proc. Roy. Soc. London A223, 296 (1954).

29. P. A. Lee, T. M. Rice, and P. W. Anderson, Solid State Commun. 14, 703 (1974).

30. T. M. Rice, in **Low Dimensional Cooperative Phenomena**, ed. H. J. Keller (Plenum, New York, 1975).

31. R. M. Fleming, in **Physics in One-Dimensional**, eds. J. Bernasconi and T. Schneider (Springer-Verlag, New York, 1981).

32. R. M. Fleming, D. E. Moncton, and D. B. McWhan, Phys. Rev. B 18, 5560 (1978).

33. R. M. Fleming and C. C. Grimes, Phys. Rev. Lett. 42, 1423 (1979).

34. P. Monceau, J. Richard, and M. Renard, Phys. Rev. Lett. 45, 43 (1980).

35. See the collection of articles in **Superconductivity**, ed. by R. D. Parks (Dekker, New York, 1969).

36. F. J. DiSalvo, R. Schwall, T. H. Geballe, F. R. Gamble, and J. H. Osiecki, Phys. Rev. Lett. 27, 310 (1971).

37. R. C. Morris and R. V. Coleman, Phys. Rev. B 7, 991 (1973).

38. R. C. Morris, Phys. Rev. Lett. 34, 1164 (1975).

39. C. A. Balseiro and L. M. Falicov, Phys. Rev. B 20, 4457 (1979).

40. R. H. Friend and D. Jerôme, J. Phys. C : Solid State Phys. 12, 1441 (1979).

41. W. L. McMillan, Phys. Rev. 167, 331 (1968).

42. J. Friedel, J. Physique Lett. 36, L279 (1975).

43. L. R. Testardi, Rev. Mod. Phys. 47, 637 (1975).

44. L. N. Bulaevskii, Sov. Phys.-Usp. 18, 131 (1975).

45. W. W. Fuller, P. M. Chaikin, and N. P. Ong, Solid State Commun. 39, 547 (1981).

46. E. R. Hoverstreydt, J. Appl. Cryst. 16, 651 (1983).

47. H. F. Braun and C. U. Segre, **Ternary Superconductors**, G. K. Shenoy, B. D. Dunlap, and F. Y. Fradin, eds. (North-Holland, New York, 1981), p. 239.

48. G. Venturini, M. Méot-meyer, E. McRae, J. F. Marêche, and B. Roques, Mat. Res. Bull. 19, 1647 (1984).

49. L. J. van der Pauw, Philips Res. Rep. 13, 1 (1958).

50. M. J. Johnson and R. N. Shelton, Solid State Commun. 52, 839 (1984).

51. A. Eiling and J. S. Schilling, J. Phys. F : Metal Phys. 11, 623 (1981).

52. C. B. Vining, Ph.D. Thesis (unpublished), Iowa State University, Ames, (1983).

53. H. F. Braun and C. U. Segre, Solid State Commun. 35, 735 (1980).

54. H. F. Braun, K. Yvon, and R. M. Braun, Acta Crystallogr. B36, 2397 (1980).

55. Ø. Fischer, Appl. Phys. 16, 1 (1978).

56. J. M. Vandenberg and B. T. Matthias, Science 198, 194 (1978).

57. R. N. Shelton, L. S. Hausermann-Berg, P. Klavins, H. D. Yang, M. S. Anderson, and C. A. Swenson, Phys. Rev. B 34, 450 (1986).

58. L. S. Hausermann-Berg and R. N. Shelton, (to be published in Phys. Rev. B).

59. L. S. Hausermann-Berg, Ph.D. Thesis (unpublished), Iowa State University, Ames (1986).

60. H. F. Braun and M. Pelizzone, **Superconductivity in d- and f- Band Metals**, W. Buckel and W. Weber eds. (Kernforschungszentrum Karlsruhe 1982), p. 245.

61. C. U. Segre and H. F. Braun, **Physics of Solids under High Pressure**, J. S. Schilling and R. N. Shelton eds. (North-Holland, Amsterdam, 1981), p. 381.

62. R. I. Boughton, J. L. Olsen, and C. Palmy, **Progress in Low Temperature Physics**, Vol. 6, C. J. Gorter, ed. (North-Holland, Amsterdam, 1970), p. 163.

63. T. F. Smith, **Superconductivity in d- and f- Band Metals**, D. H. Douglass, ed. (AIP, New York, 1972), p. 293.

64. P. B. Allen and R. C. Dynes, Phys. Rev. B 12, 905 (1975).

65. A. Birnboim, Phys. Rev. B 14, 2857 (1976).

66. K. A. Gschneidner, Jr., **Solid State Physics**, eds. F. Seitz and D. Turnbull, Vol. 16 (Academic Press, New York, 1964), p. 275.

67. L. S. Hausermann-Berg and R. N. Shelton, Physica, 138B, 400 (1985).

68. J. F. Olsen, in **Low Temperature Physics - LT13**, Vol. 3, K. D. Timmerhaus, W. J. O'Sullivan, and E. F. Hammel, eds. (Plenum, New York, 1974), p. 27.

69. A. A. Abrikosov and L. P. Gor'kov, Sov. Phys.--JETP 12, 1243 (1961); 16, 1575 (1963).

70. E. Helfand and N. R. Werthamer, Phys. Rev. 147, 88 (1966).

71. N. R. Werthamer, E. Helfand, and P. C. Hohenberg, Phys. Rev. 147, 295 (1966).

72. K. Maki, Phys. Rev. 148, 362 (1966).

73. T. P. Orlando, E. J. McNiff, Jr., S. Foner, and M. R. Beasley, Phys. Rev. B 19, 4545 (1979).

74. H. D. Yang, R. N. Shelton, and H. F. Braun, Phys. Rev. B 33, 5062 (1986).

75. R. N. Shelton, A. R. Moodenbaugh, P. D. Dernier, and B. T. Matthias, Mat. Res. Bull. 10, 1111 (1975).

76. R. N. Shelton and R. P. Dougherty, Physica 107 B, 475 (1981).

77. D. C. Johnston, R. N. Shelton, and J. J. Bugaj, Solid State Commun. 21, 949 (1977).

78. M. Decroux, M. S. Torikachvili, M. B. Maple, R. Baillif, Ø. Fischer, and J. Müller, Phys. Rev. B 28, 6270 (1983).

79. R. N. Shelton, **Superconductivity in d- and f- Band Metals**, D. H. Douglass, ed. (Plenum, New York, 1976), p. 137.

80. J. E. Schirber, Phys. Rev. Lett. 28, 1127 (1972).

81. T. M. Smith, R. N. Shelton, and J. E. Schirber, Phys. Rev. B 8, 3479 (1973).

82. P. Monceau, J. Peyrard, J. Richard, and P. Molinie, Phys. Rev. Lett. 39, 161 (1977).

83. C. Berthier, P. Molinie, and D. Jerome, Solid State Commun. 18, 1393 (1976).

84. P. W. Selwood, **Magnetochemistry**, 2nd Ed. (Interscience, New York, 1956), p. 78.

85. R. M. White, **Quantum Theory of Magnetism** (McGraw-Hill, New York, 1970), p. 86.

86. J. Chaussy, P. Haen, J. C. Lasjaunias, P. Monceau, G. Waysand, A. Waintal, A. Meerschaut, P. Molinie, and J. Rouxel, Solid State Commun. 22, 759 (1976).

87. R. L. Fleming, F. J. DiSalvo, R. J. Cava, and J. V. Waszczak, Phys. Rev. B 24, 2850 (1983).

88. J. Friedel, J. Phys. Lett. 36 L, 279 (1975).

89. G. Biebro and W. L. McMillan, Phys. Rev. B 14, 1887 (1976).

90. P. A. Lee, T. M. Rice, Phys. Rev. B 19, 3970 (1979).

91. H. G. Schuster, Solid State Commun. 14, 127 (1974).

92. L. N. Bulquevskiy, Usp. Fiz. Nauk 115, 263 (1975) [Sov. Phys. 18, 131 (1975)].

93. P. Monceau, N. P. Ong, A. M. Portis, A. Meerschaut, and J. Rouxel, Phys. Rev. Lett. 37, 602 (1976).

94. N. G. Ong, and P. Monceau, Phys. Rev. B 16, 3443 (1977).

95. J. Bardeen, Phys. Rev. Lett. 42, 1498 (1979).

96. J. Bardeen, **Highly Conducting One-Dimensional Solids**, ed. by J. T. Devreese, R. P. Evrard, and V. E. van Doren (Plenum, New York 1979), p. 373.

97. F. J. DiSalvo, **Electron-Phonon Interaction and Phase Transition**, ed. by T. Riste (Plenum, New York, 1977), p. 107.

98. a)For example, see **Molecular Metal**, Les Arcs, France, 1978, ed. by W. E. Hatfield (Plenum, New York, 1979).
b)For example, see **The Physics and Chemistry of Low Dimensional Solids**, Tomar Portugal, 1979, ed. by L. Alcacer (Reidel, Boston, 1980).

99. N. LeNagard, A. Katty, G. Collin, O. Gorochov, and A. Willing, J. Solid State Chem. 27, 267 (1978).

100. Hiroshi Fujimoto and Hajime Ozaki, Solid State Commun. 49, 1117 (1984).

101. F. J. DiSalvo and J. V. Waszczak, Phys. Rev. B 17, 3801 (1978).

102. Pei-Ling Hsieh, F. de Czito, A. Janossy, and G. Grüner, J. Phys. 44, C3-1479 (1983).

103. D. W. Murphy, F. J. DiSalvo, G. W. Hull, Jr., J. V. Waszczak, S. F. Mayer, G. R. Stewart, S. Early, J. V. Acrivos, and T. H. Geballe, J. Chem. Phys. 62, 967 (1975).

104. H. F. Braun, Phys. Lett. 75A, 386 (1980).

105. H. F. Braun, C. U. Segre, F. Acker, M. Rosenberg, S. Dey, and P. Deppe, J. Mag. and Magn. Mater. 25, 117 (1981).

106. F. Steglich, J. Aarts, C. D. Bredl, W. Lieke, D. Meschede, W. Franz, and H. Schafer, Phys. Rev. Lett. 43, 1982 (1979).

107. C. U. Segre and H. F. Braun, Phys. Lett. 85A, 372, (1981).

108. C. B. Vining and R. N. Shelton, Solid State Commun. 54, 53 (1985).

109. C. B. Vining and R. N. Shelton, Phys. Rev. B 28, 2732 (1983).

110. P. W. Williams, G. S. Parry, and C. B. Scruby, Philos.-Mag. 29, 695 (1974).

111. L. J. Sundstorm, **Handbook on the Physics and Chemistry of Rare Earths**, ed. by K. A. Gschneidner, Jr. and L. Eyring (North-Holland, Amsterdam, 1978), Vol. 1, p. 379.

112. C. A. Swenson, (to be published).

VIII. ACKNOWLEDGMENTS

I would like to extend my deepest thanks to my major professor, Dr. R. N. Shelton, for making my graduate career exciting, rewarding, and enjoyable. His scientific support, personal encouragement, and enthusiastic guidance have set an example that I will always value highly.

A special thanks is reserved for Peter Klavins. He introduced me to the experimental techniques of low temperature physics with limitless patience and thoughtful instruction. Some measurements reported in this thesis were done in cooperation with him.

The stimulating discussion with my colleagues in the group, Dr. L. S. Berg, Dr. K. S. Athreya, Dr. H. C. Ku, W. H. Lee, Youwen Xu, and C. Parengkuan, broadened my outlook and interests in many fields and helped me at important moments.

I have benefited from working with Dr. C. A. Swenson, M. S. Anderson, Dr. J. L. Staudenmann, Dr. R. D. Horning, Dr. T. P. Chen, Dr. Z. X. Zhao, and Dr. P. J. Chu. I am grateful to Drs. D. K. Finnemore, J. R. Clem, K. A. Gschneidner, Jr., and R. A. Jacobson for serving on my thesis committee.

I would like to express my general thanks to all of the faculty, secretaries, scientific and administrative staff, and fellow students who helped me along the way at ISU.

Finally and most importantly, I dedicate this work to my parents for their great love and constant support and without whom none of this would mean so much.

IX. APPENDIX: SOURCES AND PURITIES OF STARTING MATERIALS

Element	Source	Purity
Si	Research Organic/Inorganic Chemical Corp.	7N pieces
Ge	Ventron Alfa Products Lot#041377	6N+ pieces
Co	Ventron Alfa Products Lot#051573	m2N5 pieces
Rh	Purchased from USDOE stockpile P.O. A3-1197	4N powder
Ir	Research Organic/Inorganic Chemical Corp. #IR-002	3N powder
	DOE stores #01213642	3N powder
Os	Ventron Alfa Division Lot#010279 Lot#111478	3N powder
Sc	Ames Laboratory	batch 112481, rod major impurities (atomic): O 118 ppm F 109 ppm H 89 ppm C 64 ppm W 36 ppm Fe 20 ppm N 6.4 ppm Cu 6 ppm La 5 ppm Ni 5 ppm Pr 4 ppm other impurities are all less than 4 ppm

Y	Ames Laboratory	batch 12381b, rod major impurities (atomic): O 834 ppm H 704 ppm C 141 ppm W 22 ppm Pb 20 ppm F <14 ppm Fe 10 ppm Cu 5 ppm Tb 4.5 ppm Pr 4 ppm other impurities are all less than 4 ppm
Lu	Ames Laboratory	batch 51585, rod major impurities (atomic): H 346 ppm C 189 ppm O 130 ppm Fe 78 ppm N 37 ppm F <27 ppm W 5.6 ppm other impurities are all less than 5 ppm
Yb	Ames Laboratory	batch 72081-RB, rod major impurities (atomic): O 38 ppm Fe 10 ppm C 187 ppm H 1713 ppm Zn 5.3 ppm Ca 5 ppm Na <5 ppm Si <70 ppm Sr<300 ppm Rb<300 ppm Lu 7 ppm La 6 ppm Gd 6 ppm other impurities are all less than 3 ppm

Tm	Ames Laboratory	batch 32878, rod major impurities (atomic): O 10.6 ppm H 328 ppm N 24 ppm C 378 ppm Fe 25 ppm F 124 ppm Cu 11 ppm Cl 10 ppm Ce 8 ppm Si 3 ppm other impurities are all less than 3 ppm
Er	Ames Laboratory	batch 31584, rod major impurities (atomic): O 367 ppm C 139 ppm H 994 ppm N 24 ppm F <25 ppm Ta 42 ppm Fe 19 ppm Cu 3.6 ppm other impurities are all less than 3 ppm
Ho	Ames Laboratory	batch 9977, rod major impurities (atomic): O 309 ppm C 301 ppm H 653 ppm N 47 ppm F 651 ppm Ni 5 ppm Fe 47 ppm Ta 30 ppm Hf 6 ppm Cr 5 ppm Cu 3.4 ppm other impurities are all less than 3 ppm

Dy	Ames Laboratory	batch 1578, rod major impurities (atomic): O 367 ppm C 124 ppm H 322 ppm N 35 ppm F 632 ppm Ta 30 ppm Fe 632 ppm Cl 5 ppm Mn 4 ppm Al 5 ppm Ho 6 ppm other impurities are all less than 4 ppm